Determining the Effects of Wnt Signaling in the Alleviation of Cholestasis Via the Promotion of Hepatocyte Transdifferentiation and Cholangiocyte Proliferation

by

Karis Pearl Kosar

Bachelor of Arts, The College of Wooster, 2015

Submitted to the Graduate Faculty of the

School of Medicine in partial fulfillment

of the requirements for the degree of

Doctor of Philosophy

University of Pittsburgh

2021

UNIVERSITY OF PITTSBURGH

SCHOOL OF MEDICINE

This dissertation was presented

by

Karis Pearl Kosar

It was defended on

May 5, 2021

and approved by

Alejandro Soto-Gutiérrez, Associate Professor, Department of Pathology

Lance Davidson, Professor, Department of Bioengineering

Satdarshan P. S. Monga, Professor and Vice Chair, Division of Experimental Pathology, Department of Pathology

Michael Oertel, Associate Professor, Department of Pathology

Donghun Shin, Associate Professor, Department of Developmental Biology

Dissertation Director: Kari Nejak-Bowen, Associate Professor, Department of Pathology

Determining the effects of Wnt signaling in the alleviation of cholestasis via the promotion of hepatocyte transdifferentiation and cholangiocyte proliferation

Karis Pearl Kosar, PhD

University of Pittsburgh, 2021

Primary sclerosing cholangitis (PSC), is a chronic cholestatic disease that causes bile duct inflammation and fibrosis, and results in end-stage liver disease and reduced life expectancy. Therefore, an effective treatment for PSC is needed. Previously we identified specific Wnt proteins (Wnt7a, a canonical signaling ligand, and Wnt7b, a noncanonical signaling ligands) upregulated in the cholangiocytes during cholestatic liver injury and found mice lacking Wnt secretion from hepatocytes and cholangiocytes showed fewer hepatocytes expressing cholangiocyte markers, proliferating cholangiocytes, and high mortality in response to DDC diet. These findings led us to two hypotheses: 1) Canonical Wnt/β-catenin signaling induces hepatocyte-to-cholangiocyte transdifferentiation, which could alleviate cholestatic injury caused by PSC, and 2) Wnt7b induces cholangiocyte proliferation, which if knocked out would induce more severe cholestatic injury caused by PSC. After testing these hypotheses, we found that β-catenin signaling does induce hepatocyte-to-cholangiocyte reprogramming, thereby alleviating biliary injury. We also found that mice lacking Wnt7b in only the cholangiocytes, and mice lacking Wnt7b in both hepatocyte and cholangiocyte compartments did in fact have decreased cholangiocyte proliferation, but this did not result in increased biliary injury. Instead, this inability of the cholangiocytes to proliferate promoted hepatocytes to adopt a cholangiocyte-like phenotype, which resulted in the alleviation of cholestatic injury. Overall, our work has elucidated two methods to induce hepatocyte-to-cholangiocyte transdifferentiation which could be used to establish a groundwork for potential PSC treatments.

Table of Contents

List of Tables

List of Figures

Preface

Deciding to pursue my PhD was an easy decision to make, but completing graduate school has been the most challenging thing I've ever done. I would have never made it this far without the support of my friends and family. First and foremost, I would like to thank my family for constantly encouraging me to pursue my passions and empowering me to do so. Especially my mother and sister for always being there for me and willing to let me talk about my research, even though they might not understand a single word I'm saying. I would also like to thank all of the friends I have made while at the University of Pittsburgh. They have provided me with a life outside of lab, memories I will cherish forever, and a support network I will always have no matter how far apart we end up. Tuesday dinners, dungeons and dragons, and camping will never be same without them.

I would especially like to thank the members of the Nejak-Bowen lab, who created the best work environment ever. Pam for helping me throughout my time in the lab, always being a great sounding board for anything and everything, helping me come up with appropriate controls when needed, and for knowing everything there is to know about Pittsburgh and educating me as much as she could. Lizzie, Mary, and Anu for always being down to get lunch and bubble tea and for making our lab even more fun as they joined. It's thanks to all of their help and advice that I have been able to get to this point. I have always been happy to come to work and you all have made it all the better. I would also like to thank my thesis committee members for their support and insight in my scientific endeavors, without their guidance my project would not be where it is today. I would like to thank Dr. Monga for helping me throughout my graduate career. From when I first joined Dr. Nejak-Bowen's lab by letting me join his lab's weekly lab meeting when our lab was

only three people, to giving me advice on where to postdoc, his insight and knowledge have been greatly valued and he has helped me to become the researcher I am today.

Finally, I would like to thank Dr. Nejak-Bowen. She has been an incredible mentor throughout this process, and it is thanks to her guidance and support that I am the scientist I am today. She has always been supportive of both myself and my ideas and fostered my independence and critical thinking. She aided the growth of my career by encouraging me to submit abstracts, travel to, and present at conferences, apply for grants, and write papers. I can say without any doubt that my success as a graduate student has been a direct result of her outstanding mentorship. I may be Dr. Nejak-Bowen's first graduate, but I know deep down that she will continue to help shape great future scientists and she will only get better with it as she gets more experience. Although my time in her lab is finishing up, I will continue to look to her for advice and mentorship throughout my career. Thank you for everything you have done.

.

1.0 Introduction

The liver performs a multitude of functions vital to homeostasis, making it crucial to survival. The biliary system within the liver also plays a crucial role in hepatic health and function. Without the cholangiocytes within the biliary system, bile would not be modified or transported out of the liver, damaging to the liver. Therefore, it is crucial for the liver and the biliary system to possess the ability to regenerate upon injury. Both the liver and the biliary system are capable of regenerating through two methods: transdifferentiation and proliferation. However, during chronic cholestatic diseases, such as primary sclerosing cholangitis (PSC), the ability of the biliary system to repair or regenerate is severely impaired. This dissertation focuses on the role of Wnt signaling in the regeneration of injured bile ducts; canonical Wnt signaling induces hepatocyte-to-cholangiocyte transdifferentiation (Aim 1) and non-canonical Wnt signaling induces healthy cholangiocyte proliferation (Aim 2) (Figure 1). This study will define the roles of both canonical and non-canonical Wnt signaling in bile duct regeneration in cholestatic liver disease and these finding could become the foundation of a novel treatment utilizing specific Wnts for relieving intrahepatic cholestasis.

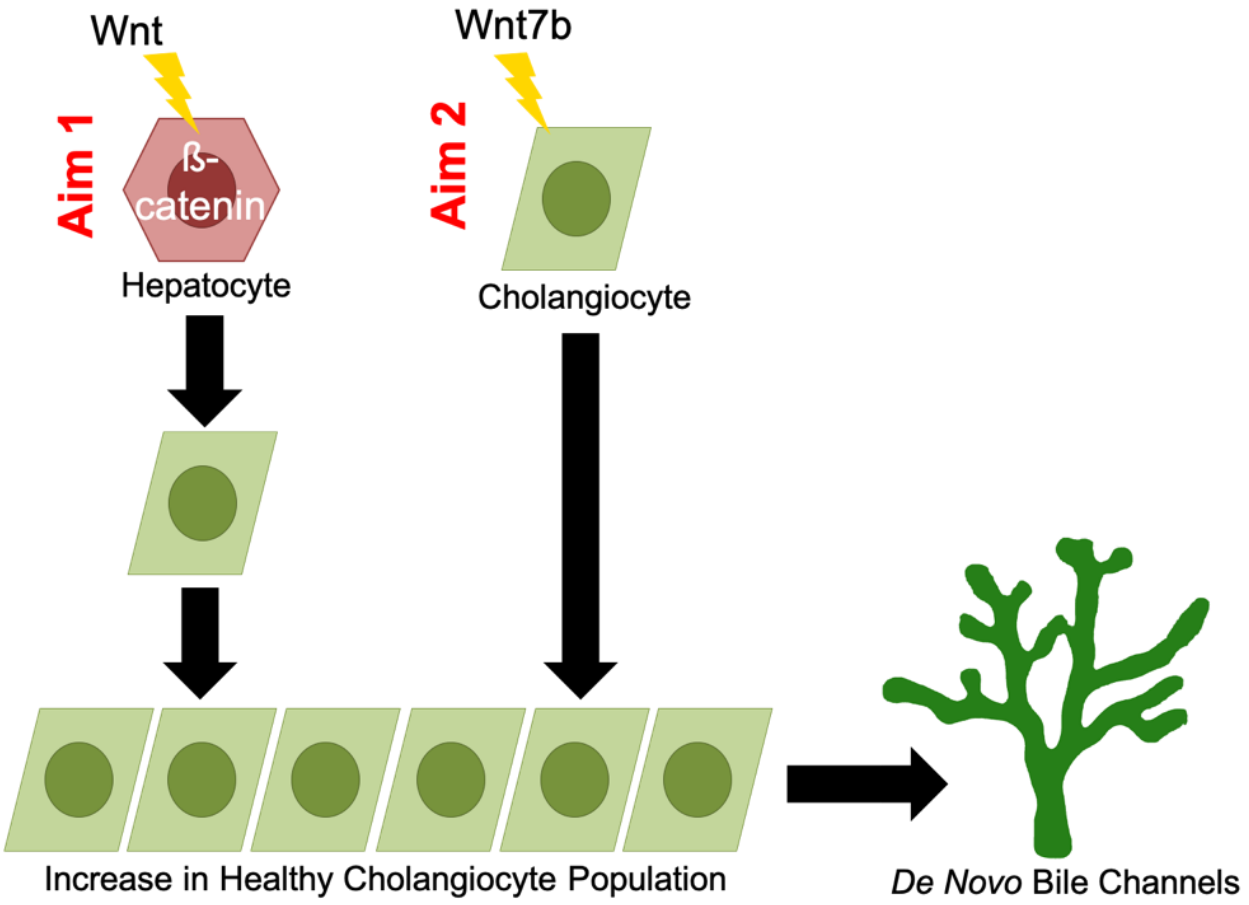

Figure 1. Schematic for Wnt Driven Bile Duct Regeneration
Bile Duct Regeneration can occur through two different means: 1) canonical Wnt/β-catenin signaling can indue hepatocyte-to-cholangiocyte transdifferentiation (Aim 1) or 2) non-canonical Wnt signaling can induce healthy cholangiocytes to proliferate (Aim 2). These newly generated cholangiocytes increase the healthy cholangiocyte population, leading to the formation of de novo bile duct channels, which could relieve cholestatic injury.

1.1 Wnt Signaling Pathways

1.1.1 Canonical Wnt/β-catenin Signaling

The Wnt signaling pathway is a highly conserved pathway found in all phyla of the animal kingdom. The canonical Wnt pathway is centered on regulating and signaling through moderating the levels of β-catenin protein in cells. Canonical Wnt signaling is highly regulated and involved

in multiple biological processes ranging from development to cancer. Signaling in the canonical Wnt/β-catenin pathway is mediated through Wnt ligands. Wnt ligands are part of a family of secreted glycoproteins that are relatively insoluble due to a hydrophobic lipid modification, palmitoylation, which is necessary for their function (1). Wnt ligands are palmitoylated by enzyme porcupine in the endoplasmic reticulum (2). Post palmitoylation, Wntless (Wls), a transmembrane protein that mediates protein trafficking between the Golgi apparatus and cell membrane, secretes the hydrophobic Wnts from the cell (3, 4).

In the absence of Wnt ligands , β-catenin levels are kept low via degradation by a β-catenin destruction complex consisting of the proteins Axin, adenomatous polyposis coli (APC), Glycogen synthase kinase 3 (GSK3), and casein kinase 1α (CK1α) (5, 6) (Figure 2). The scaffold protein Axin brings together the destruction complex components, mediating the phosphorylation of β-catenin by CK1α first at serine 45, followed by serine 33 and serine 37, and GSK3 phosphorylates threonine 41 (5, 7). Phosphorylated β-catenin is then recognized by β-transducin repeat-containing protein (βTrCP), a component of the E3 ubiquitin ligase complex, triggering the ubiquitination and proteasomal degradation of β-catenin (5, 8, 9) (Figure 2A).

To activate the canonical Wnt/β-catenin pathway, a secreted Wnt ligand binds to a Frizzled receptor (Fz) and the co-receptor low-density lipoprotein receptor-related protein (LRP) 5 or 6 (10-12). This binding of Wnt to its receptors mediates activation of the Wnt/β-catenin signaling pathway. The scaffolding protein Dishevelled (Dvl) is triggered to phosphorylate LRP5/6 (4, 13). Phosphorylated LRP5/6 then recruits Axin to the plasma membrane, removing Axin from the destruction complex (4, 13). This removal of Axin disrupts the β-catenin destruction complex, promoting stabilization and cytoplasmic levels of β-catenin to increase. β-catenin then translocates

to the nucleus where it forms a complex with T cell factor/lymphoid enhancer factor (TCF/LEF) transcription factors to mediate expression of target genes (14, 15) (Figure 2B).

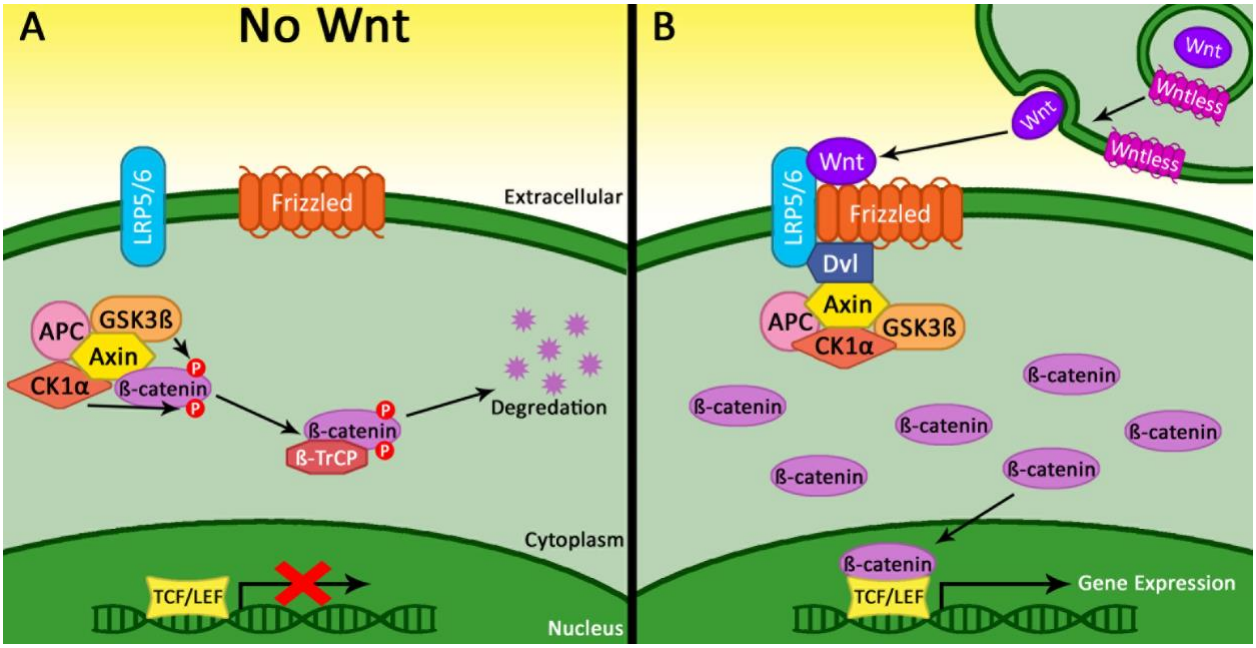

Figure 2. Canonical Wnt/β-Catenin Signaling

(A) In the absence of Wnt β-catenin is phosphorylated by its destruction complex. This phosphorylation targets β-catenin for proteasomal degradation by β-transducin repeat-containing protein (β-TrCP). (B) Wnt is released from a neighboring cell by cargo receptor Wntless. The Wnt protein binds to its receptor (Frizzled) and co-receptor (LRP5/6), triggering the scaffold protein Dishevelled (Dvl) to recruit Axin and the β-catenin destruction complex to the plasma β-catenin accumulates in the cytoplasm, and translocates to the nucleus to bind the T cell factor/lymphoid enhancer factor (TCF/LEF) family of transcription factor inducing target gene transcription.

1.1.2 β-catenin Activity Independent of Wnt Signaling

β-catenin is known to play integral roles in both gene transcription and the regulation and coordination of cell-cell adhesion. However, not all of the functions performed by β-catenin are driven by Wnt signaling. Epidermal growth factor (EGF), hepatocyte growth factor (HGF)/c-met, and Protein Kinase A (PKA) have also been shown to regulate β-catenin activity. EGF has been observed to activate β-catenin signaling to promote mesenchymal stem cell proliferation (16) and induce the extracellular-signal-regulated kinase/mitogen activated protein kinase (ERK/MAPK) pathway to phosphorylate LRP6, a co-receptor to Frizzled, to activate β-catenin signaling during

bone and cartilage formation (17, 18). HGF/c-met's activation of β-catenin is well studied in hepatoblastoma (19, 20). Pathologic activation of β-catenin via HGF/c-Met signaling is present in most tumors of hepatoblastoma and has been found to utilize a separate pool of β-catenin located at the inner surface of the cell membrane (21, 22).

1.1.2.1 PKA-Driven β-catenin Signaling

Like HGF/c-met activation of β-catenin, PKA induction of β-catenin activity is also known in the liver. Due to β-catenin's dual function in both cell-cell adhesion and gene transcription, the protein has many sites at which it can be phosphorylated to designate whether β-catenin should active or degraded and where β-catenin should be localized in the cell (7, 9, 23, 24). Interestingly, there are also two sites of phosphorylation on the β-catenin protein that are known to be phosphorylated by PKA and are distinct sites from Wnt signaling and cell-cell adhesion phosphorylation sites (25-27). These PKA driven phosphorylation sites are Ser-552 and Ser-675, and phosphorylation of these novel sites prevents β-catenin from being degraded and increases its transcriptional activity (25-27).

PKA-driven phosphorylation of Ser-675 and subsequent activation of β-catenin is known to play a couple roles in the liver. In conjunction with activated Ras-related C3 botulinum toxin substrate 1(Rac-1), PKA induced phosphorylation of β-catenin at Ser-675 has been shown to increase the motility of fibrocystin-defective cholangiocytes (28). Additionally, PKA driven phosphorylation of Ser-675 has been found to induce hepatocyte proliferation when the liver is exposed to thyroid hormone (T3) (29, 30). This proliferation was found to be promoted through β-catenin's induction of cyclin D1 expression (29, 30).

1.1.2.2 β-catenin in Adherens Junctions

β-catenin is also involved in cell-cell adhesions as a component of adherens junctions. Adherens junctions are protein complexes that form subapical junctions that promote homotypic cell-cell adhesions in epithelial tissue (31). The main component of adhesion protein complexes is a class of transmembrane proteins called cadherins, which perform the extracellular interaction during cell-cell adhesion. E-cadherin is typically the cadherin protein found in adherens junctions. To mediate cell-cell adhesion the extracellular domain of E-cadherin forms calcium-dependent complexes with E-cadherin molecules of neighboring cells (32). β-catenin's role in adherens junctions is to facilitate in anchoring E-cadherin to the actin skeleton. β-catenin acts as a bridge between E-cadherin and α-catenin, which binds directly to the actin cytoskeleton or to actin-binding proteins (33, 34). Additionally, β-catenin facilitates the assembly of the adherence junction protein complex. β-catenin binds newly synthesized E-cadherin, which promotes E-cadherin's delivery from the endoplasmic reticulum to the basal-lateral plasma membrane (35-37). β-catenin binding to E-cadherin also blocks a specific peptide sequence, which when exposed targets E-cadherin for proteasomal degradation, protecting E-cadherin from being degraded (35, 38).

However, β-catenin is not permanently integrated into adherens junctions. β-catenin can be phosphorylated to induce dissociation from the adherens junction. Specifically tyrosine phosphorylation of β-catenin at residues Y142, Y654, and Y670 by HGF/c-met activity, and Y654 by epidermal growth factor receptor (EGFR) activity, and Src activity leads to the disassembly of the β-catenin from adherens junction to increase β-catenin available for other signaling pathways (21, 39-42). β-catenin may also play a role in tight junction formation in the blood-bile barrier, which prevent the mixing of bile in the biliary canaliculi with blood in the hepatic sinusoids. It

was found that liver-specific loss of β-catenin leads to intrahepatic cholestasis, defective bile canalicular morphology, and bile secretory defects (43-45).

1.1.3 Non-Canonical Wnt Signaling

Wnt ligands are also capable of signaling independent of β-catenin, or non-canonical Wnt signaling. Two well studied pathways in which Wnt acts independently of β-catenin are the planar cell polarity (PCP) pathway and the Wnt/calcium pathway. In the PCP pathway Wnt ligands bind to Frizzled and another co-receptor receptor tyrosine kinase-like orphan receptor 2 (Ror2) (46, 47) (Figure 3A). Dishevelled is then activated and recruited to the plasma membrane, leading to the activation of RhoA and Rac, Rho-family small GTPases. RhoA and Rac subsequently activate c-Jun N-terminal kinase (JNK) and Rho-associated protein kinase (ROCK). The signaling from JNK and ROCK leads to modification of the actin cytoskeleton causing cytoskeletal rearrangement that allows for changes in cell polarity and cell migration (46, 48-50).

The other non-canonical Wnt signaling pathway is the Wnt/calcium pathway (Figure 3B). Similar to the PCP pathway, a Wnt ligand binds to Frizzled receptor and co-receptor Ror2 (51, 52). A complex consisting of Dishevelled and G-proteins is recruited to Frizzled and the complex phosphorylates Ror2 (53, 54). Phosphorylated Ror2 triggers membrane-bound enzyme phospholipase C (PLC) to activate membrane-bound phospholipid phosphatidyl inositol 4,5-bisphosphate (PIP2) and increase cellular inositol 1,4,5-triphosphate (IP3), and 1,2 diacylglycerol (DAG). IP3, in turn, promotes increased intracellular calcium levels and DAG activates Protein Kinase C (PKC) (55). The increased calcium levels activate calcium-calmodulin dependent kinase II (CaMKII) and calcineurin (CaN), which regulate cell migration and cell proliferation (53, 56).

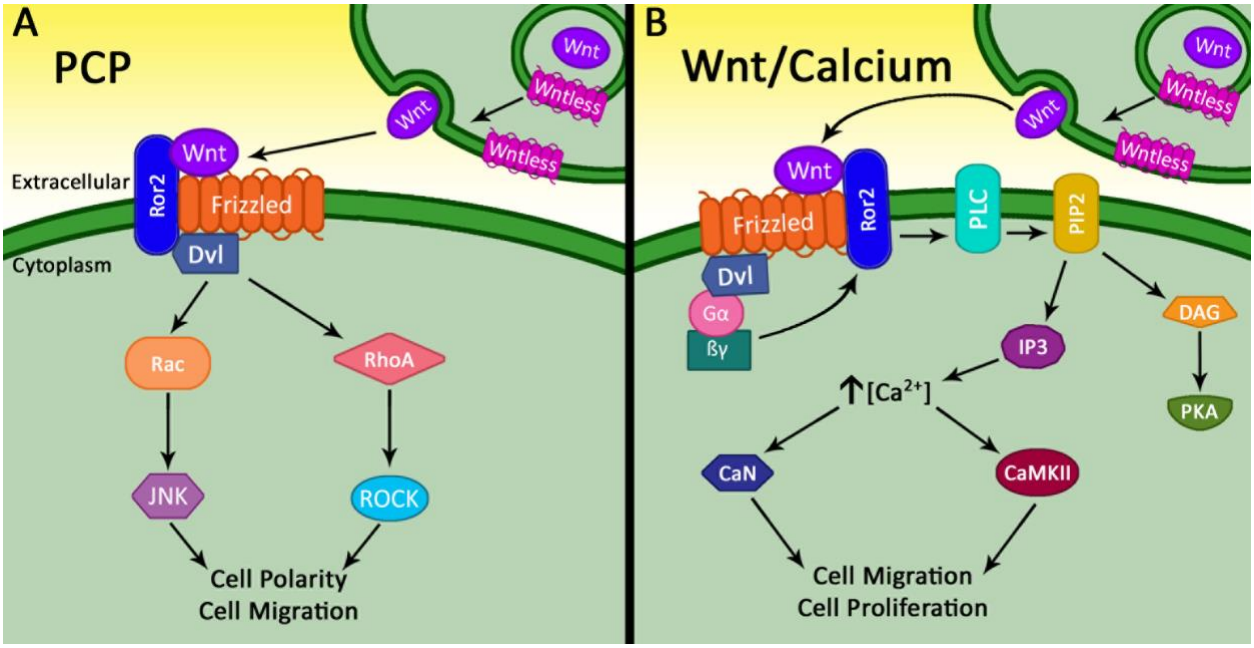

Figure 3. Non-Canonical Wnt Signaling Pathways

(A) In the Planar Cell Polarity (PCP) pathway, Wnt ligands bind to a complex consisting of certain Frizzled receptors, Ror2, and Dishevelled. This triggers activation of Rac and JNK signaling, or RhoA and ROCK signaling to regulate cell polarity and migration. (B) In the Wnt/calcium pathway, Wnt ligands bind to Frizzled receptor and Ror2 co-receptor. A tri-protein complex of Dishevelled and G-proteins is formed, and one of the G-proteins mediates phosphorylation of Ror2 co-receptor. Ror2 induces PLC to mediate PIP2's generation IP3 and DAG. DAG activates PKC, and IP3 promotes increased intracellular calcium levels. Increased intracellular calcium levels activates CaMKII and CaN, which in turn regulate cell migration and proliferation.

1.1.4 Wnt Ligands in Liver

With multiple Wnt pathways, both canonical and non-canonical, it is not surprising there are multiple Wnt ligands. There are a total 19 of Wnt ligands, all of which are evolutionarily conserved across mammals (57, 58). With this many Wnts questions arise whether the 19 Wnt ligands have unique or redundant roles. Unique Wnt roles can be determined through developmental loss-of-function studies: Wnt1 and Wnt3 are involved in midbrain and cerebellum development, Wnt2 and Wnt7b play important roles in placental development, and Wnt10b and Wnt16 participate in bone development (59-65).

However, the role of specific Wnts in liver pathobiology are not well characterized. This lack of characterization is mostly due to the lack of robust Wnt antibodies and the ability of hepatic cell populations to compensate for when Wnts are mutated or lost by upregulating other Wnts that act analogously. Despite these difficulties some Wnts and their roles have been identified in the liver. During hepatic injury liver sinusoidal endothelial cells release Wnt2 which is required to promote liver regeneration (66). Once the liver is regenerated to its full size, Wnt5a is one of the factors that terminates liver regeneration (67). Wnt2 and Wnt9b are released from endothelial cells adjacent to central vein which aids in liver zonation (68). Finally, Wnt7b and Wnt10a have been found to promote cholangiocyte proliferation during cholestatic injury (69).

1.1.4.1 Wnt7b in the Liver

Apart from Wnt7b promoting cholangiocyte proliferation, not much more is known about it in context of the liver. Wnt7b is known to be a noncanonical Wnt ligand; however, this has only been determined in cell types outside of the liver, such as osteogenic cells, dendritic cells, pancreatic progenitor cells, and in prostate cancer (70-73). Wnt7b is also known to signal through canonical Wnt signaling in pancreatic adenocarcinoma, epithelial and vascular smooth muscle cells, renal cells, and during hippocampal synapse formation (74-77). Interestingly a study did find that Wnt7b along with Wnt7a and Wnt10a were significantly upregulated during murine oval cell response, and β-catenin levels were also increased in the same cell compartments (78). These findings hint at one or more of the three Wnts found in this study being involved in canonical Wnt signaling pathway in oval cell response; however, studies have yet to completely determine Wnt7b's function and how it signals in the liver.

1.1.5 Wnt Signaling in Liver Development and Regeneration

Though the roles that specific Wnt ligands play in the liver is not completely known, Wnt signaling in the liver is pretty well understood. Wnt signaling, specifically canonical Wnt signaling, is known to play important roles in both liver development and regeneration. During development the endoderm consists of three parts: the foregut, from which the liver is derived, the midgut, and the hind gut. To begin liver formation, foregut development is initially inhibited via Wnt signaling from the mesoderm to the posterior endoderm to promote hindgut fate. The anterior endoderm simultaneously secretes Wnt antagonists to suppress Wnt/β-catenin signaling allowing the foregut to maintain its identity and to allow liver development (79, 80). Once the foregut is formed, canonical Wnt/β-catenin activation is required around embryonic day 8.5 (E8.5) for the liver specification. It has been noted that β-catenin's removal from hepatoblasts during liver development in mice results in suboptimal liver development by E12 and fetal lethality by E17, which resulted from increased oxidative stress, hepatocyte apoptosis, and lack of hepatocyte growth (81). Postnatally, β-catenin activation is also important for hepatic cell proliferation for the continuation of liver development up to 20 days postnatal. This is known because β-catenin-null mice have lower liver weight to body weight ratios during their lifespan compared to wild type mice, while mice with hyperactivate β-catenin develop larger livers before one month of age due to the increased cell cycle entry and proliferation (82-84).

Once the liver is developed it is capable of regenerating up to 70% of the organ if it is removed or acute hepatic injury occurs. This process of regeneration is mediated through the proliferation of existing differentiated hepatocytes (85). There are a few well studied models of liver injury and regeneration, however the two most prevalent models are two-thirds partial hepatectomy (PHx) model and acute liver failure from acetaminophen (APAP) overdose model.

During the PHx model two-thirds of a mouse or rat liver are removed. Within days of the removal, cellular hyperplasia and cellular hypertrophy takes place and the remaining lobes enlarge to replace liver mass that was lost (86). Wnt/β-catenin signaling is important to liver regeneration in this model. In rats, within minutes of PHx, β-catenin expression is increased 2.5-fold followed by its rapid translocation to the nucleus, which helps to promote hepatocyte proliferation through target gene expression, such as cell-cycle regulator cyclin D1 (87, 88). Mice lacking β-catenin specifically in hepatocytes and mice lacking both Wnt co-receptors LRP5 and LRP6 displayed delayed regeneration 40 hours post PHx compared to WT mice (84, 89). However, there is a subsequent increase in regeneration in the β-catenin knockout mice three days post-PHX, indicating the activation of a compensatory signaling pathway (84). Therefore, Wnt/β-catenin signaling does play a role in liver regeneration post PHx; however, Wnt/β-catenin signaling is not necessary for regeneration post PHx, unlike liver development.

Much like the PHx model, β-Catenin signaling is also required for regeneration after acute liver failure caused by APAP overdose. The APAP overdose model causes hepatotoxicity through the metabolization of APAP by cytochrome P450 enzymes, Cyp2e1 and Cyp1a2, which creates N-acetyl-p-benzoquinone imine, a toxic, reactive metabolite that covalently binds to cellular macromolecules, which induces hepatocyte death (90-92). Both *CYP2E1* and *CYP1A2* are target genes of β-catenin, so mice lacking β-catenin specifically in their hepatocytes are resistant to APAP-induced hepatotoxicity (93). However, β-catenin also promotes liver regeneration following APAP overdose. Liver-specific β-catenin knockout mice given APAP following induction of Cyp2e1 and Cyp1a2 activity presented with significant defects in hepatocyte proliferation following APAP-induced hepatic necrosis (90). Therefore, despite the protection lacking β-catenin offers hepatocytes during APAP overdose, it also hinders the hepatocytes' ability

to proliferate and regenerate post APAP overdose, so β-catenin signaling is necessary for the liver's ability to regenerate.

1.2 Biliary System

The biliary system is a 3-dimensional network of tubular structures that forms an almost tree-like shape with its branches connecting the hepatocellular parenchyma of the liver with the lumen of small intestine through its trunk. The main function of the biliary system is to transport bile from the liver to the small intestine to aid in digestion. Hepatocytes produce bile, which is secreted into the bile canaliculi, dilated intercellular spaces sealed by tight junctions between apical membranes of neighboring hepatocytes (94-96). The bile flows from canaliculi to the network of bile ducts, which are lined with cuboidal epithelial cells called cholangiocytes. Bile ducts anastomose into larger ductules, then larger ducts, which eventually form the common bile duct (Figure 4). The common bile duct enters the gall bladder, where the bile is stored until it is needed.

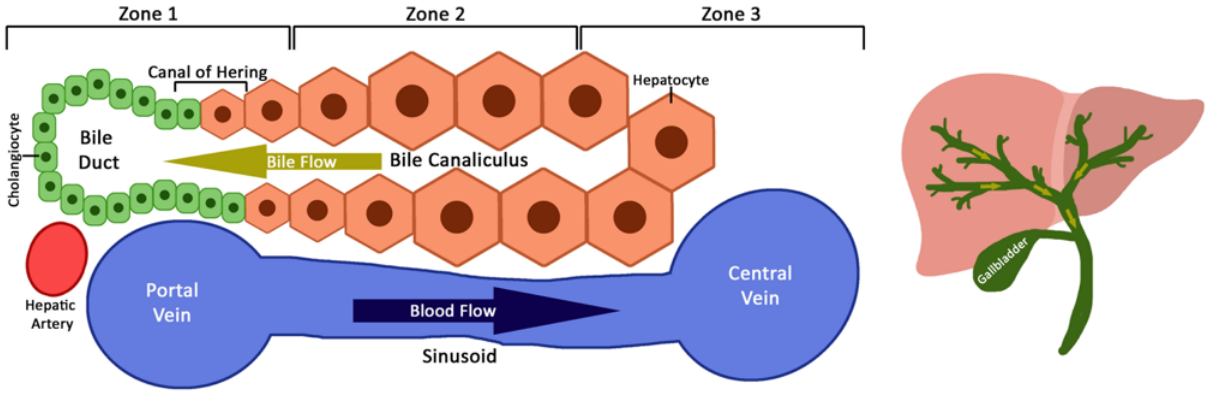

Figure 4. Liver Zonation and the Biliary System

Left Image: The structure of a liver lobule consists of three zones. Zone 1 consists of the "portal triad": the portal vein, bile ducts, (made of cholangiocyte), and hepatic artery. Oxygenated blood from the hepatic artery and portal vein mixes and flows through the hepatic sinusoids to the central vein, which is zone 3. Spaces between hepatocytes form the bile canaliculi, which transport bile excreted from the hepatocytes in the opposite direction of blood flow to bile ducts. The interface between the end of the bile canaliculus and the start of the bile duct is known as the Canal of Hering. Right Image: The bile flows down through the ducts that grow in size and join together to form a branching network that ends in the common bile duct and the gallbladder, where bile is stored.

1.2.1 Physiology and Function of Cholangiocytes

Cholangiocytes are a highly dynamic, heterogeneous population of epithelial cells lining the three-dimensional network of bile ducts known as the biliary tree. Cholangiocytes differ in size, small cholangiocytes and large cholangiocytes, as well morphology that varies between the sizes: flattened or cuboidal small cholangiocytes less than 15 µm in diameter are in small sized, often in terminal ductules and the Canal of Hering, and large columnar cholangiocytes greater than 15 µm in diameter are in large bile ducts (97-103). Small cholangiocytes also have a greater nuclear-to-cytoplasmic ratio than large cholangiocytes, which suggests small cholangiocytes may be less differentiated and have greater plasticity compared to large cholangiocytes (99, 104, 105). These differences compared to larger, more differentiated cholangiocyte implicate small cholangiocytes as a potential functional hepatobiliary progenitor cell population (105, 106).

However, small cholangiocytes' role as a hepatobiliary progenitor cell population has yet to determined experimentally.

Regardless of their size, all cholangiocytes perform reabsorptive and secretory processes on the bile, which significantly modifies the volume and composition of the bile (105, 107). After a meal secretin is released, and it interacts with its G protein-coupled receptor localized on basolateral membrane of cholangiocytes, inducing an increase in intracellular cAMP levels (108-111). The elevated cAMP subsequently stimulates the opening of cystic fibrosis transmembrane conductance regulator (CFTR), which activates the Cl^-/ HCO_3^- anion exchanger 2 (AE2) causing the release of Cl^- and HCO_3^- into the bile ducts (107, 109, 112, 113). In addition, transmembrane protein 16F (TMEM16A), a Ca^{2+}-activated Cl^- channel, can also promote HCO_3^- efflux (110, 114, 115). Cholangiocytes also release ATP, which stimulates activation of Cl^- channels and increases in Ca^{2+} concentration (116, 117). Biliary HCO_3^- release drives the movement of water through water channel aquaporin 1 (AQP1), resulting in increased biliary volume and enhanced choleresis (109, 118, 119). The maintenance of bile pH and volume through HCO_3^- and water release is very important as it creates an alkaline barrier, which prevents toxic bile acid accumulation and renders bile acids polar, de-protonated and membrane impermeable (120-122).

Cholangiocytes also modify bile through the absorption of bile acids, glucose, amino acids and ions. Bile acids, which are steroid acids, exist as either a free, unconjugated acids or acids conjugated to taurine or glycine. Unconjugated bile salts passively diffuse into cholangiocytes and are returned to hepatocytes through cholehepatic shunting (123, 124). Conjugated bile acids are absorbed from the bile through apical sodium-dependent bile salt transporter (ASBT) (125). Cholangiocyte express multidrug resistance protein 3 (MRP3) and multidrug resistance protein 4 (MRP4), which efflux organic ions from the basolateral membrane (105, 126). Cholangiocytes

also express multidrug resistance 1 (MDR1), and Mdr1a in mice, which are ATP-dependent efflux pumps with extensive substrate specificity, including glucocorticoids, lipophilic cytotoxic drugs, peptide antibiotics, and Ca+2 channel blockers (105, 127). However, in cholangiocytes MDR1/Mdr1a are believed to prevent the accumulation of organic cations in cholangiocytes via the excretion of them back into bile (105). Therefore, cholangiocytes play a vital role in both the modification of bile composition and bile flow.

1.2.2 Cholangiocytes in Development

Around E13, bipotential hepatoblasts begin to differentiate towards mature hepatocytes and cholangiocytes (128). By E15.5 the ductal plate begins to form as hepatoblasts with a cholangiocyte-like phenotype near the portal mesenchyme coalesce (129). The ductal plate will eventually give rise to primitive ductal structures that become the intrahepatic bile ducts. The complete adoption of hepatoblasts to a cholangiocyte phenotype is orchestrated through endothelial and mesenchymal cells within the portal tract expressing gradients of developmental morphogens such as Wnt/β-catenin, Notch, transforming growth factor-β (TGFβ) and fibroblast growth factor (FGF) (130-134). Interestingly, much like liver development, Wnt/β-catenin signaling is also required for bile duct development. Jagged1, a cell surface Notch ligand, also plays an important role in bile duct formation through its effects on both cell differentiation and tubulogenesis of bile ducts (129, 135, 136).

1.2.3 Bile Acid Synthesis and Transport in the Liver

Bile acids are important for nutrient absorption in the intestines and biliary secretion of lipids, toxic metabolites, and xenobiotics. Synthesized in hepatocytes by the cytochrome P450 (Cyp) enzymes, Cyp7a1 of the classic bile acid synthesis pathway and Cyp27 of the alternative synthesis pathway, bile acids are the end products of cholesterol catabolism (94, 137, 138). The major primary bile acids produced through these processes are cholic acid (CA) and chenodeoxycholic acid (CDCA), which are then conjugated with taurine or glycine rendering them more soluble, less cytotoxic, and easily secreted (139-141). Bile acids are excreted by the hepatocytes into the biliary canaliculi by apical transporters such as multidrug resistance-associated protein-2 (MRP2) and the bile salt export pump (BSEP) (140). Once secreted the bile makes its way down through the bile ducts to the intestines to aid in nutrient absorption. In the intestines, about 15% of the CA and CDCA are converted to secondary bile acids, deoxycholic acid (DCA) and lithocholic acid (LCA) (137, 142). All bile acids, both primary and secondary, are recycled through a process called enterohepatic circulation, during which the bile acids are reabsorbed through the intestines, returned to the liver via portal blood circulation and basolateral uptake transporters, and reconjugated (137, 140, 143). This enterohepatic circulation of bile acids is an important process as it helps create a feedback control for bile acid synthesis (137, 140, 143). The liver is also very proficient in monitoring and maintaining hepatic bile acid levels; when bile acid levels increase, compensatory responses are activated such as decreased bile acid synthesis and uptake, and upregulation of bile acid metabolism and basolateral membrane export pumps (137, 140, 142, 144, 145).

1.3 Biliary Injury and Regeneration

1.3.1 Intrahepatic Cholestatic Liver Disease

Intrahepatic cholestatic liver diseases are often chronic, progressive diseases of the biliary tree. They can be either acquired or genetic, observed across all age groups, and have a variety of clinical features with a high degree of variability in prognosis and presentation between the diseases (146-148). The primary target of these diseases is typically the cholangiocyte cell population. Though cholestasis is not a disease itself, it is the common symptom of intrahepatic cholestatic liver diseases. Despite the variety of diseases all are diagnosed, both clinically and biochemically, through varying degrees of jaundice, pruritus, and elevated levels of serum alkaline phosphatase (ALP), γ-glutamyl transpeptidase (GGT), conjugated bilirubin, bile acids, and cholesterol (146-149). Despite our advances in diagnosing and understanding these diseases, unfortunately, to date there are no proven therapeutic treatments for the majority of these diseases.

1.3.1.1 Primary Sclerosing Cholangitis

One intrahepatic cholestatic disease of interest is primary sclerosing cholangitis (PSC). PSC is a rare, chronic, idiopathic, heterogeneous, cholestatic liver disease characterized histologically and biochemically by cholestasis and persistent, progressive biliary fibrosis and inflammation. Typically in PSC obliterative fibrosis and chronic inflammation of the intrahepatic bile duct leads to multifocal bile duct strictures, which causes bile stasis and chronic fibrosis (150-153). These symptoms will continue to progress until patients with PSC develop cirrhosis, end-stage liver disease, and cholangiocarcinoma (150-153). Diagnostic criteria for PSC include increased levels of serum ALP persisting more than 6 months, cholangiographic findings of

multifocal bile-duct strictures, which are both used to monitor disease progression, and the exclusion of causes of secondary sclerosing cholangitis (154, 155). In general, PSC is slowly progressive with outcomes varying patient to patient. Currently there are no effective medical treatments for patients with PSC; however, if patients reach end-stage liver disease and they are eligible, they can receive a liver transplant (153, 156). Unfortunately, for patients who do require and receive a liver transplant, transplantation is not a cure, since up to 25% of patients will have recurrence of PSC within 10 years of receiving transplantation (155, 157-160). Therefore, an effective medical treatment for PSC that does not require transplantation would revolutionize the way these patients are treated.

1.3.2 Ductular Proliferation in Cholestasis

Cholangiocyte proliferation that occurs after biliary injury is categorized into three groups: "typical" proliferation, "atypical" proliferation, and oval cell proliferation. Of these types of proliferation, typical and atypical proliferation are known to take place during and after cholestatic injury. Typical cholangiocyte proliferation is confined to the portal areas and is a hyperplastic reaction, which induces an increase in the number of intrahepatic bile ducts (161, 162). During typical proliferation, the proliferating cholangiocytes create tubular structures with well-defined lumens, which form a three-dimensional network contributing to the bile ducts (161-164). This type of proliferation is observed in rodent models when exposed to α-naphthylisothiocyanate (ANIT), carbon tetrachloride (CCl_4), or lithocholic acid (LCA) in diet form, or after bile duct ligation, as well as in human patients during the early stages of chronic cholestatic liver disease and after acute obstructive cholestasis (163-171).

The second type of proliferation, atypical cholangiocyte proliferation, is irregular proliferation of the intrahepatic bile ducts which spread into the periportal and parenchymal regions of the liver (161, 162). Bile ducts formed through atypical proliferation are irregular and tortuous in shape, lack a well-defined lumen, and often functionally inefficient (161, 163, 172). This type of proliferation occurs in rat and mice models after chronic exposure to xenobiotics or chemicals such as 3,5-diethoxycarbonyl-1,4-dihydrocollidine (DDC), and is also commonly seen in human patients with prolonged cholestatic liver diseases such as primary biliary cholangitis (PBC) or PSC (163, 173, 174). Atypical proliferation can also involve an oval cell response, which is characterized by hyperplasia of bipotential cells with characteristics of both cholangiocytes and hepatocytes (175-177). Oval cell involvement in atypical proliferation has been observed in rodent models after chronic administration of DDC, D-galactosamine, and CCl_4 and in human patients with alcoholic liver diseases, long chronic extrahepatic biliary obstruction, massive hepatic necrosis, and chronic cholestatic liver diseases, such as PSC and PBC (163, 170, 172, 178-180).

Interestingly the role of the atypical ductules in cholangiopathies is controversial. During the early stages of injury, atypically proliferating cholangiocytes may contribute to hepatobiliary repair or protect against biliary insult (148). However, over time and as injury progresses proliferating atypical ductules can also release profibrotic and proinflammatory signals, which activate cells responsible for extracellular matrix deposition (181-183).

1.3.2.1 Wnt Driven Cholangiocyte Proliferation During Cholestasis

Wnt signaling is known to play many important roles in the liver and bile ducts, and some studies have found that specific may play certain roles during cholestatic injury. These study found that after DDC exposure or BDL, WT have increased expression of Wnt7a, Wnt7b and Wnt10a in EpCAM positive cells in the portal triad region of the liver compared to WT mice on normal diet

(69, 78). Wntless KO mice placed on DDC diet also had more hepatic damage, less ductular proliferation, and decreased survival compared to WT mice, which indicate these Wnts may play a protective role during cholestatic injury (69). Of these three Wnts, it was determined that Wnt7b and Wnt10a induce the proliferation of cholangiocytes in an autocrine fashion (69). These findings suggested Wnt7b and Wnt10a are a necessary signaling mechanism to promote cholangiocyte proliferation in cholestatic liver injury regardless of injury origin. These roles for Wnt7b and Wnt10a are not unheard of, as both Wnts are known to be involved in proliferation, regeneration, and self-renewal in cell types outside of the liver (184-186).

1.3.3 Activated Cholangiocytes in Inflammation and Fibrosis

Often during intrahepatic cholestatic disease, cholangiocytes are activated through a variety of ways such as infections, xenobiotics, ischemia, and cholestasis (187, 188). However, in many cholangiopathies, including PSC, what activates cholangiocytes remains unknown. When a cholangiocyte is activated its proinflammatory and profibrotic secretions increase and along with its proliferation (182, 189). Activated cholangiocytes also recruit vascular, mesenchymal, and immune cells and facilitate the crosstalk between them, and if cholangiocyte activation becomes chronic biliary fibrosis and cholangiocarcinoma can develop (190-192).

Recent findings indicate that this activated, secretory cholangiocyte phenotype is a result of cellular senescence prompted by stress and injury, which results in irreversible proliferative arrest (193-195). While in this state senescent cells are metabolically active, transitioning to cytokine and chemokine hypersecretory state, known as the senescence-associated secretory phenotype (SASP) (196, 197). SASP has been identified to be an important mechanism during

cholangiopathy development and progression, including PSC's development and progression (195, 198, 199).

1.3.4 Ductular Reaction

During many cholangiopathies there is an expansion of cells that express cholangiocyte markers, believed to be either activated cholangiocytes or hepatic progenitor cells, from the periportal region and into the surrounding parenchyma. This cellular expansion is called ductular reaction and has been defined as "a reaction of ductular phenotype, possibly but not necessarily of ductular origin"(175). Though this definition leaves the cellular origin for ductular reaction up for debate, the activation of the ductular reaction is thought to be instigated by the impairment of cholangiocytes' and hepatocytes' ability to regenerate during liver injury. Ductular reaction is generally associated with infiltration of inflammatory cells, activation of myofibroblasts, and matrix deposition, and unless reversed, can lead to periportal fibrosis, ductopenia, and eventually biliary cirrhosis (200, 201). Ductular reaction is pathologically recognized as bile duct proliferation or hyperplasia and is identified in and often a hallmark of biliary disorders such as PSC, PBC, and biliary atresia (BA) (148, 175, 201). Interestingly, despite various liver conditions presenting with ductular reaction, the way ductular reaction presents differs depending on the disease.

A recent study characterized ductular reaction in PSC and PBC, and they found that while ductular reaction is a prognostic marker for both conditions, the phenotype and activated signaling pathways different between the two diseases (202). PSC expressed lower levels of laminin and neurogenic locus notch homolog protein 1, but higher levels of wingless-related integration site (WNT) family pathway components, in the progenitor cell niche compared to PBC (202). This

increased expression of Wnt family pathway components during PSC, specifically in the progenitor cell niche, further indicates that Wnt signaling may play a role in cholangiocyte activation and proliferation or possible hepatocyte transdifferentiation. Another study used laser capture microdissection to isolate cells of the ductular reaction from patients with PSC or hepatitis C virus (HCV), then used high throughput RNA sequencing to analyze the differences between the cells (203). It was found that HCV has a more neo-angiogenesis signature and PSC has a more oxidative stress-related and pro-inflammatory gene expression signature (203).

1.3.5 Murine Models of Primary Sclerosing Cholangitis

Due to the poor understanding of PSC's pathogenesis, well-characterized animal models of PSC are invaluable. Not only do these models provide opportunities to develop and understand novel pathogenetic concepts,s they also offer opportunities to study new treatment strategies. Currently there are a variety of rodent models of PSC that utilize gene knockout, chemicals, infectious agents, or a multitude of other methods (204).

1.3.5.1 DDC as a Model of PSC

A common chemical induced method of studying PSC is the 3,5-diethoxycarbonyl-1,4-dihydrocollidine (DDC) diet model. DDC disrupts heme biosynthesis through the inhibition ferrochelatase activity (Figure 5A), which causes an excess of porphyrin to build up in the liver (205). This porphyrin is then exported out of the hepatocytes into the bile ducts, where it forms porphyrin pigment plugs in the biliary tract obstructing the bile duct and leading to a multitude of PSC like symptoms. After DDC exposure mice develop bile duct injury, cholangiocytes with a reactive phenotype, and serum markers similar to those of cholestasis (173, 206, 207). The livers

develop pericholangitis, onion skin-type periductal fibrosis, ductular reaction, bile regurgitation, and consequently portal-portal bridging, all of which are common histological markers of PSC in patients (Figure 5B) (173, 204). Finally, mice exposed to DDC diet also have a down-regulation of Mrp2, impaired glutathione excretion, and segmental bile duct obstruction (173). All of these results are hallmarks for PSC in patients and are achieved within 4 weeks of initial diet exposure, which makes DDC diet an ideal rodent model for studying PSC.

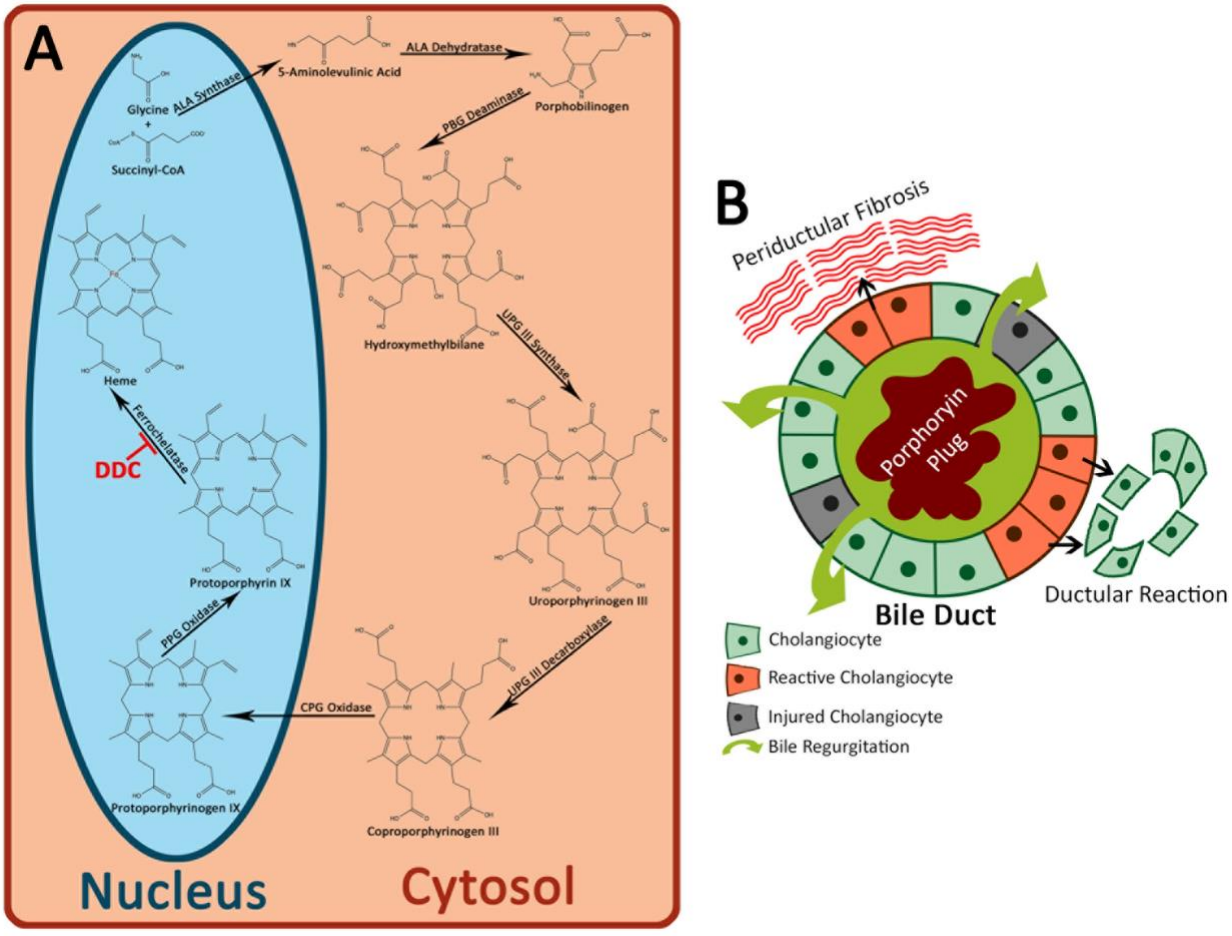

Figure 5. How DDC works as a model of PSC

(A) DDC inhibits ferrochelatase from completing the final step of the heme biosynthesis pathway, which results in an accumulation of porphyrin in the liver. (B) Porphyrin is exported from the hepatocytes into the bile ducts which accumulates and creates porphyrin plugs that obstruct the bile ducts. This obstruction results in injury to the bile duct, bile regurgitation, periductular fibrosis, and ductular reaction.

1.3.5.2 Mdr2 KO as a Model of PSC

A common genetic knockout model for studying PSC is the multidrug resistance gene (*Mdr2*) (*Abcb4*) knockout (KO) mice (Mdr2($^{-/-}$)). Mdr2 is flippase that transports phosphatidylcholine from the hepatocytes into the biliary canaliculi; Mdr2 KO mice have a genetic disruption of the *Mdr2* gene, causing a complete absence of phosphatidylcholine from bile (208-210). Phosphatidylcholine is important to bile as it reduces the cellular toxicity of bile acids (211). Therefore, Mdr2 KO mice have more toxic bile compared to their WT counterparts and the toxic bile is what causes a PSC phenotype (212, 213). Mdr2 KO mice develop extrahepatic and intrahepatic biliary strictures, onion-skin-type periductal fibrosis, and focal fibrous obliteration of bile ducts, all of which are symptoms seen in PSC patients (212, 214, 215). Interestingly as these mice age their symptoms worsen, which makes PSC in Mdr2$^{-/-}$ mice a multistep process. Ultimately the mice develop a PSC phenotype that involves regurgitation of bile from leaky ducts into the portal tracts, which leads to the induction of periductal inflammation, followed by the activation of periductal fibrogenesis (214). All of these phenotypes then go onto to cause obliterative cholangitis that is owed to atrophy and death of bile duct epithelial cells, similar to PSC patients (214). Mdr2 KO mice also start to develop all of these symptoms as early as 2 weeks old and they become more pronounced with age, therefore the Mdr2 KO model is a very quick and effective model to study PSC (204, 212, 214).

1.4 Hepatocyte-to-Cholangiocyte Transdifferentiation

The liver and the bile ducts can regenerate through two means: proliferation and transdifferentiation (Figure 6). This transdifferentiation typically only occurs during extreme hepatic or biliary injury. During this process, hepatocytes and cholangiocytes function as a type of "facultative stem cells," and undergo reprogramming from one cell type to the other rescuing the failed regeneration (216, 217). In rodent models, mature hepatocytes transdifferentiate into biliary cells when there is extensive injury and resident cholangiocytes are unable to proliferate to adequately compensate for the injury (218-221).

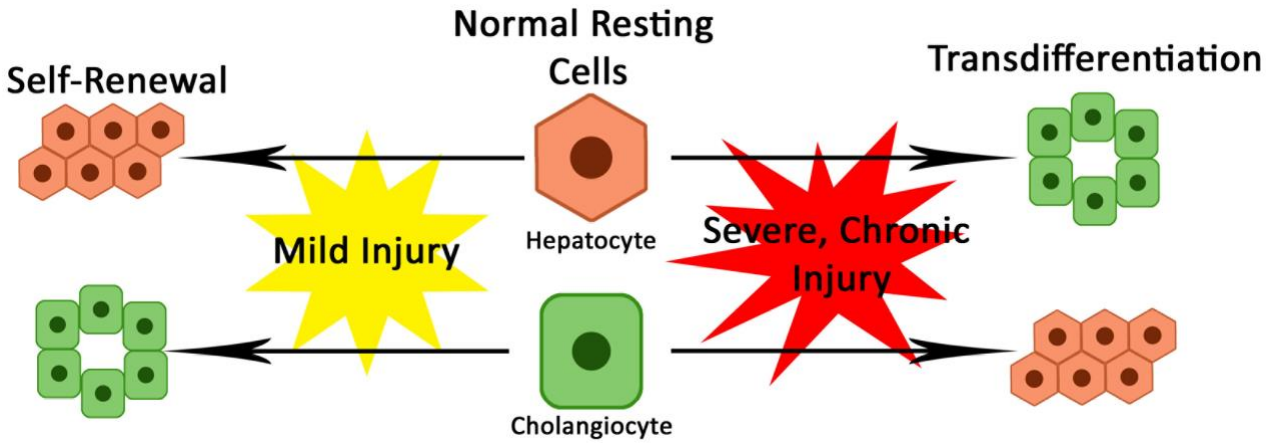

Figure 6. The type of injury drives the type of repair
During mild or acute injury to the liver hepatocytes and cholangiocytes renew their respective cells populations through proliferation. However, during severe or chronic injury hepatocytes and cholangiocytes are able to transdifferentiate into the other cell type to help alleviate the injury.

In vitro studies using hepatic organoids derived from rats have been used to demonstrate hepatocyte-to-cholangiocyte transdifferentiation (222, 223) In one organoid study rats, which do not express Dipeptidyl Peptidase IV (DPPIV), were given retrorsine, which blocks hepatocyte proliferation, and transplanted with DPPIV-positive hepatocytes, resulting in livers with colonies of donor-derived DPPIV-positive hepatocytes. Organoid cultures were then derived from these

hybrid livers and cells resembling cholangiocytes were observed on the surface of the organoid culture (223). These cholangiocytes were also found to be DPPIV-positive, indicating they originated from hepatocyte (223). In another study, rat hepatocytes were cultured in medias containing various growth factors including hepatocyte growth factor (HGF), epidermal growth factor (EGF), vascular endothelial growth factor (VEGF), platelet-derived growth factor (PDGF), stem cell factor (SCF), macrophage-stimulating protein (MSP), fibroblast growth factor-a (FGF-a), fibroblast growth factor-b (FGF-b), and fibroblast growth factor-8b (FGF-8b) (222). Through this study it was determined that HGF and EGF are required to induce the phenotypic change of hepatocytes to cholangiocytes (222).

This transdifferentiation has also been observed *in vivo*. By utilizing stain-tagging, hepatocyte-derived cholangiocyte were found in rats under conditions in which the biliary epithelium is incapable of repair due to toxic injury (220, 223). Genetic mouse models and lineage tracing has also shown that hepatocytes are capable of transdifferentiating to cholangiocytes under conditions that cause biliary toxicity and chronic liver injury (221, 224-226). Additionally, and most importantly, hepatocyte reprogramming has also been reported in human liver diseases. Hepatocytes from both pediatric and adult cholangiopathy patients have been observed to express the ductal marker OV-6 (227, 228). Additionally, hepatocytes express cholangiocyte-specific cytokeratins in patients with cholestasis (229-231). Finally patients with chronic biliary disease have been shown to have hepatocytes expressing biliary transcription factors (222, 224). Combined these results suggest that during biliary injury the number of hepatocytes expressing biliary markers increases over time; therefore, as cholestasis progresses, more and more hepatocytes compensate for the damage to and loss of the biliary epithelium.

1.4.1 Canonical Wnt Signaling in Hepatocyte-to-Cholangiocyte Transdifferentiation

Though previous studies have shown the importance of HGF and EGF to hepatocyte-to-cholangiocyte transdifferentiation, the role that Wnt signaling plays during this process has not been extensively studied. The same study determined that HGF and EGF are required for hepatocyte transdifferentiation in organoid culture also found that β-catenin and its downstream targets are upregulated in hepatic organoid cultures under conditions that promote hepatocyte reprogramming (222). This finding implicates a role for β-catenin in this transdifferentiation process. Wnt7A, which is expressed by cholangiocytes during cholestasis, has also been identified as a regulator of hepatocyte reprogramming (69). *In vitro*, Wnt7A was found to activate β-catenin and also induce hepatocytes to express biliary markers, such as SRY-related HMG box transcription factor 9 (Sox9) and epithelial cell adhesion molecule (EpCAM) (69). It has also been noted that mice transgenic (TG) for a non-degradable S45D-mutated β-catenin in the liver showed an increased number of hepatocytes positive for A6, a biliary marker, compared to WT when subjected to DDC diet and cholestatic injury (180). This finding also coincided with a decreased in serum markers of biliary injury, alkaline phosphatase (ALP) and bilirubin levels, in S45D TG mice compared to WT mice exposed to DDC diet (180). The S45D TG mice were also found to have more hepatocytes expressing cholangiocyte markers, such as Sox9, after DDC exposed compared WT on DDC diet (180). Therefore, canonical Wnt signaling may play an important role in hepatocyte-to-cholangiocyte transdifferentiation.

1.4.2 Fate of Cholangiocyte-Like-Hepatocytes

Studies have shown that hepatocyte-derived cholangiocytes incorporate into biliary ductules, but no studies have shown the pattern through which these cells integrate (221, 224, 225, 232). One possible method of incorporation is that hepatocytes surrounding dying and damaged cholangiocytes convert to replace injured biliary epithelium. If this occurs ducts would become a mosaic of hepatocyte-derived and native cholangiocytes (Figure 7A). The other possible method of incorporation is in order to expedite the removal of bile from the parenchyma hepatocytes transdifferentiate to form de novo ducts. If this occurs whole ducts would be comprised solely of hepatocyte-derived cholangiocytes (Figure 7B). Therefore, a study that determines the pattern of hepatocyte-derived cholangiocytes incorporation into bile ducts could provide unique insights into biliary repair.

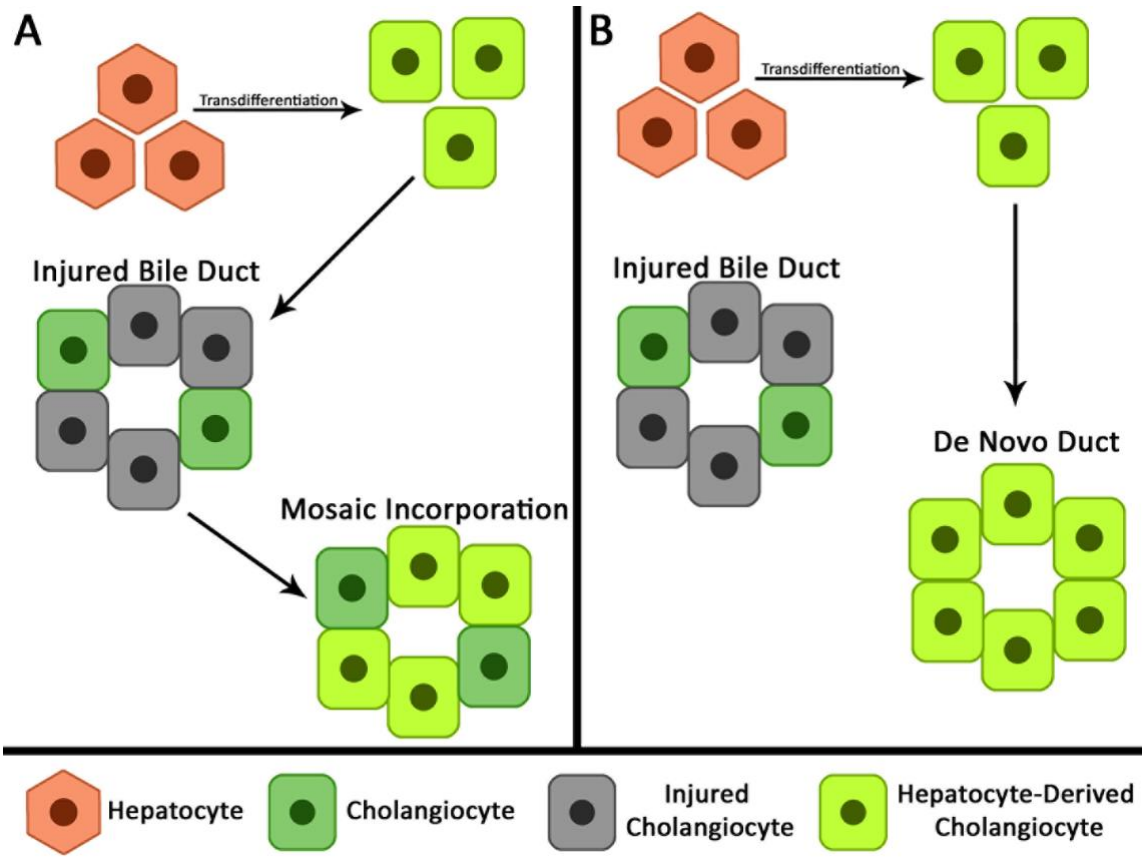

Figure 7. Hepatocyte-derived cholangiocyte incorporations into bile ducts
(A) Hepatocytes transdifferentiate into cholangiocytes and incorporate into the injured bile duct to alleviate biliary injury creating a bile duct that is a mosaic of native cholangiocytes and hepatocyte-derived cholangiocytes. (B) Hepatocytes transdifferentiate into cholangiocytes then form de novo ducts to replace the injured bile duct.

Similarly, the functional capacity of these transdifferentiated cells has yet to be compared to native cholangiocytes. It is likely that once these cells have incorporated into ducts, they perform most functions of native cholangiocytes. However, they may perform with less efficiency depending on the type of selective pressure that initiated the transdifferentiation. If there is sufficient selective pressure, such as bile duct paucity, hepatocytes are known to transdifferentiate into mature cholangiocytes that form functional bile ducts (232). However, it has also been shown under circumstances when injury is reserved reprogrammed cells can revert back to hepatocytes (225). This conversion and reversion of hepatocytes is more consistent with metaplasia than it is transdifferentiation. Finally, hepatocytes expressing biliary markers may never fully convert into a cholangiocyte (233, 234). Instead, these cells exist in a biphenotypic intermediate state. These

cells may be able to perform some cholangiocyte functions, such as forming intermediate bile channels and bile modification, which helps to prevent injury progression. This biphenotypic cell type is also beneficial because these cells are able to evade cholangiocyte-directed immune injury.

1.4.3 GC-1 as a Potential Driver of Hepatocyte-to-Cholangiocyte Transdifferentiation

Thyroid hormones, such as triiodothyronine (T3), is a commonly used therapy in patients which regulates a wide range of genes and affects many physiological processes in the body, including heart rate, metabolism, growth and development, and body temperature (235-237). In rodent livers, T3 increases hepatocyte proliferation after partial hepatectomy in a β-catenin dependent manner through interaction with thyroid hormone receptor β (TRβ) (29, 30, 238, 239). However, T3 is not liver specific as it is also known to have mitogenic effects in other organs such as the heart, and pancreas (239, 240). Luckily GC-1, or sobetirome, is a liver specific thyroid hormone which recapitulates T3's β-catenin–dependent hepatocyte proliferation after partial hepatectomy (241).

Unfortunately, GC-1 and other thyroid hormones have not been well studied in the context of cholestatic disease. However, GC-1 could be a promising therapeutic for PSC patients. This is because GC-1 induces hepatocyte proliferation through a β-catenin activity, which has also been implicated as an important signaling pathway during hepatocyte transdifferentiation. During cholestatic injury, with the proper selective pressures, GC-1 could be used to induce β-catenin dependent hepatocyte-to-cholangiocyte transdifferentiation, since GC-1 is known to activate β-catenin. Therefore, a study determining the therapeutic effects GC-1 has on biliary injury and hepatocyte-to-cholangiocyte transdifferentiation during cholestasis could be a worthwhile endeavor.

2.0 The Thyromimetic Sobetirome (GC-1) Alters Bile Acid Metabolism in a Mouse Model of Hepatic Cholestasis

In this section we characterize the exposure of mice lacking Mdr2 to the thyromimetic sobetirome (GC-1) in diet form. We predict that mice lacking Mdr2 will have increased β-catenin activity inducing proliferation and hepatocyte-to-cholangiocyte transdifferentiation after GC-1 exposure, and we will discuss our results and interpretations in detail. This study was published in The American Journal of Pathology PMID: 32205094 (242). As first author, the publisher Elsevier has granted full permission to reuse the manuscript in this dissertation.

2.1 Paper Summary

Chronic cholestasis results from bile secretory defects or impaired bile flow with few effective medical therapies available. Thyroid hormone triiodothyronine and synthetic thyroid hormone receptor agonists, such as sobetirome (GC-1), are known to impact lipid and bile acid (BA) metabolism and induce hepatocyte proliferation downstream of Wnt/β-catenin signaling after surgical resection; however, these drugs have yet to be studied as potential therapeutics for cholestatic liver disease. Herein, GC-1 was administered to ATP binding cassette subfamily B member 4 (*Abcb4*$^{-/-}$; Mdr2$^{-/-}$) knockout (KO) mice, a sclerosing cholangitis model. KO mice fed GC-1 diet for 2 and 4 weeks had decreased serum alkaline phosphatase, but increased serum transaminases compared with KO alone. KO mice on GC-1 also had higher levels of total liver BA due to alterations in expression of BA detoxification, transport, and synthesis genes, with the

net result being retention of BA in the hepatocytes. Interestingly, GC-1 does not induce hepatocyte proliferation or Wnt/β-catenin signaling in KO mice, likely a result of decreased thyroid hormone receptor β expression without Mdr2. Therefore, although GC-1 treatment induces a mild protection against biliary injury in the early stages of treatment, it comes at the expense of hepatocyte injury and is suboptimal because of lower expression of thyroid hormone receptor β. Thus, thyromimetics may have limited therapeutic benefits in treating cholestatic liver disease.

2.2 Background

Many chronic liver diseases have few to no medical therapies that are capable of halting or reversing disease progression, and the only life-extending treatment is orthotopic liver transplantation. Primary sclerosing cholangitis (PSC), a chronic cholestatic liver disease of unknown etiology, is one such example. Patients with PSC have bile duct inflammation and fibrosis, which results in end-stage liver disease and reduced life expectancy (243, 244). A significant number (40%) of PSC patients will ultimately require liver transplant and up to 25% of patients who receive liver transplant will have recurrent PSC (151). Therefore, an effective therapeutic strategy to treat PSC is a major unmet clinical need.

ATP binding cassette subfamily B member 4 (*Abcb4*$^{-/-}$; Mdr2$^{-/-}$) gene knockout (KO) mice spontaneously develop sclerosing cholangitis characterized by pericholangitis, ductular proliferation, and onion skin-type periductal fibrosis (214). This phenotype is due to lack of the Mdr2 gene, a canalicular flippase that transports phospholipids into bile (208). The loss of protective phospholipids in the KO leads to increased concentrations of free toxic bile acids (BAs), which damages cholangiocytes and causes bile to leak into the parenchyma (204). Because the

resulting liver injury resembles PSC, these mice have long been used to study the pathogenesis and signaling pathways involved in this disease, as well as to test potential therapeutics.

The Wnt/β-catenin signaling pathway has a well-described role in liver physiology and pathology, and its modulation also alters the progression of cholestatic liver disease (245). Loss or inhibition of β-catenin (alias catenin β 1) leads to improved outcomes after bile duct ligation and 5-diethoxycarbonyl-1,4-dihydrocollidine, two commonly used animal models of cholestasis (246, 247). However, it was recently shown that knockdown of β-catenin in Mdr2 KO leads to increased inflammation, oxidative stress, fibrosis, and impaired hepatocyte proliferation (44). In this case, β-catenin is essential in maintaining homeostasis in the absence of Mdr2, and its loss results in decompensation and increased injury. Thus, in some types of cholestatic conditions, such as those modeled by the Mdr2 KO mouse, activation of β-catenin may be advantageous by balancing ongoing injury with a robust regenerative response.

Thyroid hormones, such as triiodothyronine (T3), are known to have mitogenic effects in many organs, such as the liver, heart, and pancreas (239, 240). In hepatocytes, T3 increases proliferation in mice through interaction with thyroid hormone receptor β (alias TRβ) (238, 239). This occurs in a β-catenin–dependent manner via the cAMP-dependent protein kinase A pathway, which, in turn, leads to phosphorylation of β-catenin at Ser675 and subsequent activation (29, 30). However, because T3 is not liver specific, use of a selective TRβ agonist, such as GC-1 or sobetirome, is preferable because of its lack of off-target effects (241). GC-1 is also well studied in the liver and has been shown to recapitulate the mitogenic effects of T3, stimulating β-catenin–dependent hepatocyte proliferation after partial hepatectomy (29). However, whether these drugs can induce proliferation and repair during cholestatic liver disease is unknown.

In this study, wild-type (WT) and Mdr2 KO mice were treated with a GC-1–containing diet to activate β-catenin in hepatocytes. It was hypothesized that activation of β-catenin in this model of cholestasis would induce compensatory proliferation that may provide protection against injury. The study results show that biliary injury is transiently decreased in Mdr2 KO mice on GC-1 diet compared with Mdr2 KO mice on normal diet. This decrease in biliary injury is likely due to a lack of BA export by the hepatocytes, which spares cholangiocytes but leads to increased hepatic injury due to toxic BA retention. Also, although hepatocyte proliferation is increased in Mdr2 KO mice, it is not further induced by GC-1, nor is β-catenin activated in KO with GC-1. This is because KO have decreased responsiveness to GC-1 because of lesser expression of thyroid receptor β. This study shows that dysregulation of receptor targets during chronic liver disease may affect drug efficacy, and that caution should be used when considering the use of repurposed drugs to treat cholestatic liver diseases.

2.3 Materials and Methods

2.3.1 Animal Model

All animal studies were performed in accordance with the guidelines of the Institutional Animal Use and Care Committee at the University of Pittsburgh School of Medicine (Pittsburgh, PA) and the NIH (Bethesda, MD; protocol number 17071066). Five-week–old Mdr2 ($^{-/-}$) KO mice in an FVB/NJ background (Jackson Laboratory, Bar Harbor, ME; stock number 002539) or WT littermate controls were fed standard mouse chow or GC-1/sobetirome-supplemented diet (5 mg/kg of diet, GC-1/sobetirome purchased from MedChem Express, Monmouth Junction, NJ; diet

from Animal Specialties and Provisions LLC, Quakertown, PA) for up to 4 weeks. After the diet course was complete, mice were sacrificed, and blood serum and livers were collected. Livers were sectioned, fixed in 10% formalin, and processed for paraffin embedding or frozen in liquid nitrogen and stored at −80°C. For baseline, n = 3 mice per genotype. For 1-week GC-1 or normal diet, n = 4 WT, n = 3 WT + GC-1, n = 4 KO, and n = 3 KO + GC-1. For 2-week GC-1 or normal diet, n = 5 WT, n = 8 WT + GC-1, n = 6 KO, and n = 7 KO + GC-1. For 4-week GC-1 or normal diet, n = 8 WT, n = 7 WT + GC-1, n = 9 KO, and n = 8 KO + GC-1. For 12-week GC-1 or normal diet, n = 4 WT, n = 3 WT + GC-1, n = 4 KO, and n = 3 KO + GC-1.

2.3.2 Serum Biochemistry

At the time of sacrifice, blood was collected and serum was sent to the University of Pittsburgh Medical Center Clinical Chemistry laboratory for biochemical analysis of total and direct bilirubin, alkaline phosphatase (ALP), aspartate aminotransferase, and alanine transaminase.

2.3.3 Immunohistochemical Analysis

Paraffin-embedded liver tissues were divided into sections (4 μm thick). Sections were stained with hematoxylin and eosin or Picro-Sirius Red (Abcam, Cambridge, UK). Immunohistochemistry on paraffin-embedded sections was performed on mouse livers, as described elsewhere (177). Primary antibodies used were anti–sex-determining region Y-box transcription factor 9 (Sox9) antibody (1:100; Abcam), anti–cytokeratin 19 (CK19) antibody (31 μg/mL; TROMA-III-S; Developmental Studies Hybridoma Bank, Iowa City, IA), and proliferating cell nuclear antigen antibody (PC10; 1:4000; Santa Cruz Biotechnology, Dallas, TX). Secondary

antibodies were goat anti-rabbit, goat anti-rat, and donkey anti-goat (Chemicon, Temecula, CA), and were used at 1 to 400, and staining was detected with 3,3′-diaminobenzidine detection systems after incubation with the Avidin-Biotin Complex Kit (Vector Laboratories, Burlingame, CA). Apoptotic nuclei were detected by the terminal deoxynucleotidyl transferase-mediated dUTP nick-end labeling staining using the ApopTag Peroxidase kit (Millipore, Temecula, CA) at the University of Pittsburgh Department of Pathology's core immunohistochemistry laboratory. Images (1280 by 1024 pixels) were taken on an Olympus Provis scope (Olympus America, Center Valley, PA) at the Center for Biological Imaging at the University of Pittsburgh.

Sirius Red images were quantified using ImageJ Fiji version 2.0.0-rc-68/1.521 (NIH; https://imagej.nih.gov/ij) (248). Each image was split into red, green, and blue channels, from which the green channel was selected for optimal separation of staining. The staining was isolated by using threshold setting 0 for the upper level and 127 for the lower level, and the percentage of the stained area to the total image was measured. A total of five images per mouse liver (n = 3 mice) were quantified for each genotype.

CK19 images were quantified by splitting the image into red/green/blue channels with ImageJ Fiji, and then quantifying the blue channel using a threshold setting 0 for the upper level and 63 for the lower level. The percentage of the stained area to the total image was then calculated. A total of five images per mouse liver (n = 3 mice) were quantified for each genotype.

Quantification of proliferating cell nuclear antigen– and terminal deoxynucleotidyl transferase-mediated dUTP nick-end labeling–positive cells was performed by counting the number of positive hepatocytes per ×100 field. A total of five images per mouse liver (n = 3 mice) were quantified for each genotype.

2.3.4 Protein Extraction and Western Blot Analysis

Whole-cell liver lysates were prepared in radioimmunoprecipitation assay buffer containing fresh phosphatase and protease inhibitor cocktails (Sigma Aldrich, St. Louis, MO). Denatured proteins were separated on 10% SDS-PAGE gels and transferred to polyvinylidene difluoride membranes. Membranes were blocked using 5% nonfat dry milk or 5% bovine serum albumin in 0.1% Triton X-100 in Tris-buffered saline at room temperature for 1 hour and incubated at 4°C overnight with primary antibodies (diluted in 3% blocking media). The following primary antibodies were used: glyceraldehyde-3-phosphate dehydrogenase (GAPDH; 1:5000; Invitrogen, Carlsbad, CA), purified mouse anti–β-catenin (1:500; BD Biosciences, San Jose, CA), nonphosphorylated (active) β-catenin (Ser33/37/Thr41) (1:1000; Cell Signaling Technology, Danvers, MA), and phosphorylated β-catenin (Ser675; D2F1; 1:1000; Cell Signaling Technology). Membranes were washed three times for 15 minutes each in Tris-buffered saline before being probed with horseradish peroxidase–conjugated secondary antibodies (1:20,000 diluted in 3% blocking media; Santa Cruz Biotechnology) for 2 hours at room temperature. Membranes were washed three times for 15 minutes each in Tris-buffered saline and visualized using the Enhanced Chemiluminescence System (GE Healthcare, Little Chalfont, UK).

2.3.5 Quantitative Real-Time PCR

Total RNA was isolated from frozen liver tissue using Trizol reagent (Invitrogen). RT-PCR was performed as described elsewhere (177). Real-time PCR was performed on a CFX96 TouchReal-Time PCR Detection System (Bio-Rad Laboratories, Hercules, CA) using SYBR Green (Thermo Fisher Scientific, Pittsburgh, PA). Changes in target mRNA were normalized to

GAPDH mRNA for each sample, and P value is presented as fold change over the average from three normal livers. Three samples per each condition were assayed in triplicate. Primer sequences are provided in Table 1.

Table 1. List of Primers Used for Quantitative RT-PCR Analysis in Section 2.0

BSEP, bile salt export pump; CAR, constitutive androstane receptor; CK19, cytokeratin 19; Cyp, cytochrome P450; FXR, farnesoid X receptor; HNF1β, hepatocyte nuclear factor 1 homeobox B; NTCP, sodium-taurocholate cotransporting polypeptide; PXR, pregnane X receptor; SHP, small heterodimer partner; Slco1b2, solute carrier organic anion transporter family, member 1b2; MRP, multidrug resistance protein; Sox9, sex-determining region Y-box transcription factor 9; TRβ, thyroid hormone receptor β.

Primer name	Sequence
PXR (forward)	5′-CCCATCAACGTAGAGGAGGA-3′
PXR (reverse)	5′-GGGGGTTGGTAGTTCCAGAT-3′
SHP (forward)	5′-TCTGCAGGTCGTCCGACTATTC-3′
SHP (reverse)	5′-AGGCAGTGGCTGTGAGATGC-3′
FXR (forward)	5′-CTTGATGTGCTACAAAAGCTGTG-3′
FXR (reverse)	5′-ACTCTCCAAGACATCAGCATCTC-3′
CAR (forward)	5′-GGAGGACCAGATCTCCCTTC-3′
CAR (reverse)	5′-ATTTCATTGCCACTCCCAAG-3′
NTCP (forward)	5′-CACCATGGAGTTCAGCAAGA-3′
NTCP (reverse)	5′-AGCACTGAGGGGCATGATAC-3′
Slco1b2 (forward)	5′-GATCCTTCACTTACCTGTTCAA-3′
Slco1b2 (reverse)	5′-CCTAAAAACATTCCACTTGCCATA-3′
MRP2 (forward)	5′-GCTTCCCATGGTGATCTCTT-3′
MRP2 (reverse)	5′-ATCATCGCTTCCCAGGTACT-3′
MRP3 (forward)	5′-TGAGATCGTCATTGATGGGC-3′
MRP3 (reverse)	5′-AGCTGCGAGCGCAGGTCG-3′
MRP4 (forward)	5′-TTAGATGGGCCTCTGGTTCT-3′
MRP4 (reverse)	5′-GCCCACAATTCCAACCTTT-3′
BSEP (forward)	5′-ACACCATTGTATGGATCAACAGC-3′
BSEP (reverse)	5′-CACCAACTCCTGCGTAGATGC-3′
Cyp7a1 (forward)	5′-TGGGCATCTCAAGCAAACAC-3′
Cyp7a1 (reverse)	5′-TCATTGCTTCAGGGCTCCTG-3′
Cyp3a11 (forward)	5′-CCACCAGTAGCACACTTTCC-3′
Cyp8b1 (forward)	5′-GCCCTTACTCCAAATCCTACCA-3′
Cyp8b1 (reverse)	5′-TCGCACACATGGCTCGAT-3′
Cyp27 (forward)	5′-TGCCTGGGTCGGAGGAT-3′
Cyp27 (reverse)	5′-GAGCCAGGGCAATCTCATACTT-3′
Cyp3a11 (reverse)	5′-TTCCATCTCCATCACAGTATCA-3′
Cyp2B10 (forward)	5′-CAATGGGGAACGTTGGAAGA-3′
Cyp2B10 (reverse)	5′-TGATGCACTGGAAGAGGAAC-3′
CK19 (forward)	5′-GACCTGGAGATGCAGATTGAG-3′
CK19 (reverse)	5′-GCTCCTCAGGGCAGTAATTT-3′
Sox9 (forward)	5′-CAGGCAAGAATTGGGCAAAG-3′

Table 1 continued

Sox9 (reverse)	5′-CCTCCCAACACGCAGTAAA-3′
HNF1β (forward)	5′-AACCAGCCGGGAAACAATGA-3′
HNF1β (reverse)	5′-CTCCCGACACTGTGATCTGC-3′
TRβ1 (forward)	5′-GGACAAGCACCCATCGTGAAT-3′
TRβ1 (reverse)	5′-CTCTGGTAATTGCTGGTGTGAT-3′
TRβ2 (forward)	5′-CCAGAGGTACACGAAGTGTGC-3′
TRβ2 (reverse)	5′-AGGTTTCCAGGGTAACTACAGG-3′

2.3.6 Measurement of Bile Acids

Total BAs (n = 3 samples per condition) were isolated from frozen liver using 70% ethanol, as previously described (247). Bile was also extracted from gallbladders and diluted 1:5 in distilled water. The Mouse Total Bile Acids Assay Kit (Crystal Chem, Downers Grove, IL) was used to measure BAs in both liver and bile, and the calibration curve and mean change in absorbance value for each sample were used to determine the concentration of each sample.

2.3.7 Statistical Analysis

Data are presented as means, SD, and/or individual data points. Data were analyzed, and graphs were generated using Prism GraphPad 7.0c (GraphPad Software, San Diego, CA). P values were determined using the two-tailed t-test, one-way analysis of variance followed by an appropriate post hoc test, or two-way analysis of variance followed by the appropriate post hoc test. $P < 0.05$ was considered statistically significant.

2.4 Results

2.4.1 Biliary Injury Is Decreased in KO after Short-Term GC-1 Diet

WT and KO mice were fed normal diet or GC-1 supplemented diet for 1, 2, 4, and 12 weeks and assessed for serum biochemical markers of liver injury. GC-1 diet did not affect total serum bilirubin levels nor liver weight/body weight ratios in KO mice, although conjugated bilirubin levels were decreased at 12 weeks (Figure 8). Surprisingly, hepatic injury, as assessed by measurement of serum transaminases aspartate aminotransferase and alanine transaminase, was significantly increased in KO fed GC-1 as early as 2 weeks after the start of diet, although these numbers tended to normalize or decrease at 12 weeks (Figure 9A). Terminal deoxynucleotidyl transferase-mediated dUTP nick-end labeling staining also revealed increased hepatocyte death in KO + GC-1 treated livers at 2 and 4 weeks of diet (Figure 10). On the contrary, biliary injury in KO mice on GC-1 diet was significantly decreased compared with KO mice on normal diet at both 2 and 4 weeks, as shown by a reduction in serum ALP, but was comparable in KO with and without diet at 12 weeks. To investigate parenchymal injury, hematoxylin and eosin stains of liver sections were performed. KO mice fed GC-1 diet show equivalent portal damage, including inflammation and ductular reaction, as early as 2 weeks compared with KO mice on normal diet, with this trend following into 4 weeks as well (Figure 9B). Thus, despite a transient decrease in biliary injury, KO mice treated with GC-1 have an overall similar phenotype to KO on normal diet after long-term exposure.

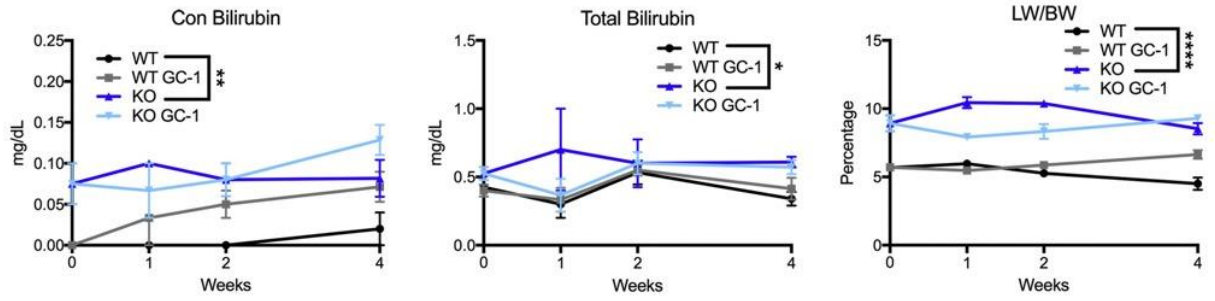

Figure 8. GC-1 does not affect serum bilirubin or the liver weight/body weight (LW/BW) ratio of ATP binding cassette subfamily B member 4 (*Abcb4*$^{-/-}$; Mdr2$^{-/-}$) knockout (KO) mice

Blood serum levels of conjugated bilirubin and total bilirubin, as well as LW/BW ratio, are significantly increased in KO mice compared with wild-type (WT) mice, but GC-1 has no effect on these parameters at most time points, although conjugated bilirubin levels were decreased at 12 weeks in KO + GC-1 compared with KO alone. n ≥ 3 mice per group. ∗P < 0.05, ∗∗P < 0.01, and ∗∗∗∗P < 0.0001 versus KO at all time points.

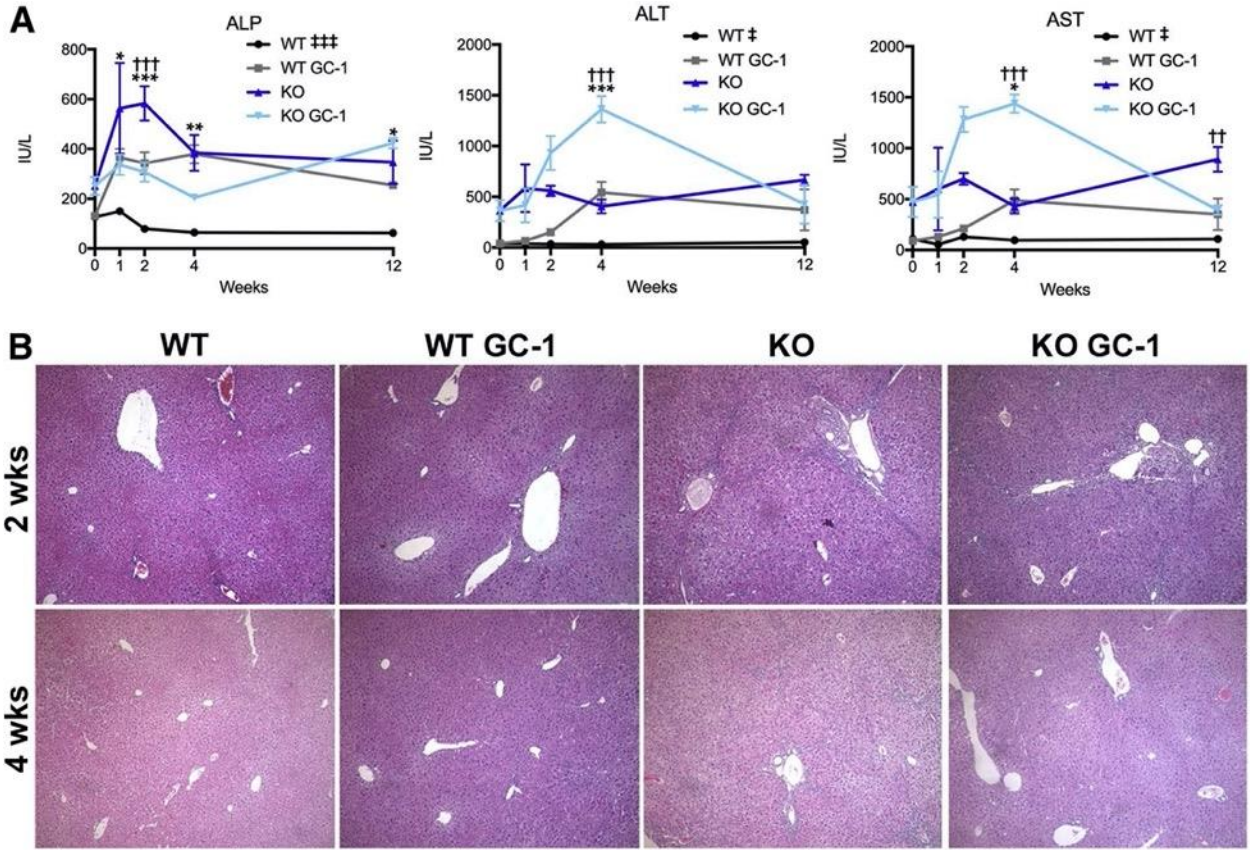

Figure 9. Biliary injury improves in ATP binding cassette subfamily B member 4 (Abcb4$^{-/-}$; Mdr2$^{-/-}$) knockout (KO) mice at 2 and 4 weeks after GC-1, at the expense of hepatic injury

(A) Blood serum levels of alkaline phosphatase (ALP) show decreased biliary injury, whereas alanine aminotransferase (ALT) and aspartate aminotransferase (AST) indicate increased hepatic injury, in KO mice on short-term GC-1 diet compared with KO mice. (B) Representative hematoxylin and eosin images show equivalent parenchymal injury in KO mice on GC-1 diet for 2 and 4 weeks compared with KO mice on normal diet. n ≥ 3 mice per group (A). ∗P < 0.05, ∗∗P < 0.01, and ∗∗∗P < 0.001 wild type (WT) versus WT GC-1; ††P < 0.01, †††P < 0.001 KO versus KO GC-1; ‡P < 0.05, ‡‡‡P < 0.001 WT versus KO at all time points analyzed. Original magnification, ×100 (B).

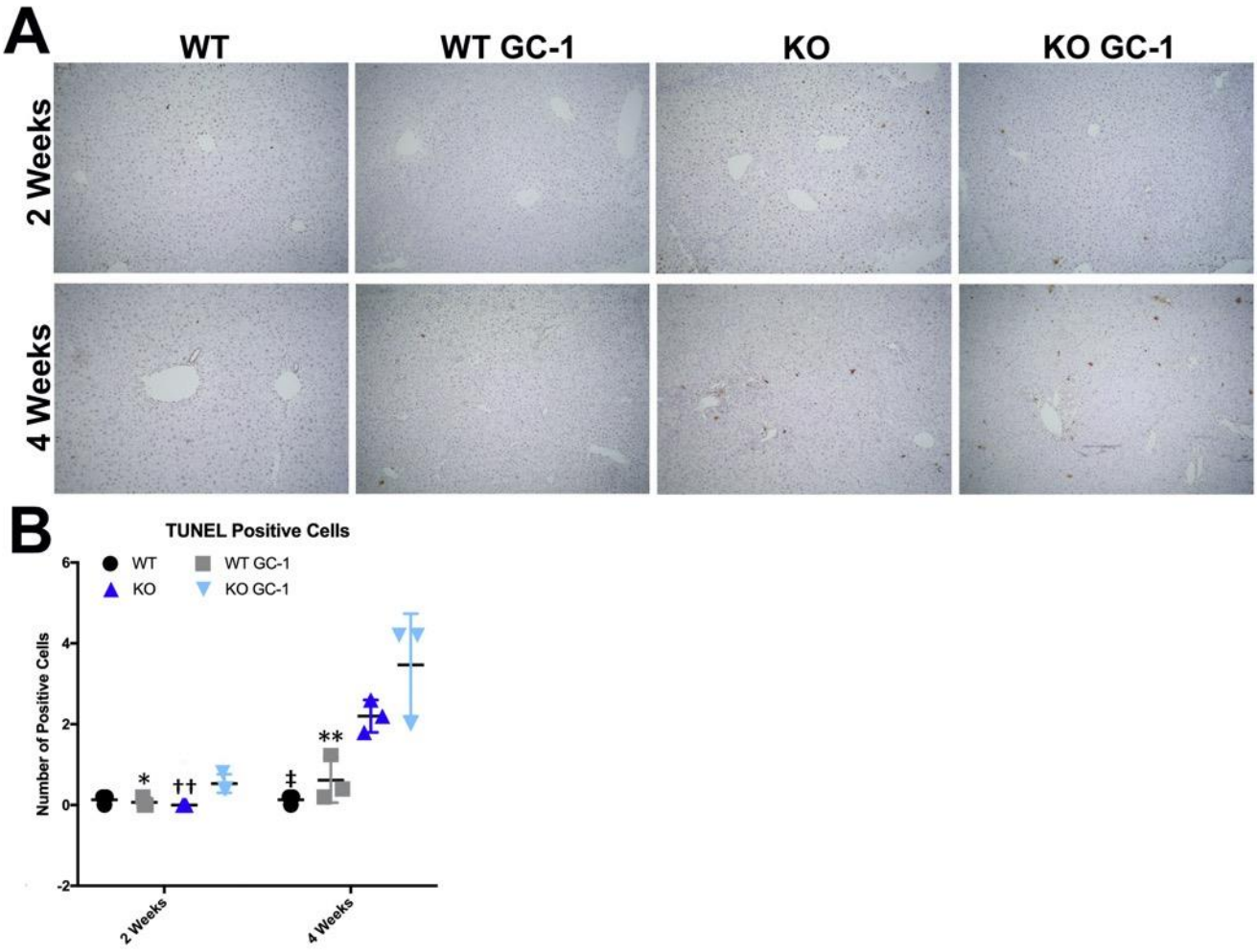

Figure 10. GC-1 treatment induces hepatocyte death *in vivo*

(A) Representative terminal deoxynucleotidyl transferase-mediated dUTP nick-end labeling (TUNEL) images show that there is more cell death in ATP binding cassette subfamily B member 4 (Abcb4−/−; Mdr2−/−) knockout (KO) mice on GC-1 at both time points compared with KO mice. (B) TUNEL quantification shows increased hepatocyte death in KO mice treated with GC-1 compared with KO mice after 2 and 4 weeks of GC-1 exposure. ∗P < 0.05, ∗∗P < 0.01 versus KO GC-1; ††P < 0.01 versus KO GC-1; ‡P < 0.05 versus KO. Original magnification, ×50 (A).

2.4.2 Fibrosis and Ductular Response Are Equivalent in KO Mice Fed GC-1

To determine if lower ALP levels in KO with GC-1 at 2 and 4 weeks correlate with decreased ductular mass and portal fibrosis, the fibrotic content of these livers was assessed by Sirius Red staining and quantification. KO mice on GC-1 diet have significantly less porto-portal bridging fibrosis after 2 weeks of diet exposure compared with KO mice, and a trend toward

decreased fibrosis at 4 weeks (Figure 11, A and C). Quantitative PCR analysis of biliary markers *Sox9*, cytokeratin 19 (official name *Krt19*), and hepatocyte nuclear factor 1 homeobox B (official name *Hnf1b*) shows that expression of common cholangiocyte markers is also decreased in KO mice on GC-1 compared with KO mice alone at both 2 and 4 weeks (Figure 11E). Immunohistochemistry for Sox9, however, indicates that the reduction in biliary markers may be due to notably fewer hepatocytes expressing biliary markers after GC-1 compared with KO mice on normal diet (Figure 12), rather than a reduction in the number of biliary structures. To directly assess biliary mass in KO after GC-1, immunohistochemistry and quantification of CK19, a marker of fully differentiated cholangiocytes, were performed. No significant differences in the amount of CK19 positivity between KO with or without GC-1 at either 2 or 4 weeks was observed (Figure 11, B and D). It is concluded that although fibrosis is transiently decreased in KO after 2 weeks of diet, on the whole, neither fibrosis nor ductular response is significantly changed over time in response to GC-1.

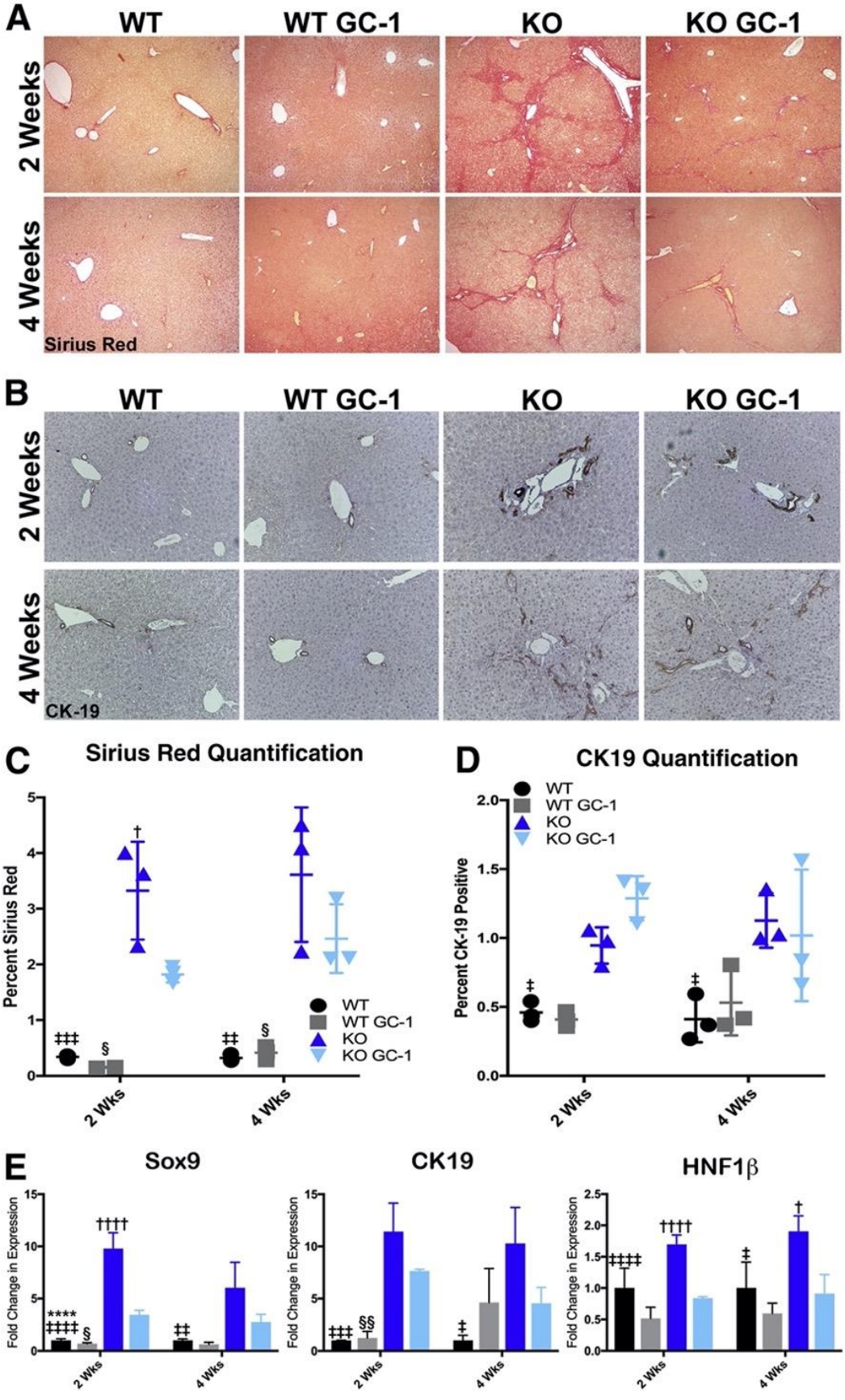
A
WT
WT GC-1
KO
KO GC-1
2 Weeks
4 Weeks
Sirius Red
B
WT
WT GC-1
KO
KO GC-1
2 Weeks
4 Weeks
CK-19
C
Sirius Red Quantification
Percent Sirius Red
WT
WT GC-1
KO
KO GC-1
2 Wks
4 Wks
D
CK19 Quantification
Percent CK-19 Positive
WT
WT GC-1
KO
KO GC-1
2 Wks
4 Wks
E
Sox9
CK19
HNF1β
Fold Change in Expression
2 Wks
4 Wks

Figure 11. ATP binding cassette subfamily B member 4 (*Abcb4*$^{-/-}$; Mdr2$^{-/-}$) knockout (KO) mice treated with GC-1 have decreased liver fibrosis but similar ductular response compared with KO mice on normal diet

(A) and (B) Representative Sirius Red (A) and cytokeratin 19 (CK19; B) images. (C) Quantification of Sirius Red stain shows less fibrosis in KO mice of GC-1 diet compared with KO mice after 2 weeks on diet. (D) Quantification of CK19 shows that KO mice both on and off GC-1 diet have increased ductular response compared with wild-type (WT) mice after 2 and 4 weeks. (E) Quantitative RT-PCR analysis of cholangiocyte markers sex-determining region Y-box transcription factor 9 (Sox9), CK19, and hepatocyte nuclear factor 1 homeobox B (HNF1β) in WT mice, WT mice fed GC-1 diet, KO mice, and KO mice fed GC-1 diet for 2 and 4 weeks shows decreased expression of these markers in KO treated with GC-1. n = 3 mice per group (E). ∗∗∗∗P < 0.0001 WT versus WT GC-1; †P < 0.05, ††††P < 0.0001 KO versus KO GC-1; ‡P < 0.05, ‡‡P < 0.01, ‡‡‡P < 0.001, and ‡‡‡‡P < 0.0001 WT versus KO; §P < 0.05, §§P < 0.01 WT GC-1 versus KO GC-1. Original magnification: ×100 (A); ×200 (B).

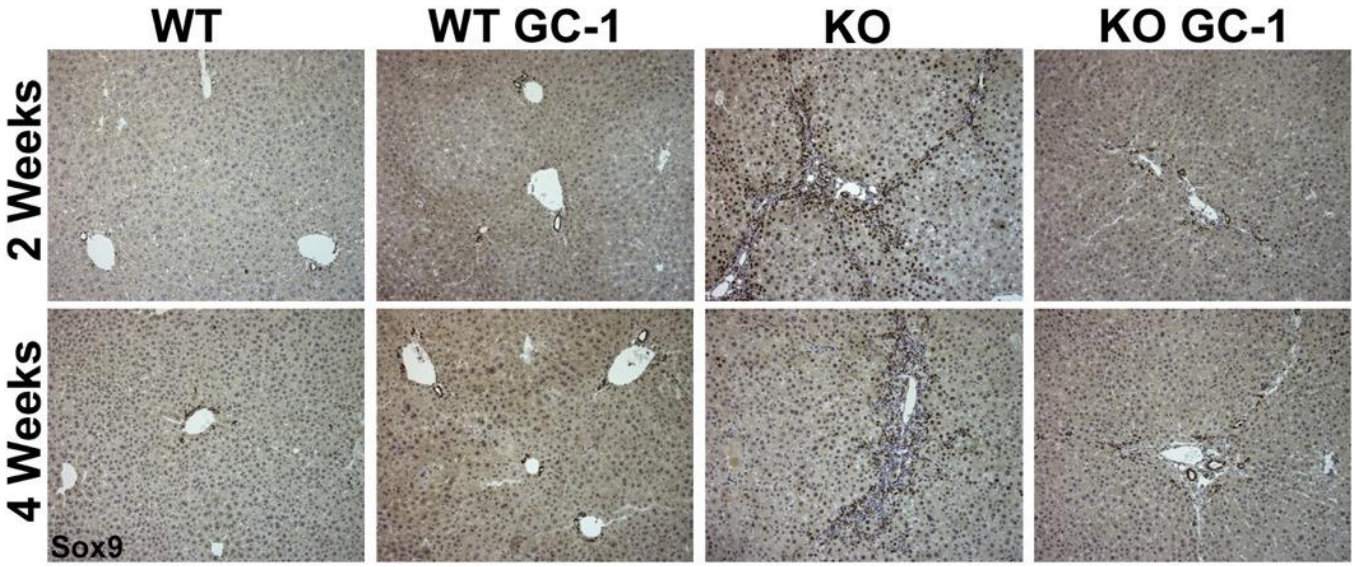

Figure 12. Sex-determining region Y-box transcription factor 9 (Sox9) immunohistochemistry shows that ATP binding cassette subfamily B member 4 (*Abcb4*$^{-/-}$; Mdr2$^{-/-}$) knockout (KO) mice and KO mice treated with GC-1 have increased ductular reaction compared with both untreated wild-type (WT) mice and WT mice treated with GC-1 at 2 and 4 weeks

Representative Sox9 images show increased ductular response in KO mice both on and off GC-1 treatment compared with WT mice, after 2 and 4 weeks. Also notable is the increased number of Sox9-positive hepatocytes in KO on normal diet compared with KO + GC-1 diet. Original magnification, ×200.

2.4.3 GC-1 Alters the Amount and Location of BAs in Mdr2 KO Mice through Differential Regulation of Hepatic BA Transporters and Synthesis Enzymes

Despite insignificant differences during the 12-week time point, this study intended to further characterize the phenotype of KO mice at the early stage of GC-1 treatment. Because hepatic injury increases simultaneously with decreased biliary injury in KO fed GC-1, it is hypothesized that alterations in BA synthesis, detoxification, or transport may be responsible.

Measurement of BAs shows that KO mice on GC-1 for 2 weeks have higher total hepatic BAs compared with both KO on normal diet and WT mice on GC-1 (Figure 13A). However, at 4 weeks, KO mice with and without GC-1 have similar levels of hepatic BAs, which are both elevated compared with WT mice (Figure 13A). At 4 weeks, a trend was also noted toward decrease in BA excretion, as KO fed GC-1 for 4 weeks have decreased biliary (gallbladder) BA levels compared with KO alone (Figure 13B). Thus, by 4 weeks, KO have compensated for increased BA accumulation after GC-1 by altering the amount and location of BA in the liver.

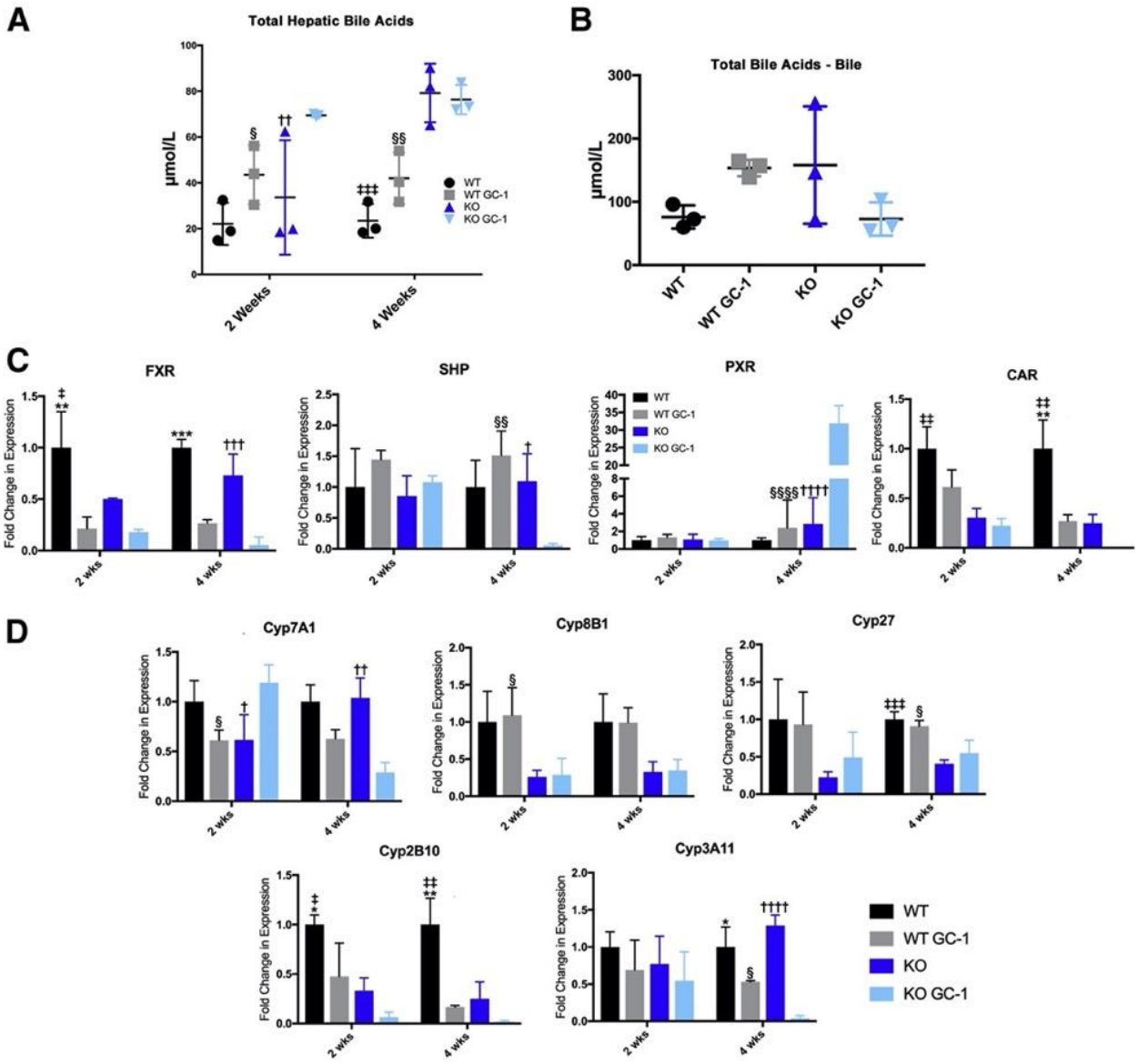

Figure 13. Bile acid excretion is dysregulated in ATP binding cassette subfamily B member 4 (*Abcb4*$^{-/-}$; Mdr2$^{-/-}$) knockout (KO) mice on GC-1 diet, concomitant with altered nuclear receptor and cytochrome P450 (Cyp) gene expression

(A) Total hepatic bile acids are increased in KO mice on GC-1 diet after 2 weeks compared with KO controls, but after 4 weeks, bile acid retention in the liver of KO on GC-1 is similar to KO on normal diet. (B) Measurement of bile acids collected from the gallbladder shows a trend toward decreased bile excretion in KO after 4 weeks of GC-1. (C) Quantitative RT-PCR analysis of farnesoid X receptor (FXR), small heterodimer partner (SHP), pregnane X receptor (PXR), and constitutive androstane receptor (CAR) shows that, after GC-1 diet, both wild-type (WT) and KO mice have decreased FXR, whereas after 4 weeks of diet, KO mice have increased PXR and decreased SHP; CAR is decreased generally in KO with and without diet. (D) Bile acid synthesis gene Cyp family 7 subfamily A member 1 (Cyp7a1) is increased in KO + GC-1 at 2 weeks, but repressed in KO after 4 weeks of GC-1 treatment, whereas Cyp family 8 subfamily B member 1 (Cyp8B1) and Cyp family 27 (Cyp27) are decreased in KO irrespective of GC-1 treatment. Detoxification genes Cyp family 3 subfamily a polypeptide 11 (Cyp3a11) and Cyp family 2 subfamily b polypeptide 10 (Cyp2b10) decreased in both WT and KO after 4 weeks of GC-1. n = 3 mice per group (A–D). ∗P < 0.05, ∗∗P < 0.01, and ∗∗∗P < 0.001 WT versus WT GC-1; †P < 0.05, ††P < 0.01, †††P < 0.001, and ††††P < 0.0001 KO versus KO GC-1; ‡P < 0.05, ‡‡P < 0.01, and ‡‡‡P < 0.001 WT versus KO; §P < 0.05, §§P < 0.01, and §§§§P < 0.0001 WT GC-1 versus KO GC-1.

Quantitative PCR analysis was then used to determine if nuclear receptors associated with BA synthesis—farnesoid X receptor [FXR; alias nuclear receptor subfamily 1 group H member 4 (*Nr1h4*)], small heterodimer partner [alias nuclear receptor subfamily 0 group B member 2 (*Nr0b2*)], pregnane X receptor [alias nuclear receptor subfamily 1 group I member 2 (*Nr1i2*)], and constitutive androstane receptor [alias coxsackie virus and adenovirus receptor Ig-like cell adhesion molecule (*Cxadr*)]—were altered after GC-1 exposure. FXR and its downstream target small heterodimer partner are master regulators of BA synthesis, whereas pregnane X receptor and constitutive androstane receptor regulate expression of cytochrome P450 (Cyp) genes involved in detoxifying and transporting BAs (249, 250). This study found that GC-1 reduced expression of FXR after 2 and 4 weeks of treatment, a finding that was consistent across both genotypes (Figure 13C). On the other hand, only KO show a decrease in small heterodimer partner after 4 weeks of GC-1 exposure, despite similar expression levels to WT at 2 weeks. Interestingly, expression of pregnane X receptor is dramatically increased in KO after 4 weeks of GC-1 diet, whereas constitutive androstane receptor expression is suppressed in KO generally, and GC-1 decreases expression further at 4 weeks (Figure 13C). Thus, the disparate regulation of some nuclear receptors, with the exception of FXR, indicates a compensatory response to GC-1 that is exclusive to KO.

To determine the impact on BA synthesis and detoxification, the expression of the Cyps involved in these processes was next analyzed. Interestingly, Cyp7a1, the rate-limiting enzyme involved in BA synthesis from cholesterol, is induced in KO mice on GC-1 for 2 weeks compared with KO mice, but significantly suppressed after 4 weeks of GC-1 exposure; expression in WT is unchanged at either time point after GC-1 (Figure 13D). Cyp8b1, which is downstream of Cyp7a1 and synthesizes cholic acid, is suppressed in the KO mice regardless of GC-1 treatment. Likewise,

Cyp27, which initiates the alternative BA synthesis pathway, is decreased in KO at both 2 and 4 weeks. Finally, expression of Cyp3a11 and Cyp2b10, which are involved in BA detoxification, significantly decreases after GC-1 diet in both WT and KO mice (Figure 13C). The results show that alternations in BA synthesis and detoxification occur early after GC-1 treatment and may subsequently affect both BA levels and toxicity.

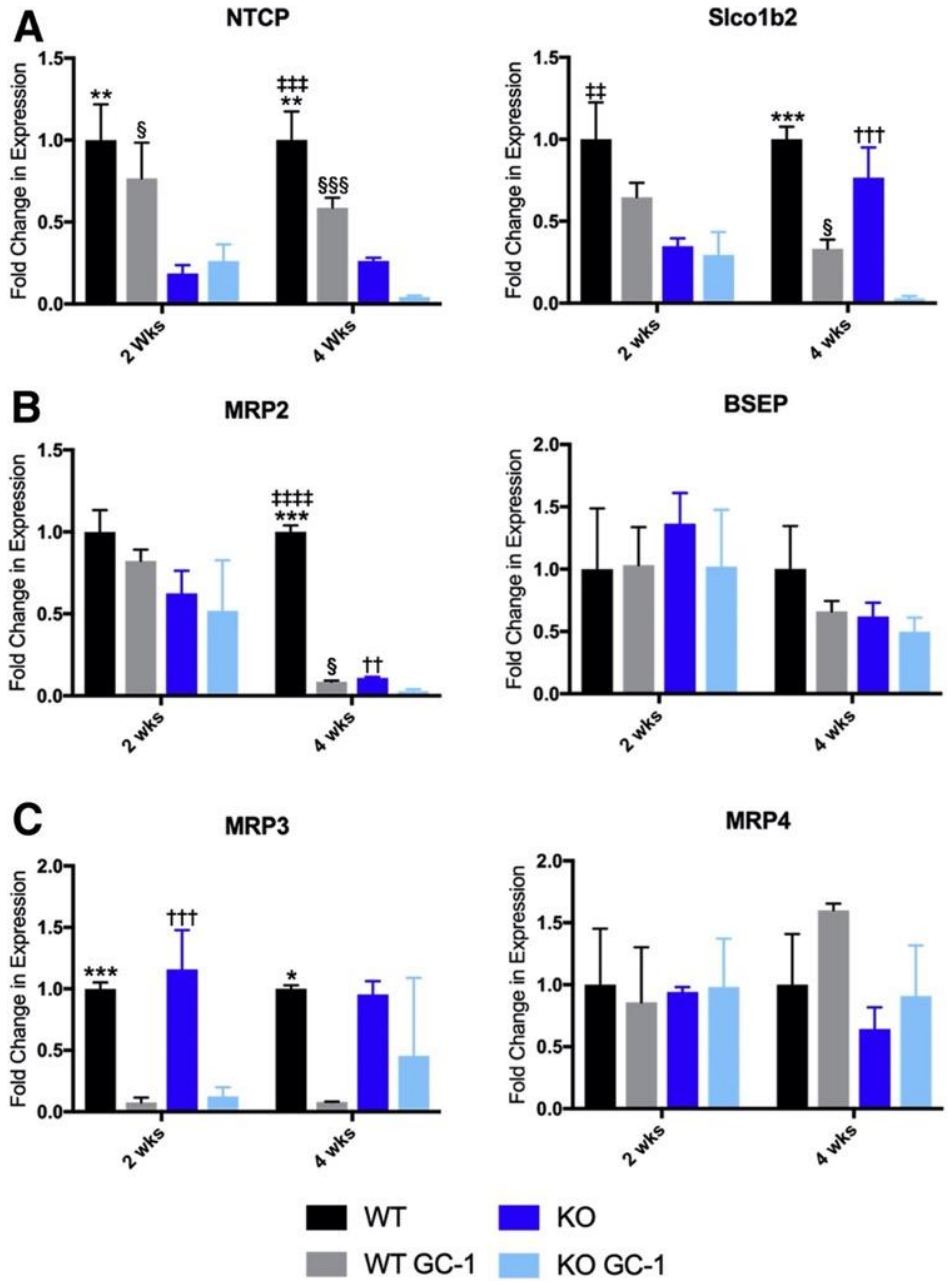

Figure 14. Bile acid transporter genes are altered after GC-1 diet, which leads to toxic bile retention in hepatocytes

(A) Quantitative RT-PCR analysis of uptake transporters sodium/taurocholate cotransporting polypeptide (NTCP) and solute carrier organic anion transporter family, member 1b2 (Slco1b2), shows decreased expression in wild-type (WT) and knockout (KO) after 4 weeks of GC-1 diet, although both are suppressed in KO on normal diet as well. (B) Efflux transporter ATP binding cassette subfamily C member 2 gene [Abcc2; alias multidrug resistance protein 2 (MRP2)] is decreased at 4 weeks in both WT and KO on GC-1 compared with controls, whereas bile salt export pump (BSEP) is unchanged. (C) ATP binding cassette subfamily C member 3 (Abcc3; alias MRP3) is significantly repressed in both WT and KO on GC-1 at 2 and 4 weeks, whereas ATP binding cassette subfamily C member 4 (Abcc4; alias MRP4) is unchanged. n = 3 mice per group (A–C). ∗P < 0.05, ∗∗P < 0.01, and ∗∗∗P < 0.001 versus WT GC-1; ††P < 0.01, †††P < 0.001 versus KO GC-1; ‡‡P < 0.01, ‡‡‡P < 0.001, and ‡‡‡‡P < 0.0001 versus KO; §P < 0.05, §§§P < 0.001 GC-1 versus KO GC-1.

Finally, the expression of genes involved in BA transport to identify any dysregulation in the presence of GC-1 was analyzed. Bile acid uptake transporters sodium-taurocholate cotransporting polypeptide [alias solute carrier family 10 member 1 (*Slc10a1*)] and solute carrier organic anion transporter family, member 1b2 [*Slco1b2*; (Slo)1b2], which are already decreased in KO mice compared with WT, are further reduced in both WT and KO after 4 weeks of GC-1 (Figure 14A). Expression of apical BA efflux transporter, ATP binding cassette subfamily C member 2 [*Abcc2*; alias multidrug resistance protein 2 (MRP2)], is decreased in both WT and KO, albeit only after 4 weeks of GC-1, whereas the bile salt export pump, another efflux transporter, is unchanged between WT and KO with or without GC-1 at either time point (Figure 14B). Decreased expression of MRP3, a basolateral BA efflux transporter, officially known as ATP binding cassette subfamily C member 3 (*Abcc3*), is also seen in both WT and KO at 2 and 4 weeks, indicating a direct repression by GC-1, whereas MRP4, another basolateral transporter officially known as ATP binding cassette subfamily C member 4 (*Abcc4*), is unchanged (Figure 14C). Overall, GC-1 induces down-regulation of FXR, BA uptake and efflux transporters, and detoxification enzymes in both WT and KO, with net result being that hepatocytes retain more toxic BAs compared with hepatocytes from mice on normal diet (Figure 15). However, KO mice on GC-1 also show increased Cyp7a1 expression at 2 weeks, which may account for the elevated levels of BAs and increased hepatic damage at this time point.

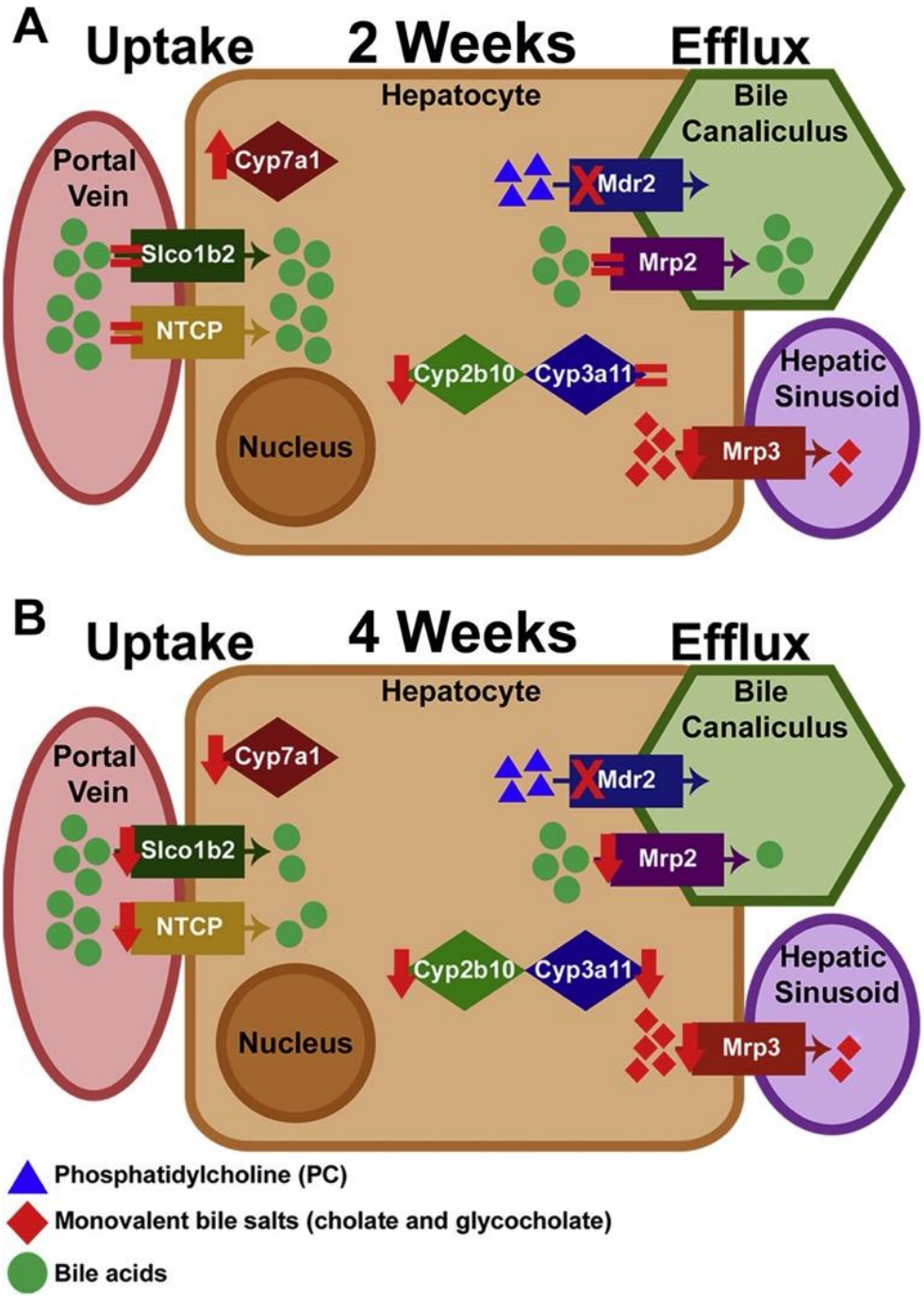

Figure 15. Schematic of changes in bile acid transporters and detoxification enzymes in ATP binding cassette subfamily B member 4 (Abcb4−/−; Mdr2−/−) knockout (KO) mice on GC-1 after 2 and 4 weeks of diet exposure compared with mice on normal diet

(A) Uptake transporter genes sodium-taurocholate cotransporting polypeptide [NTCP; alias solute carrier family 10 member 1 (Slc10a1)] and solute carrier organic anion transporter family, member 1b2 (Slco1b2), and efflux transporter [ATP binding cassette subfamily C member 2 gene (Abcc2); alias Mrp2] are equivalent in KO mice after 2 weeks of GC-1 diet, whereas Mrp3 [alias ATP binding cassette subfamily C member 3 (Abcc3)] is suppressed and cytochrome P450 (Cyp) 7a1 is increased, indicating that hepatocytes are starting to retain bile acids after 2 weeks of GC-1 diet exposure. (B) After 4 weeks of diet, uptake, efflux, synthesis, and detoxification, genes are all decreased, indicating hepatocytes are no longer capable of detoxifying or exporting bile acids.

2.4.4 GC-1 Neither Induces Hepatocyte Proliferation nor Inhibits Cholangiocyte Proliferation in Mdr2 KO Mice

Hepatocyte proliferation is an important component of the reparative response in chronic liver injury, and is often deficient in patients with cholestasis (251-254). As GC-1 has been shown to have mitogenic effects on hepatocytes, specifically after partial hepatectomy, the cell proliferation in our model was analyzed (29). Quantification of proliferating cell nuclear antigen immunohistochemistry shows increased hepatocyte proliferation in WT mice administered GC-1, as expected (Figure 16). However, hepatocyte proliferation in Mdr2 KO mice on normal diet, which was significantly elevated compared with WT, was not further induced by GC-1. A previous study has also found that thyroid hormone inhibits biliary growth both *in vitro* and *in vivo*, suggesting a cell autonomous role of thyroid receptor activation in cholangiocyte proliferation (255). However, neither WT nor KO mice exposed to GC-1 diet had any significant changes in cholangiocyte proliferation compared with mice fed normal diet (Figure 16). Thus, GC-1 diet does not affect proliferation of cholangiocytes, and hepatocyte proliferation is increased in WT but not Mdr2 KO after GC-1.

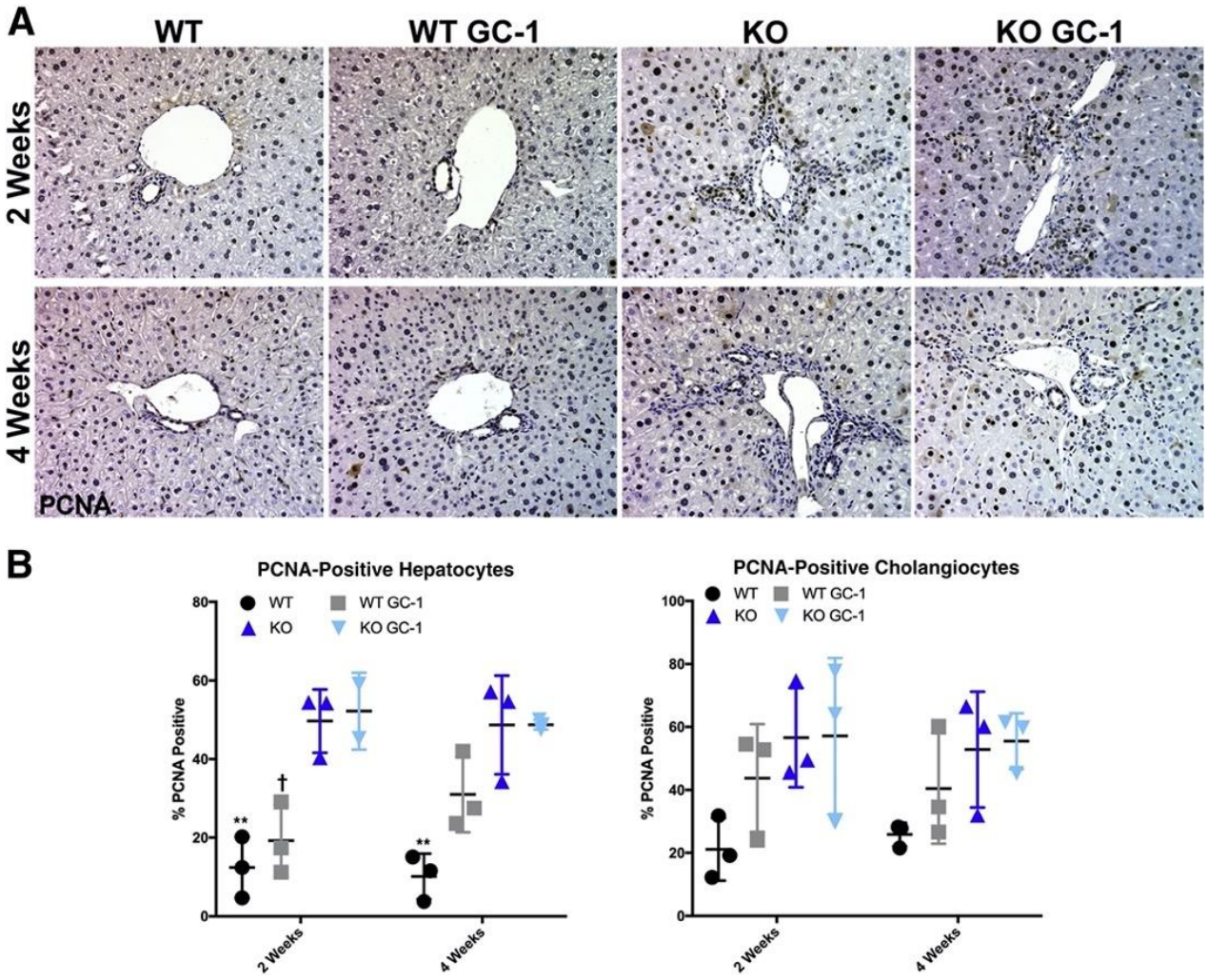

Figure 16. GC-1 has no effect on either hepatocyte or cholangiocyte proliferation in ATP binding cassette subfamily B member 4 (*Abcb4*$^{-/-}$; Mdr2$^{-/-}$) knockout (KO) mice

(A) Representative proliferating cell nuclear antigen (PCNA) images. (B) PCNA quantification shows that hepatocyte proliferation increases after GC-1 in wild type (WT) and increases significantly between WT and KO, but not between KO and KO + GC-1. Cholangiocyte proliferation in livers of KO mice fed GC-1 diet is also comparable to mice fed normal diet. ∗∗P < 0.01 versus WT GC-1; †P < 0.05 versus KO GC-1. Original magnification, ×200 (A).

2.4.5 GC-1 Does Not Activate β-Catenin in Mdr2 KO Mice

As the effect of GC-1 on hepatocyte proliferation is β-catenin dependent, a Western blot analysis of key phosphorylation sites that regulate β-catenin activation was performed. Previous studies have shown that GC-1 increases phosphorylation of β-catenin at serine 675 (S675) (29). However, KO mice fed GC-1 diet have decreased S675 phosphorylated β-catenin after 2 and 4

weeks of diet exposure compared with KO mice on normal diet (Figure 17). This decrease in S675 phosphorylated β-catenin indicates that the changes seen in the KO mice on GC-1 compared with the KO mice are not driven by protein kinase A–dependent β-catenin activation. To determine if GC-1 induces activation of β-catenin through canonical Wnt signaling, an antibody against the hypophosphorylated (nonphosphorylated) form of β-catenin was used. No significant changes in Wnt-dependent β-catenin activation were observed in KO treated with GC-1 at either the 2- or 4-week time point, although β-catenin activation was increased in KO livers compared with WT, as shown previously (44).

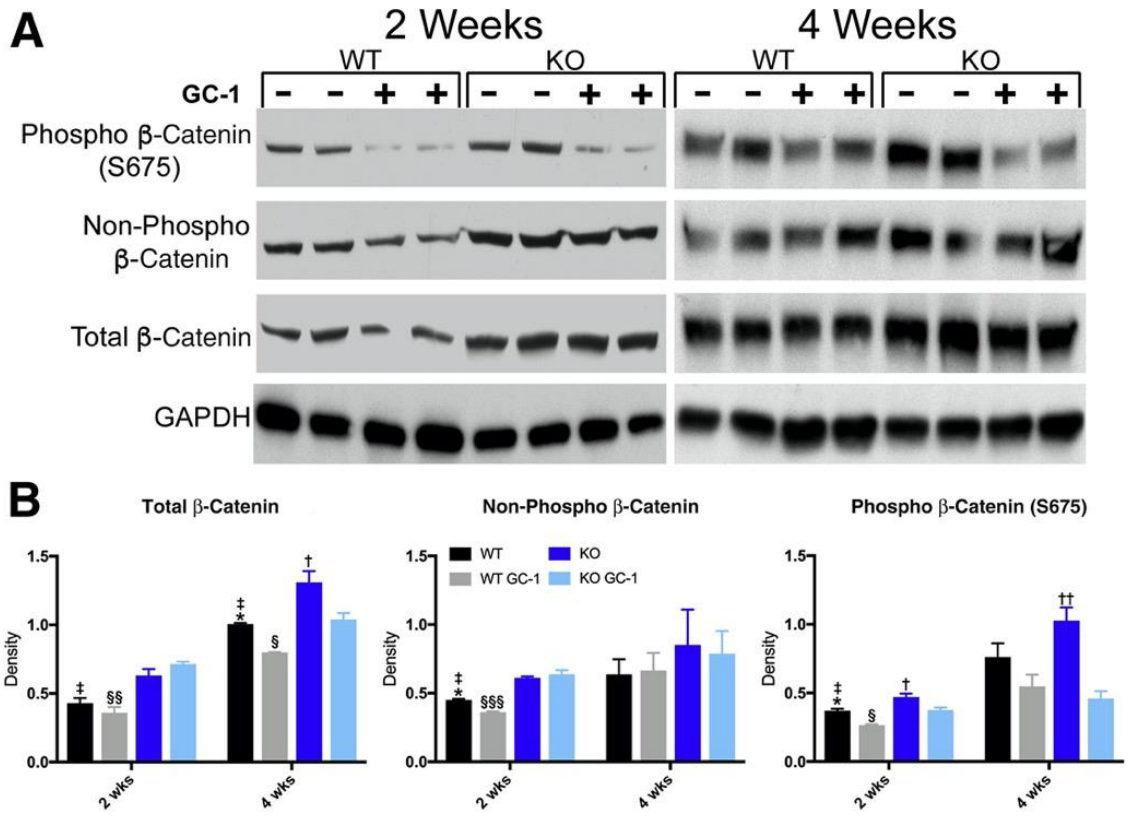

Figure 17. β-Catenin is not activated by GC-1 in ATP binding cassette subfamily B member 4 (Abcb4−/−; Mdr2−/−) knockout (KO) mice

Western blot analyses (A) and densitometry of the Western blot analyses (B) for phosphorylated (S675), nonphosphorylated active, and total β-catenin shows that KO mice given GC-1 have decreased activation of phosphorylated (S675) β-catenin compared with KO mice. ∗P < 0.05 versus WT GC-1; †P < 0.05, ††P < 0.01 versus KO GC-1; ‡P < 0.05 versus KO; §P < 0.05, §§P < 0.01, and §§§P < 0.001 versus KO GC-1. GAPDH, glyceraldehyde-3-phosphate dehydrogenase; phospho, phosphorylated; WT, wild-type.

2.4.6 TRβ Expression Is Decreased in Mdr2 KO, Resulting in a Blunted Response to GC-1

The lack of β-catenin activation led us to question whether GC-1 was being efficiently taken up and metabolized by the liver. This study sought to verify the effectiveness of GC-1 by examining expression of deiodinase, which is a TRβ target gene. Interestingly, although deiodinase is significantly up-regulated in WT, particularly at 4 weeks (approximately 30-fold over control), expression is increased only approximately 10-fold in KO after 4 weeks (Figure 18A). The study then analyzed the expression of the two TRβ isoforms in both WT and KO, and found that both were decreased in KO compared with WT at baseline (Figure 18B). Thus, GC-1 may be less effective in inducing β-catenin activation and hepatocyte proliferation in KO because of down-regulation of the receptors that interact with this thyroid hormone analog.

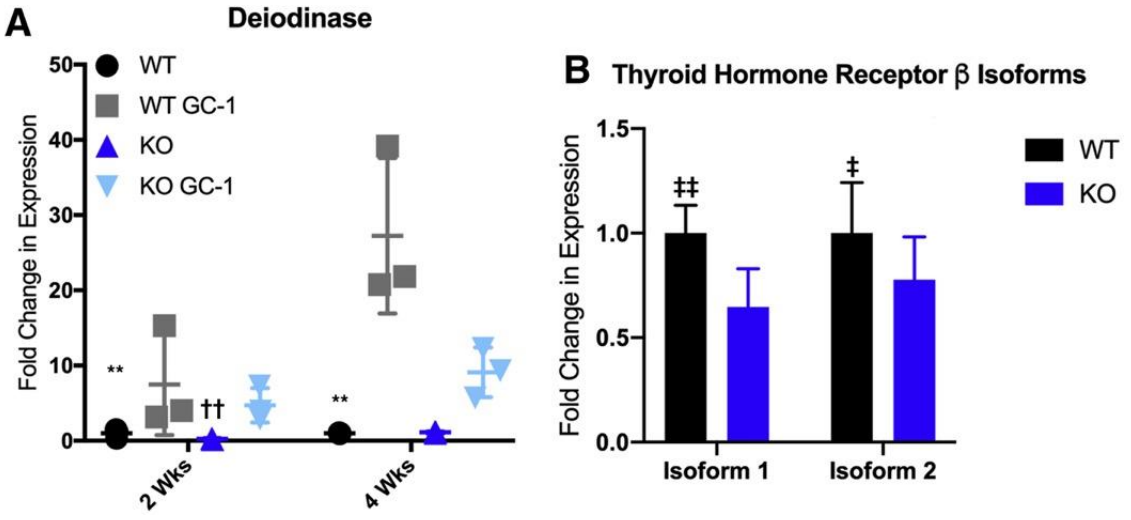

Figure 18. GC-1 induces deiodinase expression to a lesser extent in ATP binding cassette subfamily B member 4 (*Abcb4*$^{-/-}$; Mdr2$^{-/-}$) knockout (KO) livers than in wild-type (WT) livers, due to decreased expression of thyroid hormone receptor β (TRβ) receptor

(A) Quantitative RT-PCR analysis of deiodinase expression shows that KO have decreased induction after 2 and 4 weeks of GC-1 diet compared with WT mice ($P < 0.01$). (B) Expression of the two common isoforms of TRβ is decreased in baseline KO mice compared with baseline WT mice. $n \geq 3$ mice per group (A). ∗∗$P < 0.01$ versus WT GC-1; ††$P < 0.01$, †††$P < 0.001$ versus KO GC-1; ‡$P < 0.05$, ‡‡$P < 0.01$ versus KO.

2.5 Discussion

There is some evidence that activation of the Wnt/β-catenin signaling pathway may be protective in a subset of patients with cholestatic liver disease. Transgenic mice expressing a mutated, nondegradable form of β-catenin had decreased ALP, which is commonly used to monitor response to treatment in PSC patients, after long-term treatment with 5-diethoxycarbonyl-1,4-dihydrocollidine (180). Mdr2 KO mice also required β-catenin activation for maintenance of homeostasis (44). Because TRβ agonist was shown to activate β-catenin, it is hypothesized that administration of GC-1 might alleviate injury in the Mdr2 KO mouse. However, only a modest decrease in biliary injury and fibrosis in KO mice given GC-1, which was restricted to early (2- and 4-week) time points, was observed. The improvement in injury was not due to increased hepatocyte proliferation and repair, but rather a decrease in the amount of toxic bile entering the biliary tree.

Despite decreased biliary injury, KO showed a significant increase in hepatic injury, as assessed by serum aspartate aminotransferase and alanine transaminase, as well as apoptosis. Notably, serum ALP, aspartate aminotransferase, and alanine transaminase levels also increased in WT mice treated with GC-1. Interestingly, patients with familial hypercholesterolemia taking another thyroid hormone mimetic, KB2115, also showed a dose-dependent increase in transaminases and conjugated bilirubin (256). It is unknown whether these effects were off target or due to the effect of mimicking thyrotoxicosis in the liver; nonetheless, they are consistent with previous findings and led to discontinuation of treatment in some cases (256).

The pathogenesis of injury in Mdr2 KO is complex and multifactorial; however, increased concentration of free toxic BAs in the biliary tree is one major contributor. One strategy to reduce bile toxicity is to decrease BA output, which can be accomplished by treating these mice with the

dual FXR and G-protein–coupled membrane BA receptor (TGR5) agonist INT767 (257). In this study, GC-1 treatment of KO led to higher BA levels in the liver but lower levels in gallbladder bile than WT or KO on normal diet, resulting in less biliary injury. It appears that GC-1 causes retention of BAs in hepatocytes, thus sparing cholangiocytes from injury (Figure 18A). Indeed, GC-1 has important roles in lipid metabolism, including promoting conversion of cholesterol into BAs and regulating secretion of cholesterol into bile (258, 259).

It was intriguing to note that GC-1 enhanced BA toxicity and decreased their export. Increased toxicity occurs because of down-regulation of Cyp2b10 (and eventually Cyp3a11). The increase in Cyp7a1 in KO on GC-1 at 2 weeks, despite simultaneous decreases in Cyp8b1 and Cyp27, likely leads to additional BA accumulation and increased total hepatic BA levels in these mice. Alternative export of BAs from the basolateral membrane is suppressed at both 2 and 4 weeks of diet in both WT and KO by GC-1, as is export from the apical side at 4 weeks. The downregulation of BA uptake transporters from the blood is likely a secondary effect of the increasing levels of hepatic BAs, particularly in the KO. We believe that, although collectively these changes due to GC-1 result in increased biliary injury in WT due to the increased toxicity of bile, they induce hepatic injury in KO, because the toxic BAs are accumulating in hepatocytes rather than being dumped into bile. Future studies will address if some of these effects of GC-1 are indirect because of impact on cholesterol metabolism (260).

GC-1 led to an unexpected decrease in β-catenin expression and activity in Mdr2 KO. A previous study had shown GC-1 to activate both Wnt-dependent and Wnt-independent (protein kinase A–mediated Ser675 phosphorylation) activation of β-catenin (29). However, both the mode of GC-1 delivery and the length of treatment differed between the two studies, which may explain the conflicting results. The liver regeneration studies used mice injected with GC-1 for up to 8

days and harvested 1 hour after the final injection, which would allow for accurate measurement of transient events, such as protein phosphorylation. Conversely, in this study, mice consumed GC-1–containing diet ad libitum for a much longer time period (2 and 4 weeks), and were sacrificed without fasting. These conditions may not have been optimal for assessing phosphorylation events, as these are highly temporal within a cell.

Furthermore, TRβ expression was suboptimal in KO. It is possible that chronic liver injury may induce hepatocyte dedifferentiation, and decreased TRβ expression occurs as a result of this reprogramming. Thus, although compensatory hepatocyte proliferation in the Mdr2 KO likely occurs as a response to tissue damage, and may provide some protection against chronic injury, these cells are less responsive to therapies, such as thyromimetics, which rely on the presence of receptors expressed in fully differentiated hepatocytes (261). Further studies are needed to investigate the efficacy of thyromimetics in cholestatic models like Mdr2 KO after forced expression of TRβ.

Interestingly, a recent article demonstrated TRβ agonists to increase Mdr2 expression transcriptionally (262). This promoted phosphatidylcholine secretion into the bile, increasing bile flow and biliary BA output. It is unclear whether this is a reciprocal relationship, with down-regulation of Mdr2 leading to decreased TRβ, but these results suggest that this may be the case. Nonetheless, although the effect on Mdr2 induction was not tested in mouse models of cholestasis, in vitro studies using T3 and an FXR agonist showed that the effects of combination therapy are additive, resulting in stimulation of Mdr2 expression and sustained repression of Cyp7a1(262). This study demonstrates that reducing exposure of the biliary system to toxic BAs has an overall beneficial effect, and that the combination of TRβ agonists with other therapeutic modalities, such as FXR agonists, may be synergistic in reducing accumulation of BAs in hepatocytes and

subsequent hepatic injury. More optimization of TRβ expression would be necessary to test this hypothesis, but because thyromimetics are already undergoing preclinical and clinical trials, these findings have important implications for drug repurposing and personalized medicine.

3.0 Determining the Effects of Wnt Signaling in the Alleviation of Cholestasis Via the Promotion of Hepatocyte Transdifferentiation

In this section we characterize the effects β-catenin signaling has on hepatocyte transdifferentiation in mice exposed to 3,5-diethoxycarbonyl-1,4-dihydrocollidine (DDC) diet. We predict that mice expressing a transgenic, constitutively active, non-degradable from of β-catenin will have increased hepatocyte-to-cholangiocyte transdifferentiation after DDC diet exposure compared to control mice exposed to DDC diet. We will discuss our results and interpretations in detail.

3.1 Paper Summary

Primary sclerosing cholangitis (PSC) is a chronic cholestatic disease characterized by bile duct inflammation and fibrosis, resulting in end-stage liver disease and reduced life expectancy, and an effective treatment that does not rely on liver transplant is needed. Hepatocytes exhibit remarkable plasticity and are known to be capable of transdifferentiating into cholangiocytes in models of biliary injury. These newly derived cholangiocytes could create de novo ducts, repair damaged cholangiocytes, or contribute to bile detoxification. Previous studies utilizing *in vitro* organoid cultures and genetic mouse models found that β-catenin and downstream targets are upregulated in hepatic organoid cultures, and mice expressing excess β-catenin in the liver had an increased number of hepatocytes expressing cholangiocyte markers compared to wild type (WT) when subjected to cholestatic injury. These findings led to the hypothesis that Wnt/β-catenin

signaling drives hepatocyte-to-cholangiocyte transdifferentiation during biliary injury. To test this hypothesis, we utilized lineage tracing in hepatic organoid cultures and TG mice expressing a mutated non-degradable form of β-catenin (S45D) in liver. We show that hepatocytes transdifferentiate to cholangiocytes in organoid cultures, and the cholangiocytes present are not from native contaminating cholangiocytes. We also determined that TG mice fed 3,5-diethoxycarbonyl-1,4-dihydrocollidine (DDC) diet, which induces bile stasis, have improved serum ALP over time, indicating less biliary injury and bile ducts populated with hepatocyte-derived cholangiocytes. Through these studies we demonstrate that Wnt/β-catenin signaling catalyzes hepatocyte-to-cholangiocyte transdifferentiation, and activation of this pathway alleviates cholestasis in mouse models of PSC.

3.2 Background

As previously stated, primary sclerosing cholangitis (PSC), along with other intrahepatic cholestatic liver diseases, can cause serious irreparable damage to bile ducts resulting in end stage liver disease that also reduces life expectancy. Currently the only "treatment" for PSC is a liver transplant, and that is only if the patients are eligible to receive a donor organ (153, 156). Unfortunately, patients have a potential of disease recurrence after transplant (155, 157-160); thus, a treatment for PSC that is not reliant on liver transplant is an unmet clinical need.

Interestingly, a previous study found mice transgenic for a non-degradable S45D-mutated β-catenin in the liver (S45D) exposed to 3,5-diethoxycarbonyl-1,4-dihydrocollidine (DDC) diet long-term started to show improved biliary injury markers in their serum and had an increased number of hepatocytes positive for A6, a biliary marker, compared to WT mice on DDC diet (180).

This study along with data showing that Wnt7A, a known canonical Wnt ligand, induces hepatocytes to express biliary markers (69), led us to believe that the alleviation of cholestatic disease seen in the S45D mice after long-term DDC exposure is likely due to hepatocyte transdifferentiating into cholangiocytes and repairing injured ducts.

Therefore, we developed the hypothesis that β-catenin signaling will induce hepatocyte-to-cholangiocyte transdifferentiation alleviating cholestatic injury. To test this hypothesis, we bred S45D mice with R26-stop$^{flox/flox}$-EYFP which allowed us to lineage trace the origin of cholangiocytes in bile ducts after biliary injury. We used these mice for both an *in vitro* organoid study and an *in vivo* study, in which these mice were exposed to DDC diet for up to 6 months and monitored hepatocyte transdifferentiation as time progressed. We found that cholangiocytes present in organoid cultures are not from native contaminating cholangiocytes, instead they are hepatocyte-derived cholangiocytes. We determined that S45D mice fed DDC diet have improved serum ALP over time and have bile ducts populated with hepatocyte-derived cholangiocytes, which results in alleviated biliary injury over time. Through these studies we demonstrate that β-catenin signaling catalyzes hepatocyte-to-cholangiocyte transdifferentiation, and activation of this pathway alleviates cholestasis in mouse models of PSC.

3.3 Materials and Methods

3.3.1 Animal Model

All animal studies were performed in accordance with the guidelines of the Institutional Animal Care and Use Committee (IACUC) at the University of Pittsburgh School of Medicine

(Pittsburgh, PA) and the NIH (Bethesda, MD; protocol number 17071066). All mice were in a C57Bl6 background and maintained in ventilated cages under 12h light/dark cycles with access to enrichment, water and food ad libitum. To label cells with GFP, 8-week-old transgenic mice (TG) expressing a mutated non-degradable form of β-catenin in the liver and wild type controls (WT) were injected with $5x10^{11}$ viral particles adeno-associated virus serotype 8 carrying thyroid binding globulin-green fluorescent protein (AAV8-TBG-GFP, Penn Vector Core, Philadelphia, PA) diluted in sterile PBS. The AAV8 construct is specific for hepatocytes and does not infect other cell types of the liver, including biliary epithelial cells (BECs), stellate cells, or Kupffer cells. After a 12-day washout period, all animals were fed a control diet of standard mouse chow or 0.1% 3,5-diethoxycarbonyl-1,4-dihydrocollidine (DDC) diet (Bio-Serv, Flemington, NJ) for 1 month. After the diet course was complete, mice were sacrificed, and blood serum and livers were collected. Livers were sectioned, fixed in 10% formalin, and processed for paraffin embedding or frozen in liquid nitrogen and stored at −80°C. n = 4 for WT, n = 3 for WT + DDC, n = 8 for TG, and n = 3 for TG + DDC.

To permanently label hepatocytes to allow for lineage tracing during our studies TG mice were bred to R26-stop$^{flox/flox}$-EYFP mice (ROSA) to generate TG-R26-stop$^{flox/flox}$-EYFP mice (S45D). To label hepatocytes, 8-week-old ROSA and S45D mice were injected with $5x10^{11}$ viral particles adeno-associated virus serotype 8 carrying thyroid binding globulin-driven Cre recombinase (AAV8-TBG-Cre, Penn Vector Core, Philadelphia, PA) diluted in sterile PBS. The AAV8 construct is specific for hepatocytes and does not infect other cell types of the liver, including biliary epithelial cells (BECs), stellate cells, or Kupffer cells.

After a 12-day washout period all animals were fed a control diet of standard mouse chow or or 0.1% 3,5-diethoxycarbonyl-1,4-dihydrocollidine (DDC) diet (Bio-Serv, Flemington, NJ) for

2 months. Unfortunately, we received a couple batches of DDC diet from Bio-Serv that were fatal to the ROSA after about 5 weeks of exposure, so we changed diet distributors and continued our long-term DDC diet study. n = 3 ROSA, n = 3 ROSA + DDC, n = 7 S45D, and n = 7 S45D + DDC.

For our long-term study, after a 12-day washout period, all animals were fed a control diet of standard mouse chow or 0.1% 3,5-diethoxycarbonyl-1,4-dihydrocollidine (DDC) diet (Animal Specialty and Provisions LLC, Quakertown, PA). Animals were sacrificed after 2 months, 4 months, and 6 months of DDC diet exposure and blood serum and livers were collected. Livers were sectioned, fixed in 10% formalin, and processed for paraffin embedding or frozen in liquid nitrogen and stored at −80°C. For 2-months DDC or normal diet, n = 7 ROSA, n = 8 ROSA + DDC, n = 3 S45D, and n = 6 S45D + DDC. For 4-months DDC or normal diet n = 5 ROSA, n = 9 ROSA + DDC, n = 5 S45D, and n = 4 S45D + DDC. For 6-months DDC or normal diet, n = 6 ROSA, n = 9 ROSA + DDC, n = 5 S45D, and n = 8 S45D + DDC. Both male and female mice were used for experimentation.

3.3.2 Serum Biochemistry

At the time of sacrifice, blood was collected, and serum was sent to the University of Pittsburgh Medical Center Clinical Chemistry laboratory for biochemical analysis of total and conjugated bilirubin, alkaline phosphatase (ALP), aspartate aminotransferase (AST), and alanine transaminase (ALT).

3.3.3 Bile Flow Analysis

After 2 months of control diet or Bio-Serv DDC diet exposure, ROSA mice and S45D mice were analyzed for alterations in bile flow. Mice were anesthetized and their common bile ducts were catheterized. Bile was collected and measured every minute for up to twenty minutes. The bile was flash frozen using liquid nitrogen and stored in cryogenic storage for future analysis.

3.3.4 Hepatocyte Isolation and Roller Bottle Organoid Culture

Eight-week-old R26-stop$^{flox/flox}$-EYFP mice were injected with $5x10^{11}$ viral particles AAV8-TBG-Cre diluted in sterile PBS. After a 12-day washout period 2 mice were perfused via two step-collagenase perfusion as described elsewhere (263, 264). Freshly isolated hepatocytes from the livers were combined and added to roller bottles (850 cm^2 surface) from Falcon (Franklin Lakes, NJ). 250 ml of MGM medium was added to the bottles, and the bottles were rotated at a rate of 2.5 rotations per minute and kept in an incubator maintained at 37°C, saturated humidity, and 5% CO2 for 21 days. Either immediately after hepatocyte isolation or 21 days in roller bottles cells/organoids were harvested and analyzed for cholangiocyte markers.

3.3.4.1 Composition of the MGM Cell Culture Medium

The media was mixed in a similar manner to a previously published media (263, 264). Eagle's Minimum Essential Medium (EMEM) powder, HEPES, glutamine, and antibiotics were purchased from Life Technologies, Inc and ITS mixture (insulin, transferrin, selenium) was purchased from Lonza. All other additives were cell-culture grade and purchased from Sigma-Aldrich. MGM consisted of EMEM supplemented with purified bovine albumin (2.0 g/L),

galactose (2.0 g/L), ornithine (100 mg/L), proline (30 mg/L), $ZnCl_2$ (0.544 mg/L), $ZnSO_4$:$7H_2O$ (0.750 mg/L), $CuSO_4$:$5H_2O$ (0.20 mg/L), $MnSO_4$ (0.025 mg/L), and glutamine (5.0 mmol/L). Penicillin and streptomycin were added to the MGM at 100 mg/L and 100 μg/L and the MGM mixture was sterilized by filtration through a 0.22-μm low-protein-binding filter system, stored at 4°C. Dexamethasone (10^{-6} mol/L), ITS (1.0 g/L), HGF (40 ng/ml), and EGF (20ng/ml) was added after filtration, immediately before use.

3.3.5 Immunohistochemical Analysis

Paraffin-embedded hepatic organoid tissues and liver tissues were divided into sections (4 μm thick). Immunohistochemistry on paraffin-embedded sections was performed on hepatic organoids, as described elsewhere (177). Primary antibodies used were anti–cytokeratin 19 (CK19) antibody (31 μg/mL; TROMA-III-S; Developmental Studies Hybridoma Bank, Iowa City, IA). Secondary antibodies were goat anti-rat (Chemicon, Temecula, CA), and were used at 1 to 400, and staining was detected with 3,3′-diaminobenzidine detection systems after incubation with the Avidin-Biotin Complex Kit (Vector Laboratories, Burlingame, CA).

3.3.6 Immunofluorescence Staining

Paraffin-embedded hepatic organoid tissues and liver tissues were divided into sections (4 μm thick). Immunofluorescence staining was performed on these paraffin-embedded sections. Sections were deparaffinized using 3 washes of xylene and dehydrated using a series two 100% ethanol washes and two 95% ethanol washes. For antigen retrieval 1x Dako Target Retrieval Solution (Agilent, Santa Clara, CA) was used and the slides and solution were microwaved at 60%

power for 6 minutes, the evaporated antigen solution was replaced, and then microwaved for an additional 6 minutes at 60% power. The slides were allowed to cool to room temperature, washed once in PBS, then the tissues were permeabilized using 0.1% Triton X-100 in PBS for 20 minutes at room temperature. The slides were washed three times in PBS, then the slides were blocked with 2% Goat serum (Abcam, Cambridge, UK) in PBST (0.1% Tween in PBS) for 30 minutes at room temperature. Primary antibodies anti-GFP (1:200, Abcam, Cambridge, UK), and anti-Pan Cytokeratin (1:200 DAKO/Agilent, Santa Clara, CA) or anti–cytokeratin 19 (CK19) antibody (31 μg/mL; TROMA-III-S; Developmental Studies Hybridoma Bank, Iowa City, IA) were diluted in 2% Goat serum in PBST and incubated overnight at 4ºC. Slides were washed three times in PBS, then secondary antibodies Alexa Fluor 555 goat anti-chicken IgG and Alexa Fluor 488 goat anti-rabbit IgG or Alexa Fluor 488 goat anti-rat IgG diluted 1:800 in 2% goat serum in PBST were incubated for 2 hours at room temperature. Slides were three times with PBS, incubated with DAPI (1mg/100ml, Sigma, St. Louis, MO) for 30 seconds at room temperature, washed with PBS three more times, then coverslipped using gelvatol. Images were taken on a Nikon Eclipse Ti.

3.3.7 Quantitative Real-Time PCR

Total RNA was isolated from frozen liver tissue using Trizol reagent (Invitrogen, Carlsbad, CA). RT-PCR was performed as described elsewhere (177). Real-time PCR was performed on a CFX96 TouchReal-Time PCR Detection System (Bio-Rad Laboratories, Hercules, CA) using SYBR Green (Thermo Fisher Scientific, Pittsburgh, PA). Changes in target mRNA were normalized to GAPDH mRNA for each sample, and P value is presented as fold change over the average from three normal livers. Three samples per each condition were assayed in triplicate. Primer sequences are provided in Table 2.

Table 2. List of Primers Used for Quantitative RT-PCR Analysis in Section 3.0

EpCAM, epithelial cell adhesion molecule; CK19, cytokeratin 19; Sox9, sex-determining region Y-box transcription factor 9.

Primer name	Sequence
EpCAM (forward)	5′- GTGAATGCCAGTGTACTTCCTA-3′
EpCAM (reverse)	5′- GCTGTGAGTCATTTCTGCTTTC-3′
CK19 (forward)	5′- GACCTGGAGATGCAGATTGAG-3′
CK19 (reverse)	5′- GCTCCTCAGGGCAGTAATTT-3′
Sox9 (forward)	5′- CAGGCAAGAATTGGGCAAAG-3′
Sox9 (reverse)	5′- CCTCCCAACACGCAGTAAA-3′

3.3.8 Diet Comparison Study

To compare the DDC diet used in this study diet DDC diet used in previous studies, eight-week-old C57BL/6J (WT), ROSA, and S45D mice were placed on either 0.1% DDC diet from Animal Specialty and Provisions LLC or 0.1% DDC diet from Bio-Serv for 2 months. After 2 months on diet mice were sacrificed and blood serum and livers were collected. n= 3 WT + Animal Specialty, n = 3 WT + Bio-Serv, n= 5 ROSA + Animal Specialty, n= 3 ROSA + Bio-Serv, n= 3 S45D + Animal Specialty, n=3 S45D + Bio-Serv.

3.3.9 Statistical Analysis

Data are presented as means, SD, and/or individual data points. Data were analyzed, and graphs were generated using Prism GraphPad 9.0 (GraphPad Software, San Diego, CA). P values were determined using the two-tailed t-test, one-way analysis of variance followed by an appropriate post hoc test, or two-way analysis of variance followed by the appropriate post hoc test. $P < 0.05$ was considered statistically significant.

3.4 Results

3.4.1 After 1 Month of Bio-Serv DDC exposure TG mice have more cholangiocyte marker expressing hepatocytes than WT mice

Before we permanently labeled hepatocytes with EYPF, we performed an initial pilot study utilizing AAV8-TBG-GFP, which would only label the cells that were infected with the virus and not their progeny. We treated WT mice and TG with AAV8-TBG-GFP and then exposed them to Bio-Serv DDC diet for 1 month. After 1 month of Bio-Serv DDC diet exposure we found that both WT and TG mice have elevated serum biochemical markers for both biliary and hepatic injury. Both WT and TG mice on DDC diet have equally high levels of alkaline phosphatase (ALP), conjugated bilirubin, and total bilirubin (Figure 19A), which indicates that both mice have comparable biliary injury. Similarly, both types of mice also have equally high serum alanine aminotransferase (ALT) and aspartate aminotransferase (AST) levels (Figure 19B) as well, which indicates that both mice have comparable levels of hepatic injury. These results are expected, since DDC is known to induce biliary and subsequent hepatic injury in mice.

However, despite there being no differences in serum markers of injury, we noted that after 1 month of DDC diet exposure TG mice started to show more hepatocytes positive for a cholangiocyte marker, Pan-Cytokeratin (PanCK), compared to WT mice on DDC diet (Figure 19C). These PanCK positive hepatocytes in the TG mice exposed to DDC diet also appear to be forming duct like shapes, which are not present in the WT mice on DDC diet (Figure 19C). Unfortunately, this study was not pursued further since the labeling method used to monitor the hepatocyte-to-cholangiocyte transdifferentiation in this model was not permanent.

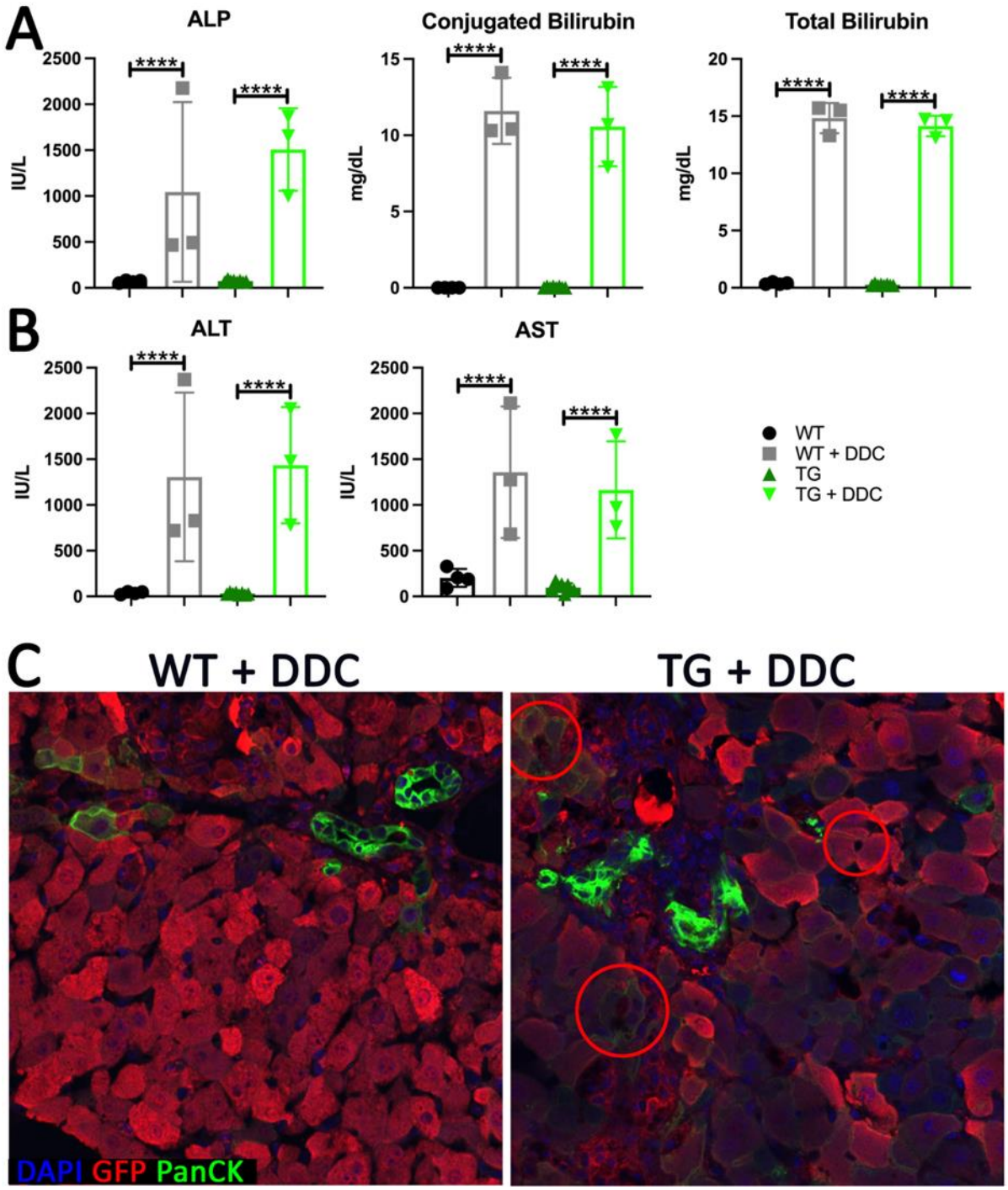

Figure 19. After 1 Month of Bio-Serv DDC exposure TG mice have more cholangiocyte marker expressing hepatocytes, but similar biliary and hepati injury compared to WT mice exposed to DDC diet

After 1 month exposed to Bio-Serv DDC diet WT and TG mice have similar levels of blood serum biliary injury markers (A) alkaline phosphatase (ALP), conjugated bilirubin, and total bilirubin and hepatic injury markers (B) alanine aminotransferase (ALT) and aspartate aminotransferase (AST). (C) After 1 month of Bio-Serv TG had more cholangiocyte marker expressing hepatocytes and hepatocytes forming bile duct-like shapes compared to WT mice exposed to DDC diet. Red circles indicate hepatocytes forming duct-like shaped. Cells were labeled with GFP using AAV8-TBG-GFP. (x200)

3.4.2 Mouse Hepatocytes Reprogram to Cholangiocyte in *In Vitro* Organoid Models

To demonstrate hepatocytes' capability to convert to cholangiocytes and the practicality of our lineage tracing model, we isolated primary hepatocytes permanently labeled with EYFP from 8-week-old ROSA mice, and utilized them to create hepatic organoids. We found that after 21 days of culture, cholangiocyte developed in hepatic organoids as seen in a CK-19 stain (Figure 20A). These findings were further confirmed through a QPCR analysis of the cholangiocyte markers EpCAM, Sox9, and CK19 (Figure 20B). In organoids cultured for 21 days all three cholangiocyte markers were significantly increased compared to hepatocyte isolated before being cultured to develop the organoids (Figure 20B). These findings indicate that the cholangiocytes present were likely functional, as fully converted cholangiocytes rather than cholangiocyte-like hepatocytes. Finally, the cholangiocytes present in these organoids were also hepatocyte-derived cholangiocytes, not the contaminating cholangiocytes that can make it through the hepatocyte isolation process. In the organoids the cholangiocyte population present were EYFP positive, indicating these cholangiocytes were derived from the EYFP positive hepatocytes and not native cholangiocytes that contaminate the hepatocyte isolation (Figure 20C). This study helps to demonstrate that our lineage tracing model is a viable method to follow hepatocyte-to-cholangiocyte conversion and it solidifies the ability of hepatocytes to convert to cholangiocytes.

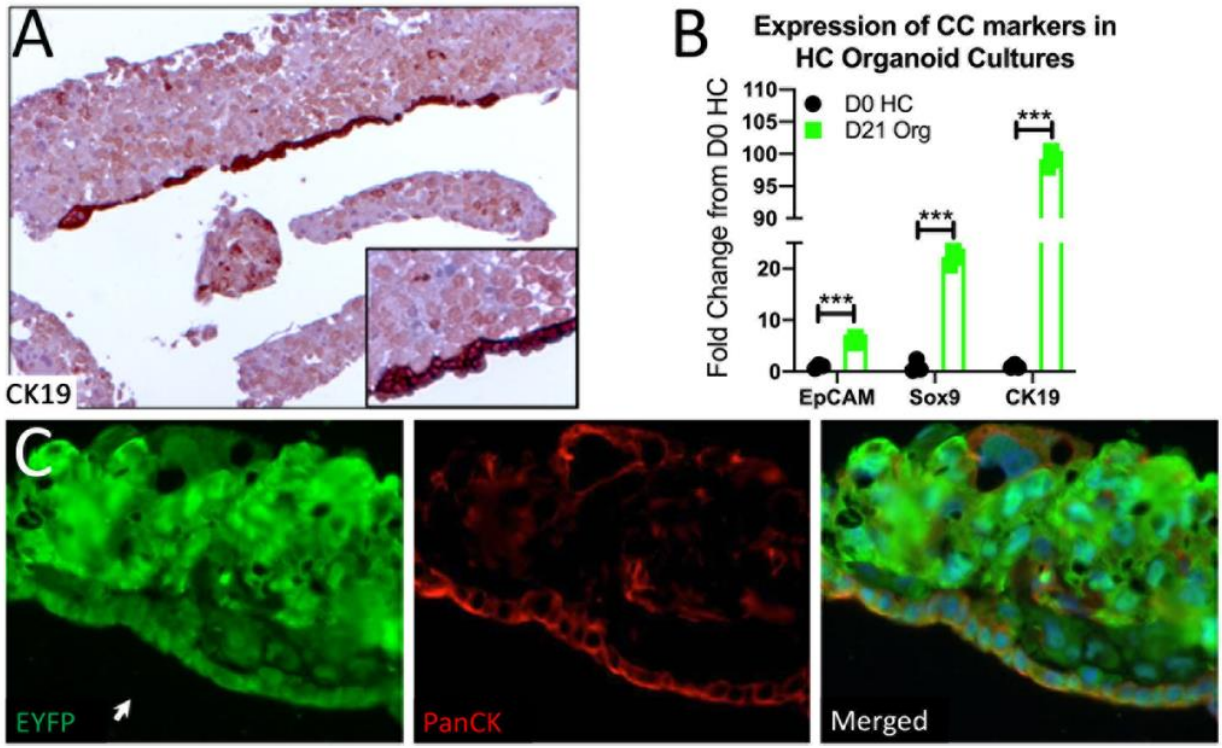

Figure 20.Cholangiocytes present in hepatic organoids are hepatocyte-derived
(A) Representative cytokerain 19 (CK19) image shows that hepatic organoids develop a cholagioncyte layer after 21 days of culture (x100, insert x200), (B) Quantitative RT-PCR analysis of epithelial cell adhesion molecule (EpCAM), sex-determining region Y-box transcription factor 9 (Sox9), and cytokeratin 19 (CK19) demonstrates that organoids culutred for 21 days have increased cholaginocyte markers compared to day 0 isolated primary hepatocytes, (C) Representative EYFP, pan-cytokeratin (PanCK), and merged images show that cholangiocytes present in organoid culture are hepatocyte derived and not from native contaminating cholangiocytes (x200). ***P < 0.001

3.4.3 S45D Mice exposed to Bio-Serv DDC Diet for 2 Months have Increased Bile Flow

After determining our lineage tracing model would work to monitor hepatocyte-to-cholangiocyte transdifferentiation we then moved into a mouse model to see how β-catenin activity would affect the rate of hepatocyte conversion and severity of biliary injury. To study this, we placed ROSA or S45D mice on Bio-Serv DDC diet with the intent to perform a long-term study and collecting timepoints at 2, 4, and 6 months of DDC diet exposure. Unfortunately, we were not able to utilize Bio-Serv DDC diet to do so, as we received several batches of DDC diet from Bio-Serv that were fatal to ROSA mice after 5 weeks on diet, which led us to change diet

manufacturers. However, before the Bio-Serv diet started to kill the ROSA mice we did manage to get some ROSA mice to 2 months on Bio-Serv DDC. During this time, we performed a bile flow study on these mice to determine if β-catenin expression helped to promote hepatocyte reprogramming and if those reprogrammed hepatocytes assisted with bile flow in these DDC exposed mice. Interestingly S45D mice on Bio-Serv DDC diet for 2 months have the fastest bile flow, over all timepoints, compared to S45D on control diet and ROSA mice both on and off of DDC diet (Figure 21). ROSA mice on Bio-Serv DDC diet had the slowest bile flow (Figure 21). These findings indicate that S45D mice after 2 months of Bio-Serv DDC diet exposure likely have more cholangiocyte-like hepatocytes, or hepatocytes that have converted to cholangiocytes.

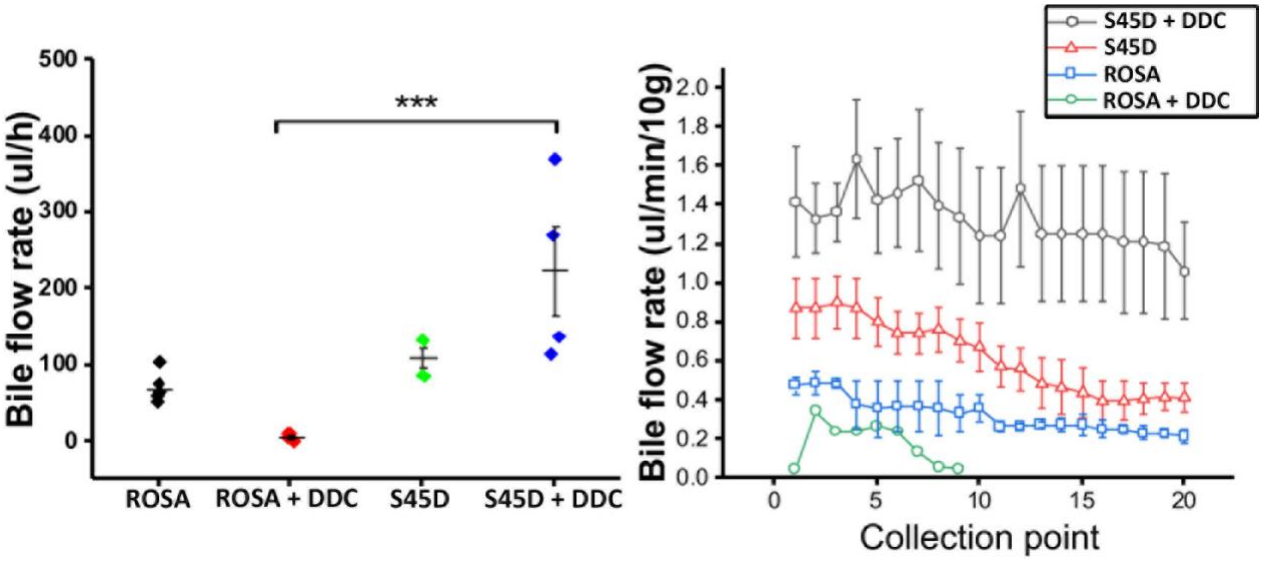

Figure 21. Bile flow is increased in S45D mice after 2 months of Bio-Serv DDC diet exposure
After 2 months of normal or DDC diet exposure the common bile duct of ROSA or S45D was canaliculated and bile flow was measured in µl/min for 20 miutes. S45D mice on DDC diet had significantly increased average bile flow (left graph) and and bile flow at individual time points (right graph) compared to ROSA mice on DDC diet. ***P < 0.001

To determine if S45D had more hepatocyte-derived ducts allowing for better bile flow we analyzed these livers for EFYP positive cholangiocytes. We found that after 2 months on Bio-Serv DDC diet, S45D mice do have EYFP positive, hepatocyte-derived cholangiocytes present and

these cells were integrated into the bile ducts (Figure 22). Unfortunately, we were unable to collect ROSA mice at this time point on the Bio-Serv diet as well to image for comparison to the S45D mice, since the livers used for the bile flow study could not be utilized for imaging. These findings were promising, and we wanted to study how this hepatocyte reprogramming was affected during long-term DDC diet exposure, so we decided to change DDC diet manufacturers in the hope that the new manufacturer would not be fatal to the ROSA mice as well.

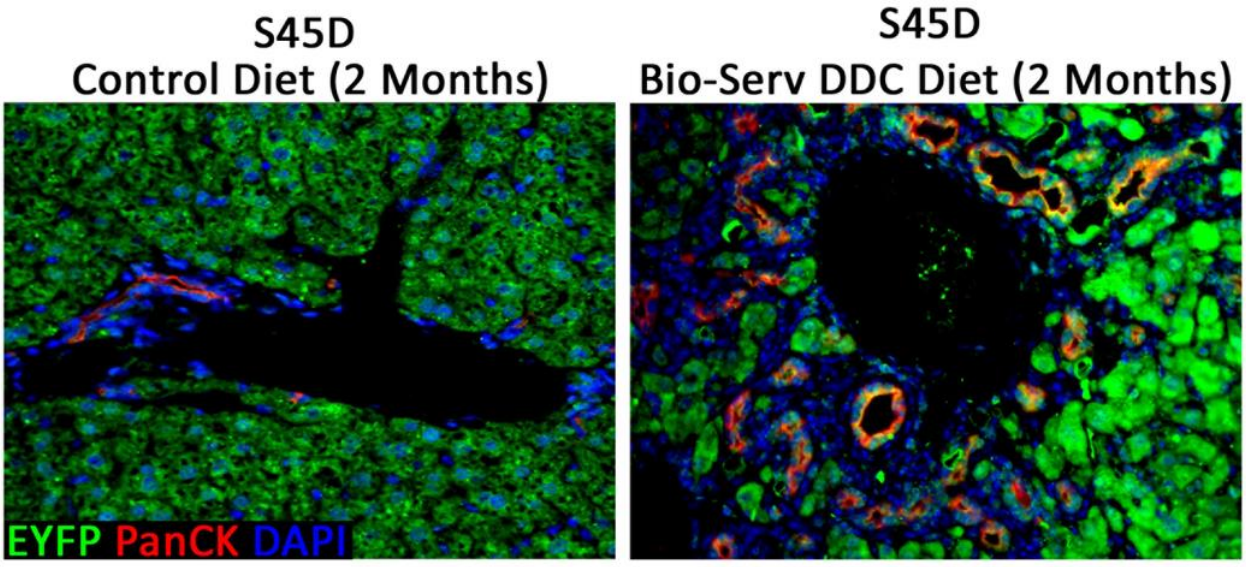

Figure 22. S45D mice on Bio-Serv DDC diet for 2 months have hepatocyte-derived cholagniocytes present
S45D mice fed DDC Bio-Serv DDC diet for 2 months have EYFP positive, hepatocyte-derived cholagnaiocytes integrated into the bile ducts. (x200)

3.4.4 Biliary Injury Improves Over Time in Mice Fed DDC Diet Long-Term

After changing diet producers and the ROSA mice surviving to 2 months and longer on DDC diet, we found that regardless of β-catenin activity, mice exposed to DDC diet long term had improved cholangiocyte injury over time. This can be observed in the decrease of serum ALP, conjugated bilirubin, and total bilirubin of both the ROSA and S45D mice fed DDC over time (Figure 23A). Both ROSA and S45D mice on DDC diet have the highest level of biliary injury at

2 months, which steadily decrease as time progresses, with their lowest level of biliary injury being at 6 months, as seen in their serum ALP, conjugated bilirubin, and total bilirubin (Figure 23A). ROSA mice following a similar trend of decreasing biliary injury as the S45D mice which was unexpected, since previous studies show that biliary injury remains high in control mice exposed to long term DDC diet (180).

Unlike biliary injury, hepatic injury remains high in both ROSA and S45D mice fed DDC diet. This is observed in the levels of serum ALT and AST in both mice on DDC diet (Figure 23B). At all-time points both ROSA and S45D mice on DDC diet have increased serum ALT and AST indicated that hepatic injury remains high in both mouse types (Figure 23B). This is not unexpected, since DDC diet is known to induce hepatic injury along with biliary injury (173, 204, 207).

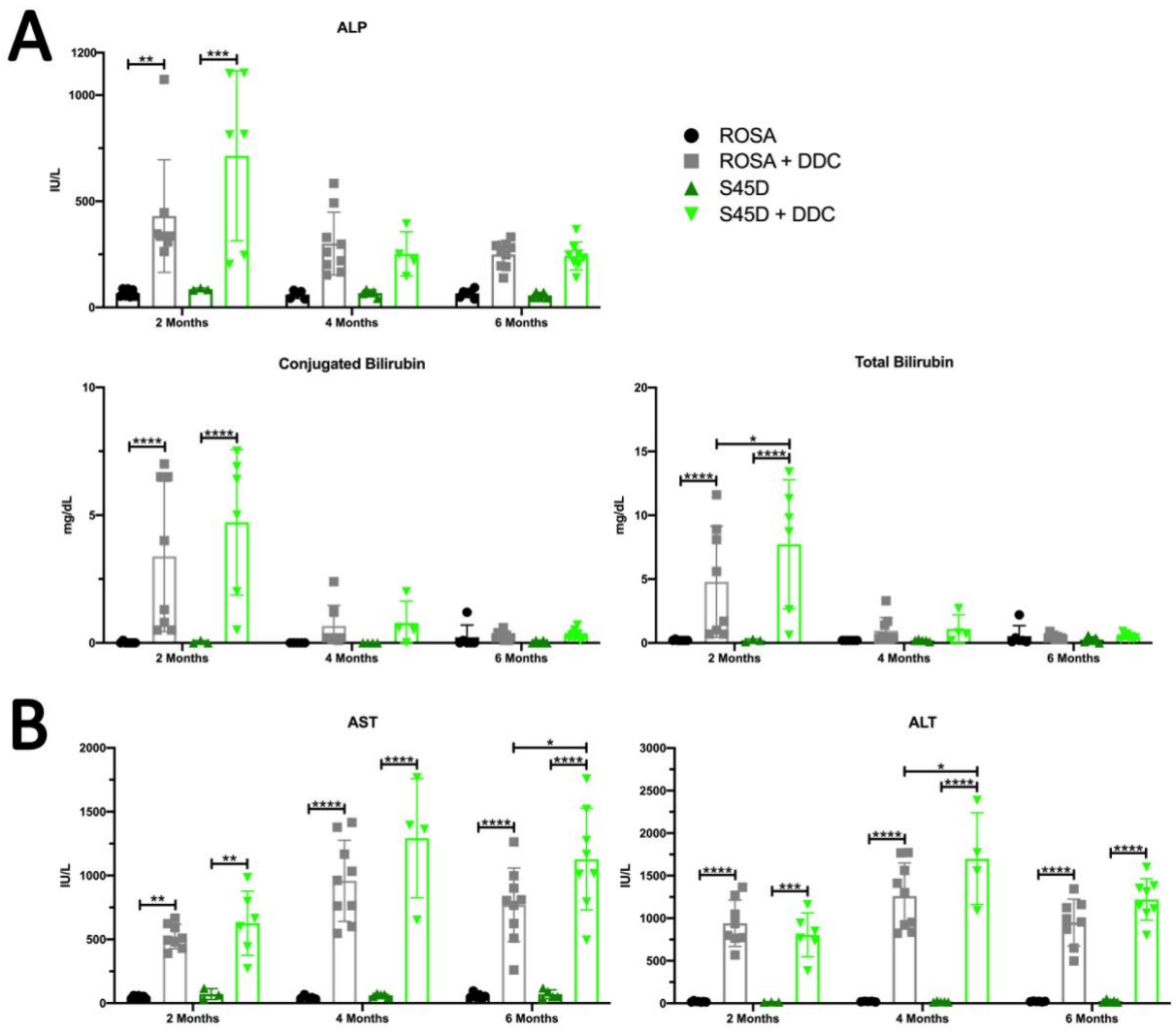

Figure 23. Biliary injury improves over time, but hepatic injury remains high in both ROSA and S45D mice fed DDC diet

(A) Blood serum levels of alkaline phosphatase (ALP), conjugated bilirubin, and total bilirubin shows as DDC diet exposure increases biliary injury decreases in both ROSA and S45D mice, whereas (B) serum levels of alanine aminotransferase (ALT) and aspartate aminotransferase (AST) indicate that hepatic injury remains high at all time points in both ROSA and S45D mice fed DDC diet. ∗P < 0.05, ∗∗P < 0.01, ∗∗∗P < 0.001, and ****P < 0.0001

3.4.5 DDC Diet Exposure Promotes Increased Hepatocyte Reprogramming in S45D Transgenic Mice

After determining that biliary injury improves in both S45D and ROSA mice exposed to DDC over time, we then decided to see if this improvement was related to hepatocyte-to-

cholangiocyte transdifferentiation. Utilizing the lineage tracing method we established in our *in vitro* organoid study we were able to observe whether cholangiocytes were derived from hepatocytes or not. After 2 months of DDC diet exposure both ROSA and S45D mice did not have any EYFP positive, hepatocyte-derived cholangiocyte (Figure 24). After 4 months of DDC diet exposure, both ROSA mice and S45D mice started to have EYFP positive, hepatocyte-derived cholangiocytes present in their bile ducts (Figure 24). Interestingly, S45D mice on DDC diet for 4 months tended to have more hepatocyte-derived cholangiocytes compared to ROSA mice on DDC diet and also started to have small bile ducts completely consisting of hepatocyte-derived cholangiocytes. This trend of hepatocyte-derived cholangiocytes only increased with DDC diet exposure in both ROSA and S45D mice. After 6 months of DDC diet both types of mice had even more EYFP positive, hepatocyte-derived cholangiocytes present in their bile ducts than they did after 4 months of diet exposure (Figure 24). However, S45D mice on DDC diet for 6 months had significantly more EYFP positive cholangiocytes than ROSA mice on DDC diet for 6 months. The S45D mice also had whole EYFP positive bile ducts, while the ROSA mice did not (Figure 24).

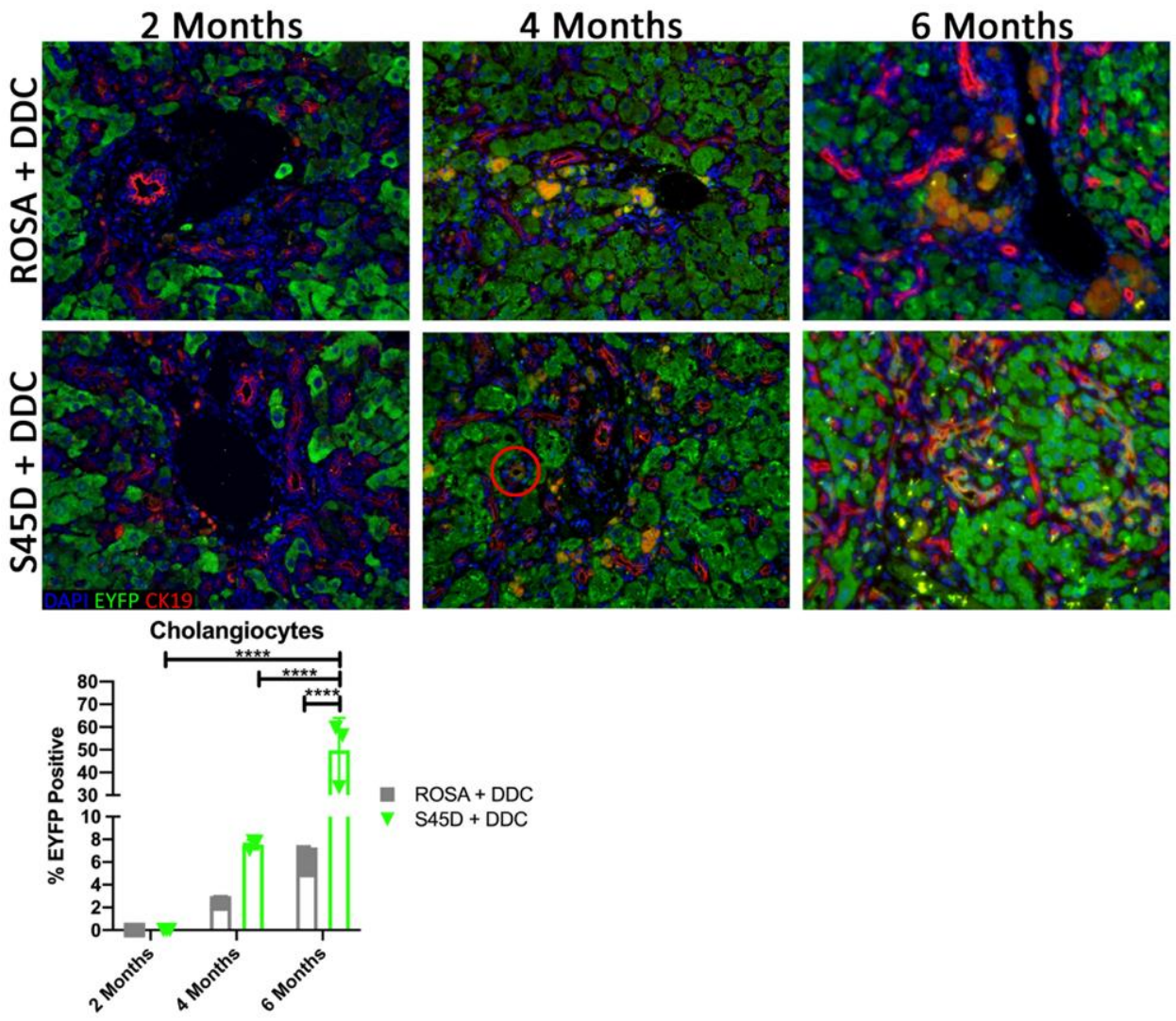

Figure 24. As DDC diet exposure increases S45D mice have more hepatocyte-derived choalginocytes present than ROSA mice

Representative EYFP, cytokeratin 19 (CK19) and DAPI images (top) and the precentage of EYFP positive cholaginocytes (bottom) in ROSA mice and S45D mice fed DDC diet for 2, 4, and 6 months. The red circle in the S45D + DDC at 2 months indicates a small bile duct that consists completely of hepatocyte-derived cholaginocytes (x200). ****P < 0.0001

3.4.6 DDC Diet Producers Induce Differing Levels of Biliary Injury in ROSA and S45D Mice

After comparing our results to previous findings, we noted that our long-term diet studies did not yield the similar results to those previously published (180). Therefore, we decided to do a DDC diet comparison between the Animal Specialty DDC diet and the Bio-Serv DDC diet to determine if diet manufacturers can affect biliary injury. Interestingly we found that after ordering a new batch of DDC diet from Bio-Serv, after we had completed our long-term study using Animal Specialty DDC diet, ROSA mice were able to survive past 5 weeks on the Bio-Serv diet. We also found that the different diet manufacturers do yield different levels of biliary injury in the mice fed DDC diet for 2 months. ROSA mice on Bio-Serv DDC diet have increased serum ALP, conjugated, and total bilirubin compared to ROSA mice on Animal Specialty DDC diet (Figure 25A). S45D mice on Bio-Serv DDC diet have decreased serum ALP and equal conjugated and total bilirubin compared to S45D mice on Animal Specialty DDC diet (Figure 25A). However, unlike biliary injury, hepatic injury markers were not altered by the different diet producers in the ROSA and S45D mice. Both ROSA and S45D mice on both types of DDC diet had consistently high serum ALT and AST levels after 2 months on DDC diet regardless of diet producer (Figure 25B).

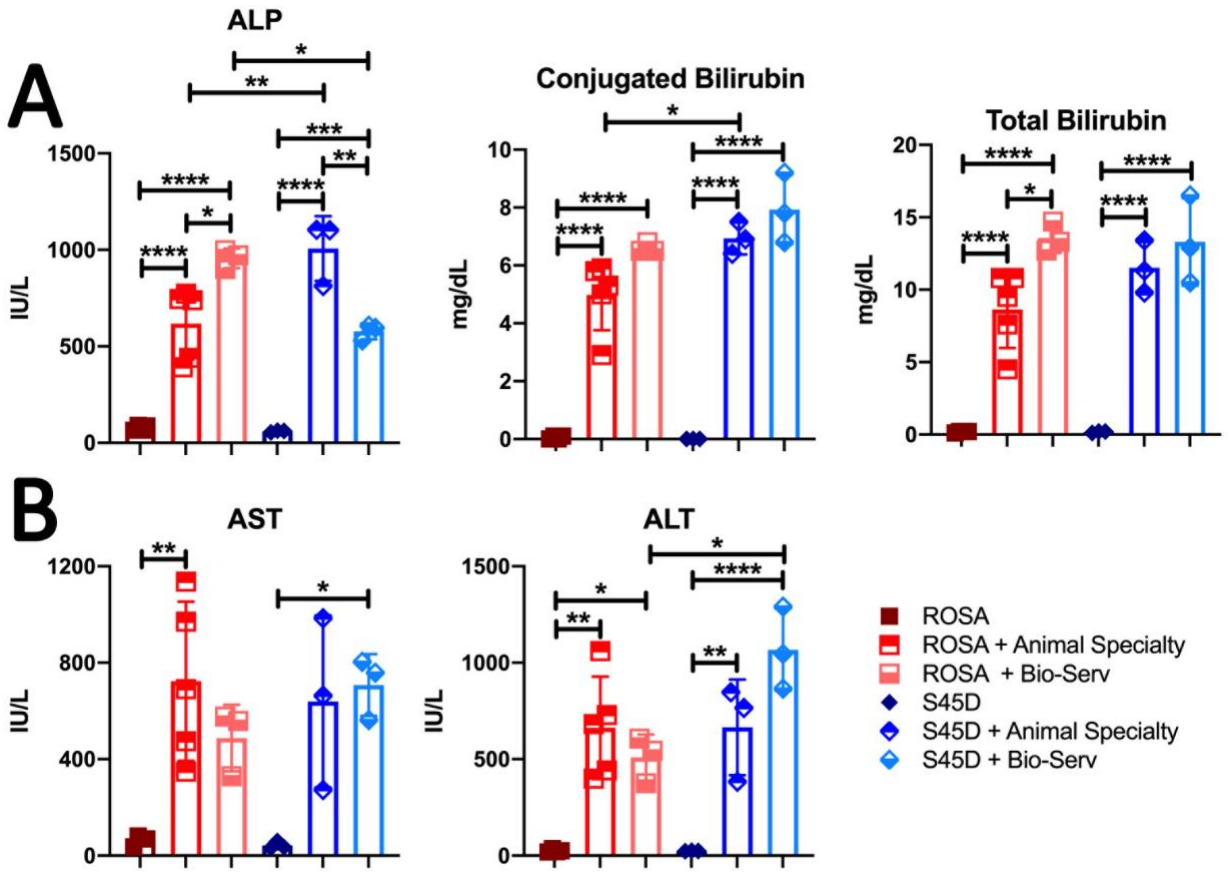

Figure 25. After 2 months of exposure to DDC diets from different producers ROSA and S45D mice have differing levels of biliary injury, but comparable levels of hepatic injury

(A) Blood serum levels of alkaline phosphatase (ALP), conjugated bilirubin and total bilirubin show that DDC diet produced by Bio-Serv casues increased levels of biliary injury in ROSA mice and decrased levels of biliary injury in S45D mice compared to Animal Specialty DDC diet. (B)Sserum levels of alanine aminotransferase (ALT) and aspartate aminotransferase (AST) indicate that hepatic injury remains high in both DDC diet types in both ROSA and S45D mice. ∗P < 0.05, ∗∗P < 0.01, ∗∗∗P < 0.001, and ****P < 0.0001

3.5 Discussion

Wnt/β-catenin activity may be protective in a subset of patients with cholestatic liver disease. A previous study found that transgenic mice (TG) expressing a mutated, nondegradable form of β-catenin after long-term treatment with DDC diet had decreased serum ALP, a serum marker used by clinicians to monitor PSC patients and their disease progression (180). These TG mice exposed to long-tern DDC diet also had significantly more A6, a cholangiocyte marker,

positive hepatocytes than the WT control on DDC diet (180). These findings led us to our hypothesis β-catenin signaling will induce hepatocyte-to-cholangiocyte transdifferentiation alleviating cholestatic injury. Excitingly using our lineage tracing model we found that S45D transgenic mice on DDC diet did have significantly more hepatocyte-derived cholangiocytes than ROSA mice after 6 month of DDC diet. We also found that these hepatocyte-derived cholangiocytes appeared to form their own ducts in the S45D mice, while the hepatocyte-derived cholangiocytes in the ROSA mice appeared to integrate into already existing bile ducts. These findings support our hypothesis and indicate that β-catenin does promote hepatocyte-to-cholangiocyte transdifferentiation.

However, something that was unexpected during our study was the trend the biliary injury serum markers followed in the ROSA mice exposed to DDC diet. Surprisingly, not only did biliary injury serum markers decrease in S45D mice on DDC diet over time, they also decreased in the ROSA mice exposed to DDC diet. This was unexpected because in a previous study, it was found that after 150 days of DDC diet, TG mice had significantly decreased biliary injury compared to the WT mice (180). In the mice exposed to long term DDC diet, WT mice had total bilirubin that was trending towards increased levels compared to TG mice (Figure 26). This study also found that WT mice had significantly higher levels of serum ALP after long-term DDC exposure compared to TG mice (Figure 26). Both of these results indicate that WT mice exposed to DDC diet long-term had increased biliary injury compared to TG mice exposed to DDC diet long-term. These findings were partially the reasoning for our initial hypothesis, so when we did not see this data recapitulated in our own findings we were surprised.

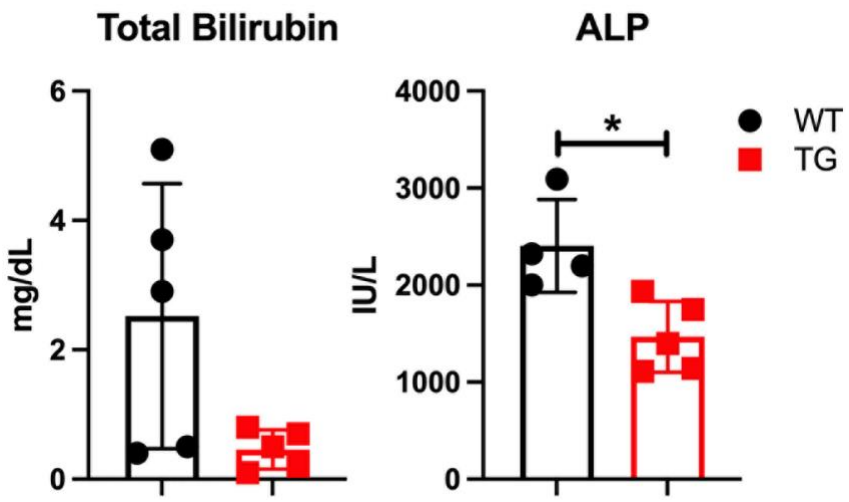

Figure 26. Transgenic mice have decreased biliary injury compared to WT mice after 150 days of DDC diet exposure

A graphicial representation of data collected in a previous study performed by Thompson MD et al., which found that after long-term DDC diet exposure (150 days) mice transgenic (TG) for non-degradable S45D-mutated β-catenin in the liver have decreased serum total bilirubin and alkaline phosphatase (ALP) compared to WT mice (180). ∗P < 0.05

One possible explanation for our ROSA mice not having increased biliary injury compared to our S45D mice is the DDC diet we used in this study. The previous study used a DDC diet produce by the company Bio-Serv, which we initially intended to put our mice on as well. However, our ROSA mice would not survive longer than 5 weeks on the Bio-Serv DDC diet. This was unusual since other studies had managed to keep WT mice on diet for much longer, so we were perplexed as how to continue our long-term DDC diet studies. The WT/ROSA mice not surviving longer than 5 weeks on the Bio-Serv diet continued through two distinctly different batches of Bio-Serv DDC diet and us contacting the company to see if anything had changed in their diet making procedure to try to determine why this was occurring. After being reassured by Bio-Serv that nothing had changed in the diet making process, we assumed the mice not surviving on the Bio-Serv diet was something that was out of our control and found a new DDC diet producer. Luckily for our study the DDC diet from our new diet producers, Animal Specialty and Provisions LLC, did not kill the control mice after 5 weeks of exposure and we were able to keep

the mice alive for the long-term diet studies. However, after analyzing the serum results from our ROSA and S45D mice we were surprised to find that the ROSA control mice had decreasing serum biliary injury markers much like the S45D mice. We determined these changes in control serum levels was likely due to the difference in the diet producers. Therefore, we decided to do a comparison of the DDC diet produced by Bio-Serv and Animal Specialty and Provisions LLC to see how the different DDC diets affect serum results in our ROSA and S45D mice after 2 months of exposure.

Surprisingly, we found that different DDC diet manufacturers do yield different results in the mice exposed to the diet for 2 months. ROSA mice on Bio-Serv DDC diet have increased biliary injury compared to ROSA mice on Animal Specialty DDC diet. S45D mice on Bio-Serv DDC diet have decreased biliary injury markers compared to S45D mice on Animal Specialty DDC diet. However, unlike biliary injury, hepatic injury markers were not altered by the different diet producers in either genotype.

These results indicate that DDC diet from different producers cause different levels of biliary injury. Therefore, it seems that Bio-Serv would be a better DDC diet producer for this study than Animal Specialty. This is because the ROSA mice on Bio-Serv DDC diet have higher biliary injury after 2 months on diet compared to S45D mice, which is similar to the long-term results seen in the previous study (Figure 26) (180). This is also enlightening, since a comparison of the DDC diet producers has not been previously studied. In this comparison we show that feeding mice DDC diet from these different producers can alter the serum results, which can ultimately affect the final results of a study. These findings lead us to believe that long-term exposure to Animal Specialty diet does not yield the same results in control animals that long-term exposure

to Bio-Serv diet does because the initial injury caused by the Animal Specialty diet is not as high the Bio-Serv diet.

Additionally, our pilot study utilizing AAV8-TBG-GFP and WT and TG on Bio-Serv DDC diet for 1 month showed that TG mice on DDC diet have more hepatocytes positive for cholangiocyte markers forming duct like shapes compared to WT mice on DDC diet. Unfortunately, this study was not pursued further since the labeling method used to monitor the hepatocyte-to-cholangiocyte transdifferentiation in this model was not permanent. However, this study and these findings did lead us to create and use the ROSA and S45D mice, which allowed us to permanently label hepatocytes with EYFP and monitor hepatocyte-to-cholangiocyte transdifferentiation more effectively.

Also of note, we did manage to get some ROSA mice to 2 months on Bio-Serv DDC diet before we received the batches of diet that caused the ROSA mice to die. During this time, the bile flow study performed on these mice showed that S45D mice on Bio-Serv DDC diet for 2 months have the fastest bile flow and the ROSA mice on Bio-Serv DDC diet had the slowest bile flow. These findings indicate that S45D mice after 2 months of Bio-Serv DDC diet exposure likely have more cholangiocyte-like hepatocytes or hepatocytes that have converted to cholangiocytes, which can be observed to an extent. S45D mice do have EYFP positive, hepatocyte-derived cholangiocytes present in and integrated into the bile ducts, unfortunately we were unable compare these results to ROSA mice. However, if the bile flow findings are indicative, it is likely the ROSA mice would not have any or very few hepatocyte-derived cholangiocytes. This is because these hepatocyte-derived cholangiocytes are likely helping to create new bile flow channels allowing bile to better escape the liver, which is why the S45D mice on DDC have increased flow. The ROSA mice likely have decreased bile flow because the hepatocytes are not being driven to

transdifferentiate, since these mice do not have β-catenin activity like the S45D mice. All of these preliminary findings, using Bio-Serv DDC diet, indicate that if injury is higher earlier, as is caused by Bio-Serv DDC diet, β-catenin activity does drive hepatocyte-to-cholangiocyte transdifferentiation, starting around 2 months of DDC diet exposure. However, it is currently unknown how transdifferentiation is affected in both the ROSA and S45D mice beyond 2 months and if the hepatocyte-derived cholangiocytes remain cholangiocytes on long term DDC diet exposure. Therefore, it is necessary that all previous experiments using Animal Specialty DDC diet must be performed again using Bio-Serv DDC diet, since the diets have been shown to yield different results at 2 months of exposure.

4.0 Wnt7b Regulates Cholangiocyte Proliferation and Function During Murine Cholestasis

In this section we characterize the effects Wnt7b β-catenin independent signaling has cholangiocyte proliferation during cholestatic injury. We predict that mice lacking Wnt7b in their cholangiocyte compartment and cholangiocyte and hepatocyte compartments will have exacerbated biliary injury after DDC diet exposure compared to control mice exposed to DDC diet. We will discuss our results and interpretations in detail.

4.1 Paper Summary

Previously we identified an upregulation of specific Wnt proteins in the cholangiocyte compartment during cholestatic liver injury and found that mice lacking Wnt secretion from hepatocytes and cholangiocytes showed fewer proliferating cholangiocytes and high mortality in response to 3,5-diethoxycarbonyl-1,4-dihydrocollidine (DDC) diet, a murine model of PSC. In vitro studies demonstrated that Wnt7b, one of the Wnts upregulated during cholestasis, induces proliferation of cholangiocytes in an autocrine manner and increases secretion of pro-inflammatory cytokines. Therefore, we hypothesized that loss of Wnt7b may exacerbate some of the complications of cholangiopathies by decreasing the ability of bile ducts to induce repair. Wnt7b-flox mice were bred with Krt19-cre mice to deplete Wnt7b expression in only cholangiocytes (CC), or with Alb-cre mice to delete Wnt7b expression in both hepatocytes and cholangiocytes (HC + CC). These mice were placed on DDC diet for one month then sacrificed for evaluation. Contrary to our expectations, we found that mice lacking Wnt7b from CC and HC + CC compartments had

improved biliary injury, but equivalent hepatic injury compared to controls. CC KO had sustained expression of biliary markers such as EpCAM, Sox9, and CK-19 and decreased fibrosis compared to control and HC + CC KO mice despite decreased cholangiocyte proliferation. CC and HC + CC KO mice on DDC diet also had more hepatocytes expressing cholangiocyte markers compared to WT mice on DDC diet, indicating that Wnt7b suppression promotes hepatocyte reprogramming. **Conclusion:** Wnt7b induces a pro-proliferative, pro-inflammatory program in cholangiocytes, and its loss is compensated for by conversion of hepatocytes to a biliary phenotype during cholestatic injury.

4.2 Background

Primary sclerosing cholangitis (PSC) is a chronic cholestatic liver disorder that is characterized by inflammation and fibrosis of the bile ducts, which can lead to end-stage liver disease and reduced life expectancy. Because the etiology of this disease is not fully understood, effective medical therapies are scarce and, in most cases, the only life extending treatment currently available is liver transplantation. Of the patients fortunate enough to receive a liver transplant up to 20% will have recurrence of disease (159, 265, 266). Therefore, an effective treatment for PSC is critically needed, as the demand for organs available for transplant increases each year.

It is well known the liver is the only internal organ capable of regeneration; however, the bile duct is often overlooked when touting the liver's regenerative ability. Much like hepatocytes, cholangiocytes, the epithelial cells that comprise the bile ducts, also exhibit a remarkable ability to regenerate. Following injury, cholangiocytes proliferate to form the tubular structures necessary

to ensure bile modification and transport. The restitution of these biliary networks is critical in maintaining liver function and preventing further injury due to cholestasis. During regeneration after acute liver injury, hepatocytes and cholangiocytes typically proliferate to repopulate their own cell types. However, during severe biliary or hepatic injury, regeneration of one of the two epithelial cell compartments can become compromised. This is when a secondary method of regeneration can occur: hepatocyte-to-cholangiocyte or cholangiocyte-to-hepatocyte transdifferentiation (221, 224, 225, 267). These two cell populations can become and act as facultative stem cells for one another, interconverting to maintain tissue integrity (217). Thus, a therapy that induces a healthy cholangiocyte population, either from hepatocyte-derived cholangiocytes or native cholangiocytes, to proliferate and repair bile ducts could be a crucial treatment for patients suffering from cholestatic liver diseases.

The Wnt/β-catenin signaling pathway is an important regulatory axis in liver physiology and pathology, due in large part to its role as a promoter of regeneration and repair (245). Recent studies have also demonstrated that Wnts are expressed during biliary disease as well. Activation of Wnt signaling is seen in the livers of PSC patients, and Wnt ligands are associated with proliferating biliary cells in 3,5-diethoxycarbonyl-1,4-dihydrocollidine (DDC) diet, a model for biliary injury and chronic cholestasis (202, 268). Other studies have shown upregulation of specific Wnts in cholangiocytes after DDC diet, and in a mouse model of cholangiocarcinoma, these ligands induced cholangiocyte proliferation (78, 269). Our lab has also shown that Wnt proteins are expressed in the cholangiocyte population during cholestatic liver injury, and that mice lacking Wnt secretion from both hepatocytes and cholangiocytes had fewer proliferating cholangiocytes and high mortality in response to DDC diet (69). However, a recent manuscript has shown that during biliary injury cholangiocytes produce Wnts that promote the formation of ductal scars by

acting via the Wnt-PCP pathway to induce fibrogenic cytokine production (270). Therefore, further mechanistic analyses are needed to determine the role of specific Wnts in the process of biliary injury and repair.

One of the Wnts that has been identified to be upregulated during cholestasis is Wnt7b, which was shown to induce cholangiocyte proliferation in an autocrine manner independent of β-catenin activity (69, 269). Therefore, we hypothesized that loss of Wnt7b may exacerbate some of the complications caused by cholangiopathies by decreasing the ability of bile ducts to induce repair. To test this hypothesis, we created both cholangiocytes (CC)-specific Wnt7b knockouts (KO) or KO in which Wnt7b is deleted from both hepatocytes and cholangiocytes (HC + CC) and subjected these mice to cholestatic liver injury. We found that both CC KO and HC + CC KO mice had improved biliary injury; however, this is not due to changes in ductular mass but rather to increased numbers of hepatocytes expressing biliary markers, which compensates for the inability of cholangiocytes to proliferate due to the lack of Wnt7b.

4.3 Materials and Methods

4.3.1 Cell Lines, Transfection, and Luciferase Assay

Small cell cholangiocytes (SMCCs) were plated at $2x10^5$ cells/well in a 6 well plate and transfected with 2.5 μg control or Wnt7b plasmid, described elsewhere (69), and 50μM negative or β-catenin siRNA (Thermo Fisher Scientific, Waltham, MA) using Lipofectamine 3000 (Invitrogen, Carlsbad, CA), as per the manufacturer's instructions. Cell proliferation was measured 48 hours post transfection using a colorimetric cell viability kit I (WST-8) (PromoCell, Heidelberg,

Germany) or thymidine incorporation assay as described previously (271). Along with the control and Wnt7b plasmids, cells were also transfected with 2.5 µg of a luciferase TOPFlash plasmid (Upstate Biotechnology, Lake Placid, NY)(69) using Lipofectamine 3000. 48 hours post transfection, luciferase activity was analyzed using the Dual-Luciferase Reporter Assay System (Promega, Madison, WI), as per the manufacturer's instructions.

For the ELISA array, SMCCs were plated and transfected with control or Wnt7b plasmid as described above. 24 hours post-transfection cell media was changed, and 48 hours later, the now conditioned media was collected and analyzed using the chemiluminescent per the manufacturer's instructions. WST-8, luciferase assay, and ELISA assay results were collected using a Synergy™ HTX Multi-Mode Microplate Reader from BioTek Instruments.

4.3.2 Animal Models

All animals were housed in light- and temperature-controlled facilities and maintained in accordance with the Guide for Care and Use of Laboratory Animals and the Animal Welfare Act, and all studies were performed in accordance with the guidelines of the Institutional Animal Use and Care Committee at the University of Pittsburgh School of Medicine and the National Institutes of Health (protocol number 20077675). Control mice ($K19^{CreERT}$/Rosa-$stop^{flox/flox}$-EYFP) were produced by breeding $K19^{CreERT}$ (Jackson Laboratories, Bar Harbor, ME) with Rosa-$stop^{flox/flox}$-EYFP (Jackson Laboratories, Bar Harbor, ME). CC KO mice ($K19^{CreERT}$/Rosa-$stop^{flox/flox}$-EYFP/ $Wnt7b^{c3}$ mice) were produced by breeding the control $K19^{CreERT}$/Rosa-$stop^{flox/flox}$-EYFP mice with $Wnt7b^{c3}$ mice (Jackson Laboratories). HC + CC KO mice (Albumin-Cre/ Rosa-$stop^{flox/flox}$-EYFP/ $Wnt7b^{c3}$) were produced by breeding the Rosa-$stop^{flox/flox}$-EYFP mice with $Wnt7b^{c3}$ mice, then breeding the Rosa-$stop^{flox/flox}$-EYFP/$Wnt7b^{c3}$ offspring with Albumin-$Cre^{+/-}$ mice (Jackson

Laboratories, Bar Harbor, ME). To delete Wnt7b and label cholangiocytes in $K19^{CreERT}$/Rosa-$stop^{flox/flox}$-EYFP/ $Wnt7b^{c3}$ mice, 3 doses of 10 mg/kg tamoxifen were given every other day starting at 21 days old. At 8 weeks of age all mice were then placed on 0.1% 3,5-diethoxycarbonyl-1,4-dihydrocollidine (DDC) diet (Animal Specialties and Provisions LLC, Quakertown, PA) or left on standard mouse chow as a control for 1 month. Mice were then sacrificed, and livers and blood serum collected. Livers were divided and fixed in 10% formalin and processed for paraffin embedding, or frozen in liquid nitrogen and stored at −80 °C. For WT on control diet n = 10, for WT on DDC diet n = 6, for CC KO on control diet n = 13, for CC KO on DDC diet n = 8, for HC + CC KO on control diet n = 4, and for HC + CC KO on DDC diet n = 8. Both male and female mice were used for experimentation. All mice were in a C57Bl6 background and maintained in ventilated cages under 12h light/dark cycles with access to enrichment, water and either standard chow or DDC diet ad libitum.

4.3.3 Serum Biochemistry

Blood serum was sent to and biochemically analyzed by The University of Pittsburgh Medical Center Clinical Chemistry lab. Alkaline phosphatase (ALP), aspartate aminotransferase (AST), alanine transaminase (ALT), total bilirubin and direct bilirubin were measured in all samples.

4.3.4 Immunohistochemical Analysis

Paraffin-embedded liver tissues were sectioned at 4 μm thick. Sections were stained with hematoxylin and eosin (H&E) or Picro-Sirius Red (Abcam, Cambridge, UK) and Sirius red images

were quantified using ImageJ Fiji ImageJ Fiji (version 2.0.0-rc-68/1.521; https://imagej.nih.gov/ij/). Images were split into red, green and blue channels, and the green channel was selected for further analysis due to the optimal color separation of the staining. The fibrotic regions were isolated by using the Threshold setting 0 for the upper level and 145 for the lower level. The percentage of the stained area to the total image was determined. Five images per mouse liver (n=3 mice) were quantified for each genotype and diet.

Immunohistochemistry on paraffin-embedded sections was performed on mouse livers as described elsewhere.(177) Primary antibodies used were A6 (26 µg/ml DSHB, University of Iowa) and PCNA antibody (1:4000, Santa Cruz Biotechnology, Dallas, TX). Secondary antibodies were goat anti-rabbit, and donkey anti-goat (Chemicon, Temecula, CA) and were used at 1:400, and staining was detected with 3,3′-diaminobenzidine detection systems after incubation with the Avidin–Biotin Complex Kit (Vector Laboratories, Burlingame, CA). For immunofluorescence staining the primary antibodies were anti-GFP (1:200, Abcam, Cambridge, UK) and Anti-Cytokeratin (1:200 DAKO, Glostrup, Denmark) and the secondary antibodies were Alexa Fluor 555 goat anti-chicken IgG (1:500, Invitrogen) and Alexa Fluor 488 goat anti-rabbit IgG (1:500, Invitrogen). Images were taken on a Nikon Eclipse Ti.

Ductular response was quantified using A6 IHC stains using ImageJ Fiji in a similar manner to quantify fibrosis. For A6 IHC blue channel was selected for further analysis due to the optimal color separation and the A6 positive regions were isolated by using the Threshold setting 50 for the upper lever and 115 for the lower level. These Threshold levels allowed for quantification of only stained cells and not porphyrin plugs caused by DDC exposure. The percentage of the stained area to the total image was determined. Five images per mouse liver (n=3 mice) were quantified for each genotype and diet.

4.3.5 Quantitative Real-Time PCR

Total RNA was isolated from frozen liver tissue using a tissue Homogenizer150 (Thermo Fisher Scientific) and Trizol reagent (Invitrogen). Reverse-transcription PCR was performed as described elsewhere (177). Real-time PCR was performed using SYBR Green (Thermo Fisher Scientific) on a CFX96 Touch™ Real-Time PCR Detection System (Bio-Rad Laboratories, Hercules, CA). Changes in target mRNA were normalized to glyceraldehyde-3-phosphate dehydrogenase (GAPDH) mRNA for each sample. P values are presented as fold change over the average from 3 normal livers. Each sample was run in triplicate. Sequences of primers are available in **Table 3**.

Table 3. Primers used for quantitative RT-PCR analysis in Section 4.0

CK19, cytokeratin 19; Sox9, sex-determining region Y-box transcription factor 9; EpCAM, epithelial cell adhesion molecule.

Primer name	Sequence
Wnt7b (forward)	5′-ACCGCATGAAGCTGGAATGTA-3′
Wnt7b (reverse)	5′-CCTCGCGGAACTTAGGTAGC-3′
Wnt7b Exon 3 (forward)	5′-CAGCTACGCAGCTACCAGAA-3′
Wnt7b Exon 3 (reverse)	5′-GTCCTCCTCGCAGTAGTTGG-3′
β-catenin (forward)	5′-GGGTCCTCTGTGAACTTGCTC-3′
β-catenin (reverse)	TTCTTGTAATCCTGTGGCTTGTCC-3′
CK19 (forward)	5′-GACCTGGAGATGCAGATTGAG-3′
CK19 (reverse)	5′-GCTCCTCAGGGCAGTAATTT-3′
Sox9 (forward)	5′-CAGGCAAGAATTGGGCAAAG-3′
Sox9 (reverse)	5′-CCTCCCAACACGCAGTAAA-3′
EpCAM (forward)	5′-GTGAATGCCAGTGTACTTCCTA -3′
EpCAM (reverse)	5′-GCTGTGAGTCATTTCTGCTTTC-3′
Wnt7a (forward)	5′-CGGACGCCATCATCGTCATA-3′
Wnt7a (reverse)	5′-CAGTTCCAACGGCCATTTCG -3′

4.3.6 Protein Extraction and Western Blot Analysis

Proteins were extracted, and Western blot analysis was performed as previously described (242). Briefly, proteins were extracted from whole-cell liver lysates, and denatured proteins were separated on 10% SDS-PAGE gels and transferred to polyvinylidene difluoride membranes. Membranes were blocked using 5% nonfat dry milk or 5% bovine serum albumin in 0.1% Triton X-100 in Tris-buffered saline and incubated with primary antibodies (diluted in 3% blocking media). The following primary antibodies were used: glyceraldehyde-3-phosphate dehydrogenase (GAPDH; 1:5000; Invitrogen, Carlsbad, CA), purified mouse anti–β-catenin (1:500; BD Biosciences, San Jose, CA), nonphosphorylated (active) β-catenin (Ser33/37/Thr41) (1:1000; Cell Signaling Technology, Danvers, MA), and phosphorylated β-catenin (Ser675; D2F1; 1:1000; Cell Signaling Technology). Horseradish peroxidase–conjugated secondary antibodies (1:20,000 diluted in 3% blocking media; Santa Cruz Biotechnology) were used and blots were visualized using the Enhanced Chemiluminescence System (GE Healthcare, Little Chalfont, UK).

4.3.7 Confocal microscopy and image analysis of mRNA expression by RNAscope

In situ detection of GFP, WNT7b, and glutamine synthetase mRNA expression was achieved by using the RNAscope kit (Advanced Cell Diagnostics, Hayward, CA) according to the manufacturer's protocol. Glutamine synthetase served as a positive control. In short, fixed frozen liver sections were pretreated with protease and incubated with probe targeting Wnt7b, GFP, and Glul (glutamine synthetase) (Advanced Cell Diagnostics) for 2h at 40°C. The slides were washed using wash buffer (Advanced Cell Diagnostics) at room temperature after each hybridization step, and lastly DAPI (Advanced Cell Diagnostics) was applied for visualization of the nuclei. Images

were acquired with an Olympus IX73 inverted microscope (Olympus America, Center Valley, PA) with a Hamamatsu ORCA-ER digital camera (Hamamatsu Corporation, Bridgewater, NJ) at 60x magnification. Image stacks (1344x1024 pixels; 0.2 μm z-steps) of 100% of the tissue thickness were taken across the liver section and were stereologically selected using a grid of 100μm^2 frames spaced by 1000μm. Image collection and processing were performed using Slidebook 6.0 (Intelligent Imaging Innovations, Inc., Denver, CO) and Matlab (MathWorks, Natick, MA) software. First, an average projection of image stacks for a site was created to make a 2-dimensional image of cells and their corresponding punctate mRNA grains. Then, a Gaussian channel was constructed for each channel by calculating a difference of Gaussians using sigma values of 0.7 and 2. Images were then separated into quantitative TIFF files of each individual channel and transferred to the HALO image analysis platform equipped with a fluorescent *in situ* hybridization add-on (Version 3.0, Indica Labs, Albuquerque, NM, USA). Using HALO software, DAPI-stained nuclei were quantified as any 40-355μm^2 object; puncta corresponding to Wnt7b and GFP were quantified as any 0.1-0.5μm^2 object. After determining the average puncta density levels for each probe (Wnt7b/wildtype: 0.43 puncta/DAPI-stained nucleus; GFP/wildtype: 1.28 puncta/DAPI-stained nucleus), thresholds were set: 1 mRNA grain for Wnt7b, 4 mRNA grains for GFP. These thresholds represented ~3 times the smaller observed density level and were used as cutoffs for positive cells to eliminate false positives that occur due to nuclei neighboring positive cells. Therefore, a DAPI-stained nucleus was deemed Wnt7b$^+$ if it contained a minimum of 1 Wnt7b puncta within 5 μm of the nucleus edge, and a cell was determined to be GFP$^+$ if it contained a minimum of 4 GFP puncta within 5μm of the nucleus edge.

4.3.8 Statistical Analysis

Data was analyzed and presented as mean, standard deviation, and/or individual data points using Prism GraphPad 7.0c. P values were determined using appropriate analyses for the data. The tests used were two-tailed Student t test and one-way analysis of variance (ANOVA) or two-way ANOVA followed by an appropriate post-hoc test. $P < 0.05$ was considered statistically significant.

4.4 Results

4.4.1 Overexpression of Wnt7b in cholangiocytes induces cell proliferation independent of β-catenin signaling *in vitro*

Previously, we showed that Wnt7b secreted by cholangiocytes induces proliferation in biliary cells through non-canonical Wnt signaling mechanisms (69). To verify these findings, we transfected small cell cholangiocytes (SMCCs) with control or Wnt7b plasmid, treated with β-catenin or control siRNA, and measured cell proliferation. We were able to achieve 6.5-fold higher Wnt7b expression in cells transfected with the Wnt-carrying plasmid compared to control, while β-catenin expression was decreased by 75% compared to control (Figure 27). Using both thymidine incorporation and a colorimetric proliferation assay (WST-8), we confirmed that overexpression of Wnt7b promotes cholangiocyte proliferation in an autocrine manner (Figure 28A-B), and that this process occurs independent of β-catenin activity, as knockdown of β-catenin does not affect cell proliferation induced by Wnt7b (Figure 28B). Furthermore, Wnt7b

overexpression in SMCCs reduces, rather than induces, β-catenin activity, as seen by the decrease in TOPFlash luciferase activity compared to cells without Wnt7b expression (Figure 28C).

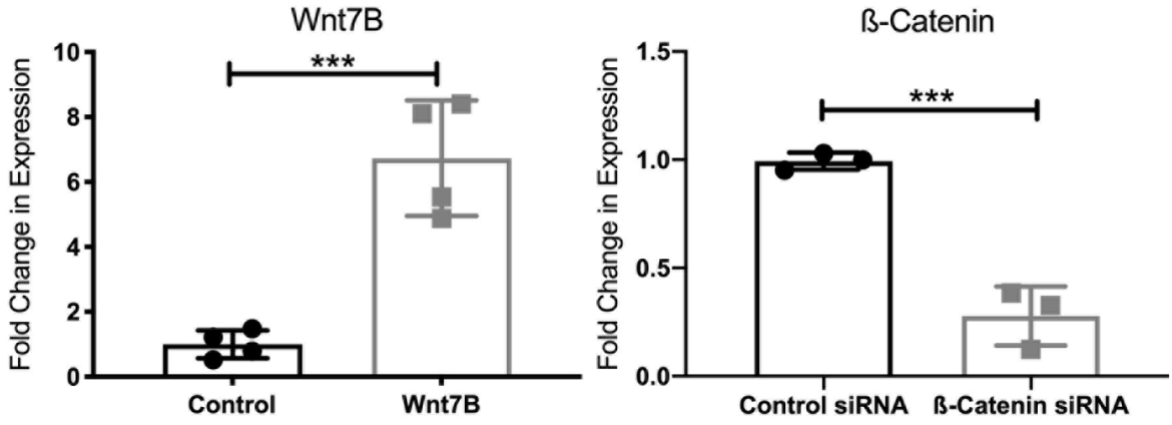

Figure 27. Quantitative RT-PCR analysis demonstrates Wnt7b overexpression and β-catenin suppression in SMCCs

SMCCs transfected with Wnt7b plasmids have significantly increased expression of Wnt7B compared to cells transfected with control plasmid. SMCCs treated with β-catenin siRNA have significantly downregulated expression of β-catenin compared to cells treated with control siRNA. ∗∗∗P < 0.001.

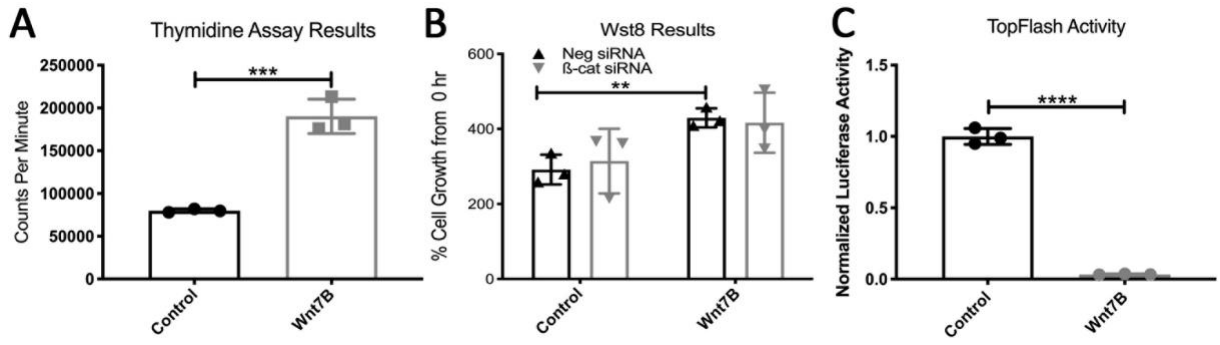

Figure 28. Overexpression of Wnt7B in SMCC culture induces cells proliferation independent of β-catenin activity.

(A) Thymidine incorporation assay demonstrates that Wnt7b overexpression induces cholangiocyte proliferation *in vitro*. (B) Wst8 colorimetric assay demonstrates that Wnt7b overexpression induces cholangiocyte proliferation which is not inhibited in the presence of β-catenin siRNA. (C) Luciferase reporter of β-catenin activity, TOPFlash, demonstrates that Wnt7b overexpression does not induce β-catenin activity. ∗∗P < 0.01, ∗∗∗P < 0.001, and ∗∗∗∗P < 0.0001.

4.4.2 Overexpression of Wnt7b induces an inflammatory phenotype in cultured cholangiocytes

Cholangiocyte proliferation, which is observed during cholestasis, is often associated with an "activated" phenotype that is characterized by increased secretion of cytokines and growth factors (272). As Wnt7b induces cholangiocyte proliferation in an autocrine manner, we wanted to determine if it also induced production of these inflammatory mediators. Using a mouse cytokine ELISA kit, we found that TNF-α and IL-12 were upregulated significantly in conditioned media from Wnt7b-expressing SMCCs compared to those with control plasmid, while other cytokines and growth factors such as IL-1α, PDGF-BB and IL-6 trended higher as well (Figure 29). Thus, Wnt7b enhances the immunomodulatory response in cholangiocytes during cholestasis.

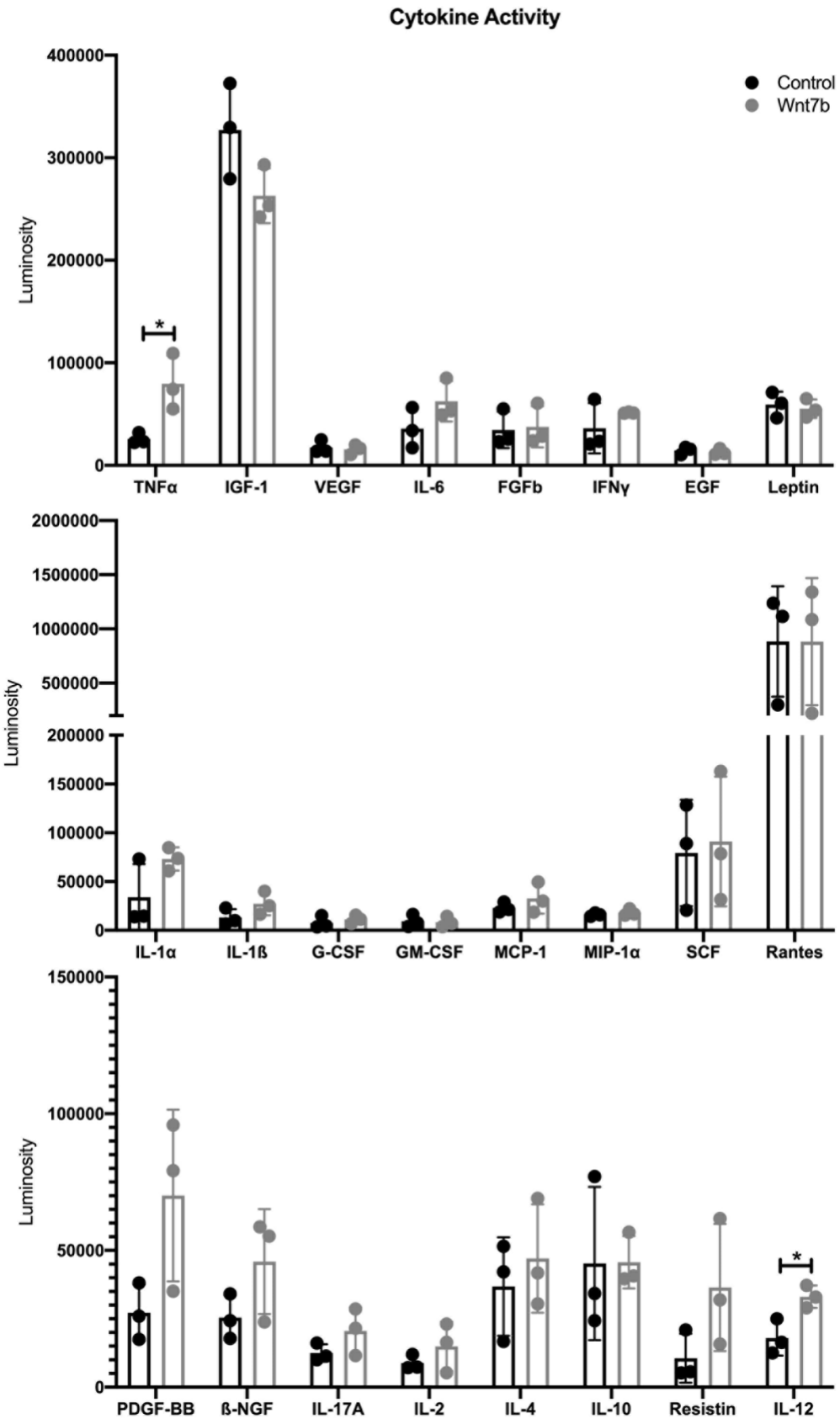
Cytokine Activity
Control
Wnt7b
Luminosity
400000
300000
200000
100000
0
*
TNFα
IGF-1
VEGF
IL-6
FGFb
IFNγ
EGF
Leptin
2000000
1500000
1000000
500000
200000
150000
100000
50000
0
IL-1α
IL-1ß
G-CSF
GM-CSF
MCP-1
MIP-1α
SCF
Rantes
150000
100000
50000
0
PDGF-BB
ß-NGF
IL-17A
IL-2
IL-4
IL-10
Resistin
IL-12
*

Figure 29. Wnt7b overexpression in cholangiocyte cell culture promotes upregulation of commonly altered cytokines

ELISA analysis of (top graph) tumor necrosis factor alpha (TNFα), insulin-like growth factor 1 (IGF-1), vascular endothelial growth factor (VEGF), interleukin 6 (IL-6), basic fibroblast growth factor (FGFb), interferon gamma (IFNγ), epidermal growth factor (EGF), leptin, (middle graph) interleukin 1 alpha (IL-1α), interleukin 1 β (IL-1β), granulocyte colony stimulating factor (G-CSF), granulocyte-macrophage colony-stimulating factor (GM-CSF), monocyte chemoattractant protein-1 (MCP-1), macrophage inflammatory protein 1-alpha (MIP-1α), stem cell factor (SCF), Rantes (Regulated on Activation, Normal T Expressed and Secreted), (bottom graph) platelet-derived growth factor (PDGF-BB), nerve growth factor β (β-NGF), interleukin 17A (IL-17A), interleukin 2 (IL-2), interleukin 4 (IL-4), interleukin 10 (IL-10), resistin, and interleukin 12 (IL-12) show that Wnt7b overexpression promotes upregulation of common cytokines and growth factors. *$P < 0.05$.

4.4.3 Wnt7b deletion *in vivo* improves biliary injury after 1 month of DDC exposure

In order to generate conditional KO of Wnt7b, Wnt7b-flox mice were bred with Krt19-cre mice to deplete Wnt7b expression in only cholangiocytes (CC), or with Alb-cre mice to delete Wnt7b expression in both hepatocytes and cholangiocytes (HC + CC). Both CC KO and HC + CC KO mice carry the Rosa-stop$^{flox/flox}$-EYFP gene, which was used to assess efficiency of Wnt7b deletion from these cell populations. Figure 30A shows that approximately 50% of cholangiocytes in the CC KO mice were EYFP+, while 100% of cholangiocytes and hepatocytes were positive for EYFP in the HC + CC KO. RNAscope for Wnt7b also confirms a greater than 50% decrease in Wnt7b expression in cholangiocytes from CC KO mice (Figure 31).

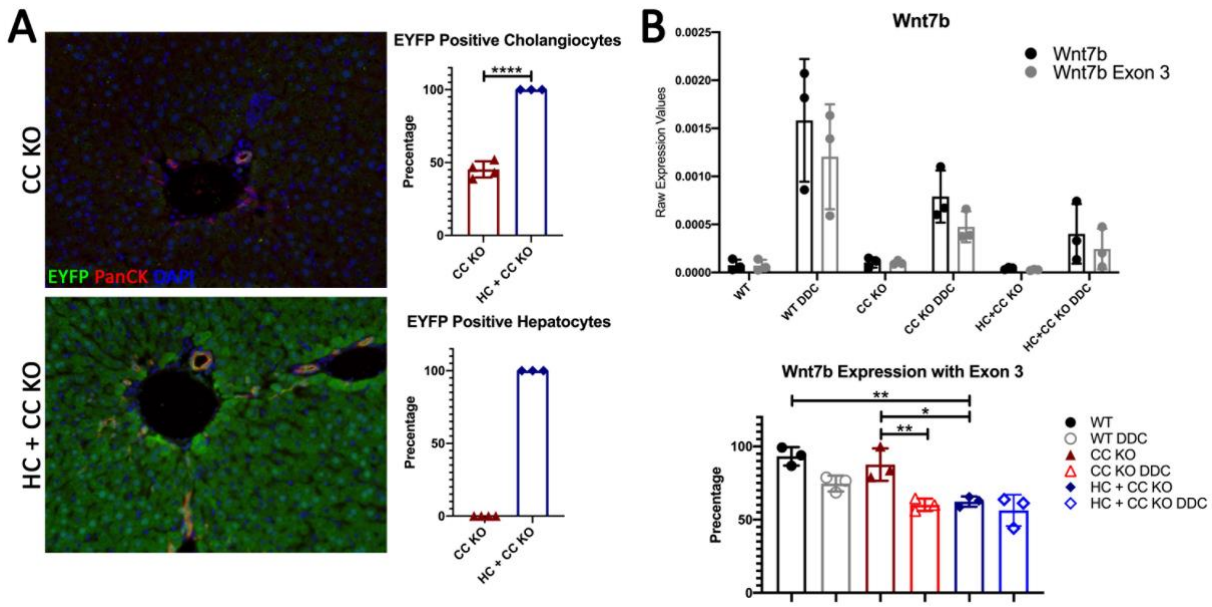

Figure 30. Confirmation of Wnt7b depletion in cholangiocyte-specific and liver-specific KO

(A) EYFP (green), PanCK (red), and DAPI (blue) immunofluorescence and quantification shows that about 50% of cholangiocytes and 0% of hepatocytes are positive for EYFP expression in CC KO mice, indicating 50% efficiency of Wnt7b deletion in the cholangiocyte population. In HC + CC KO mice, 100% of cholangiocytes and hepatocytes have EYFP expression, indicating that Wnt7b knockout is complete in both cell populations. (B) Raw values from the quantitative RT-PCR analysis show loss of Wnt7b in KO mice (top). Cre-mediated removal of exon 3 from Wnt7bc3 floxed mice creates the Wnt7bd3-null allele. Primers were designed to distinguish between functional Wnt7b protein (Wnt7b Exon 3) and the combination of Wnt7b and the untranslated null product (Wnt7b). Although Wnt7b expression increases in all genotypes after DDC diet, the expression is significantly less in CC KO and HC + CC KO than in WT. Additionally, the percentage of Wnt7b expression that contains exon 3 decreases in the KO after DDC by at least 40% (bottom). The persistence of full-length Wnt7b transcript in the KO indicates that either deletion from the cell types of interest is incomplete, or its loss is compensated for by other cell types. *P < 0.05, **P < 0.01, and ****P < 0.0001. Original magnification, 200x.

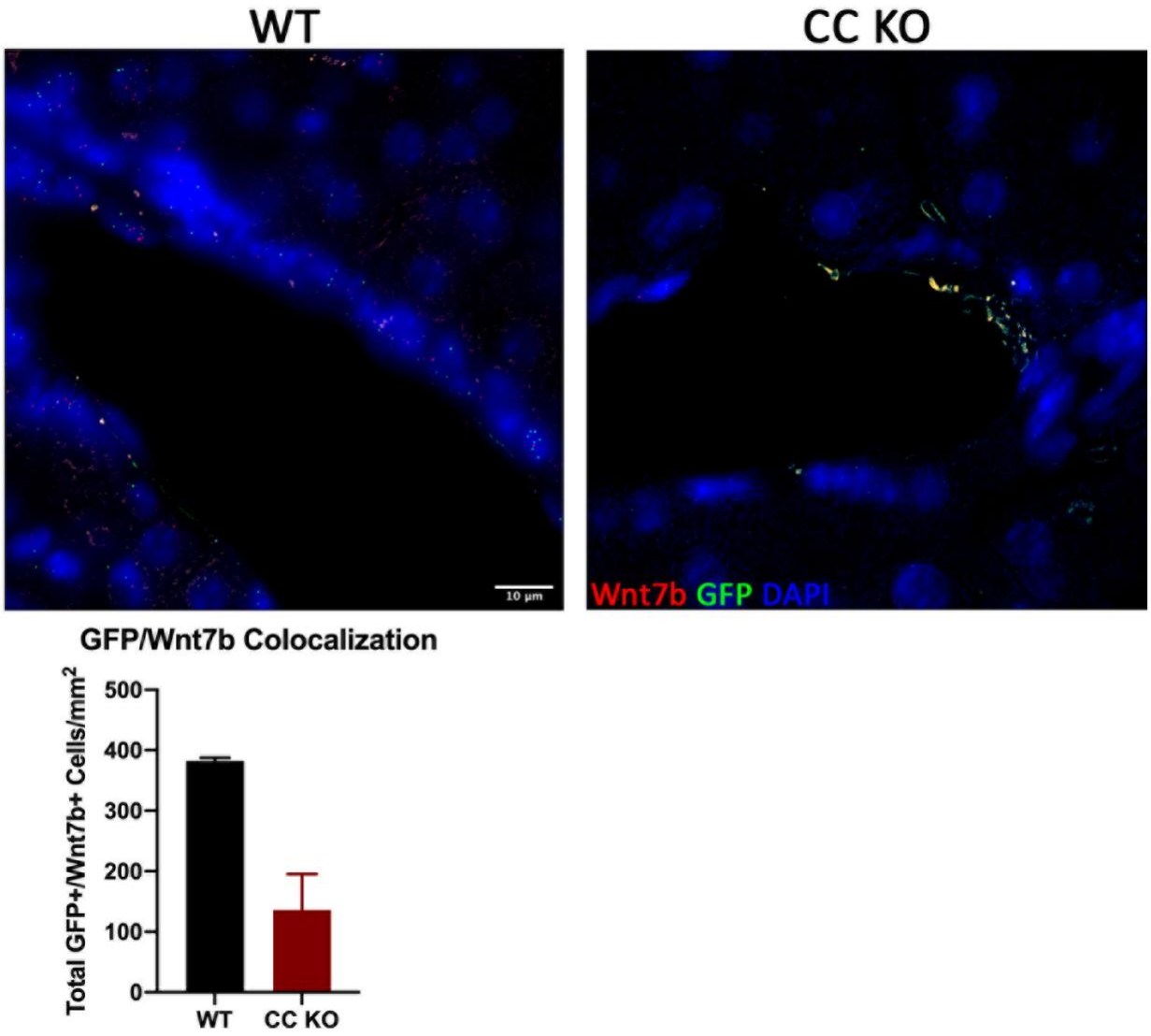

Figure 31. RNAscope for Wnt7b confirms deletion in CC KO

Top, in situ hybridization (ISH) for Wnt7b RNA (red) shows that it is present in cholangiocytes of WT mice (left image), but not in cholangiocytes of CC KO mice (right). GFP RNA expression in both WT and CC KO confirms efficient recombination of Rosa-stopflox/flox-EYFP by tamoxifen in cholangiocytes. Representative images of zone 1 are shown (original magnification, x600). Below, quantification of Wnt7b expression as a percentage of GFP+ cells shows that expression of Wnt7b in CC KO is about 30% that of WT.

To assess the impact of Wnt7b loss in the setting of cholestatic liver disease, we then fed WT, CC KO and HC + CC KO mice control or DDC diet. Figure 30B shows that while Wnt7b expression increases in all genotypes after DDC diet, CC KO and HC + CC KO have significantly less full-length Wnt7b protein than WT, confirming loss of Wnt7b from these cell types. Analysis

of serum biochemistry after one month showed that CC KO and HC + CC KO mice fed DDC diet have significantly decreased alkaline phosphatase (ALP) levels compared to WT mice on DDC (Figure 32A), indicating that both types of KO have less biliary injury compared to WT mice. Interestingly HC + CC KO DDC-treated mice have normalized conjugated and total bilirubin levels compared to both WT and CC KO mice fed DDC diet, suggesting that the HC + CC KO mice have even less cholestatic injury compared to the other mice. However, hepatic injury is sustained across all three mouse models as indicated by serum alanine aminotransferase (ALT) and aspartate aminotransferase (AST) (Figure 32B). ALT is equally high in all three mouse models fed DDC diet, and AST also remains high among the three models, but HC + CC KO mice on DDC have significantly decreased AST levels compared to WT mice on DDC. Thus, rather than worsening the phenotype, deletion of Wnt7b protected mice from biliary injury during DDC-induced cholestasis.

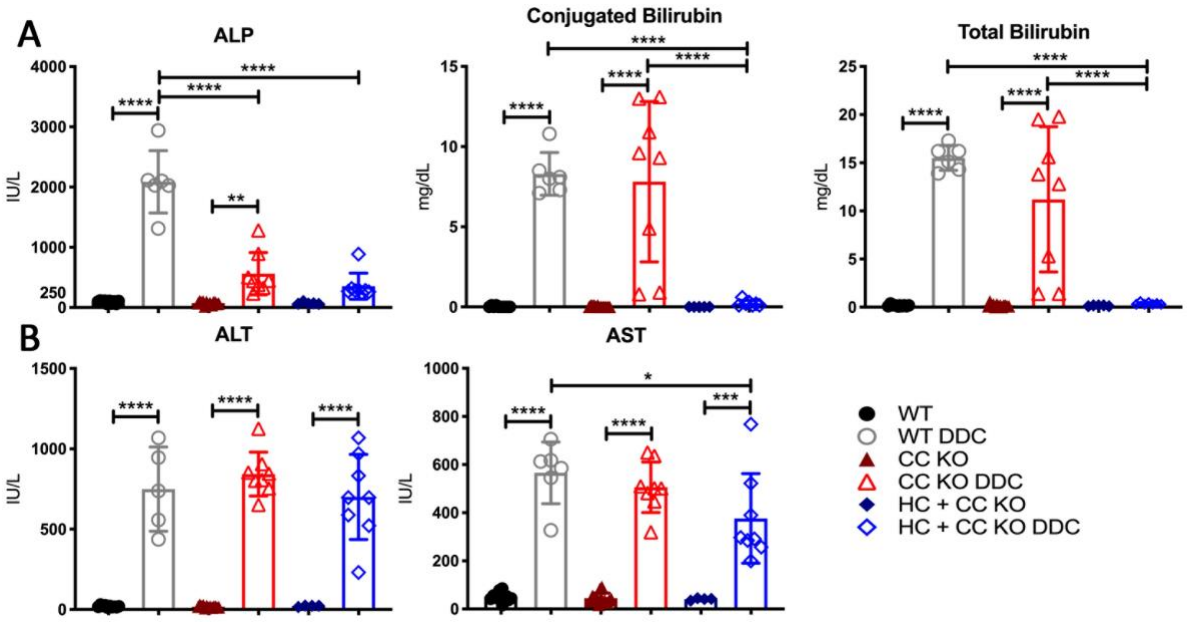

Figure 32. Blood serum results indicate Wnt7b knockout improves biliary injury after 1 month of DDC exposure

(A) Blood serum levels of ALP, conjugated bilirubin and total bilirubin show decreased biliary injury in mice lacking Wnt7b in both cholangiocytes only and cholangiocytes and hepatocytes when exposed to DDC diet for 1 month compared to WT mice. (B) Blood serum levels of ALT and AST indicate no changes in hepatic injury in mice lacking Wnt7b compared to WT mice on DDC diet for 1 month. $*P < 0.05$, $**P < 0.01$, $***P < 0.001$, and $****P < 0.0001$

4.4.4 Wnt7b knockout has no effect on parenchymal injury or fibrosis

To investigate parenchymal injury between the different genotypes, hematoxylin and eosin (H&E) stains of liver sections were performed. Both types of KO mice fed DDC diet have portal damage, including inflammation and ductular response, that is comparable to WT fed DDC (Figure 33A). Therefore, Wnt7b knockout has no effect on cholestasis-induced parenchymal injury. To determine if lower ALP levels in Wnt7b KO mice on DDC diet correlate with decreased portal fibrosis, Sirius Red staining and quantification was used to assess the fibrotic content of these livers. Fibrosis in CC KO mice on DDC trended lower than in WT, while fibrosis in HC + CC KO mice on DDC was comparable to WT (Figure 33B). Therefore, we found no direct correlation between serum ALP and ductular fibrosis in our models.

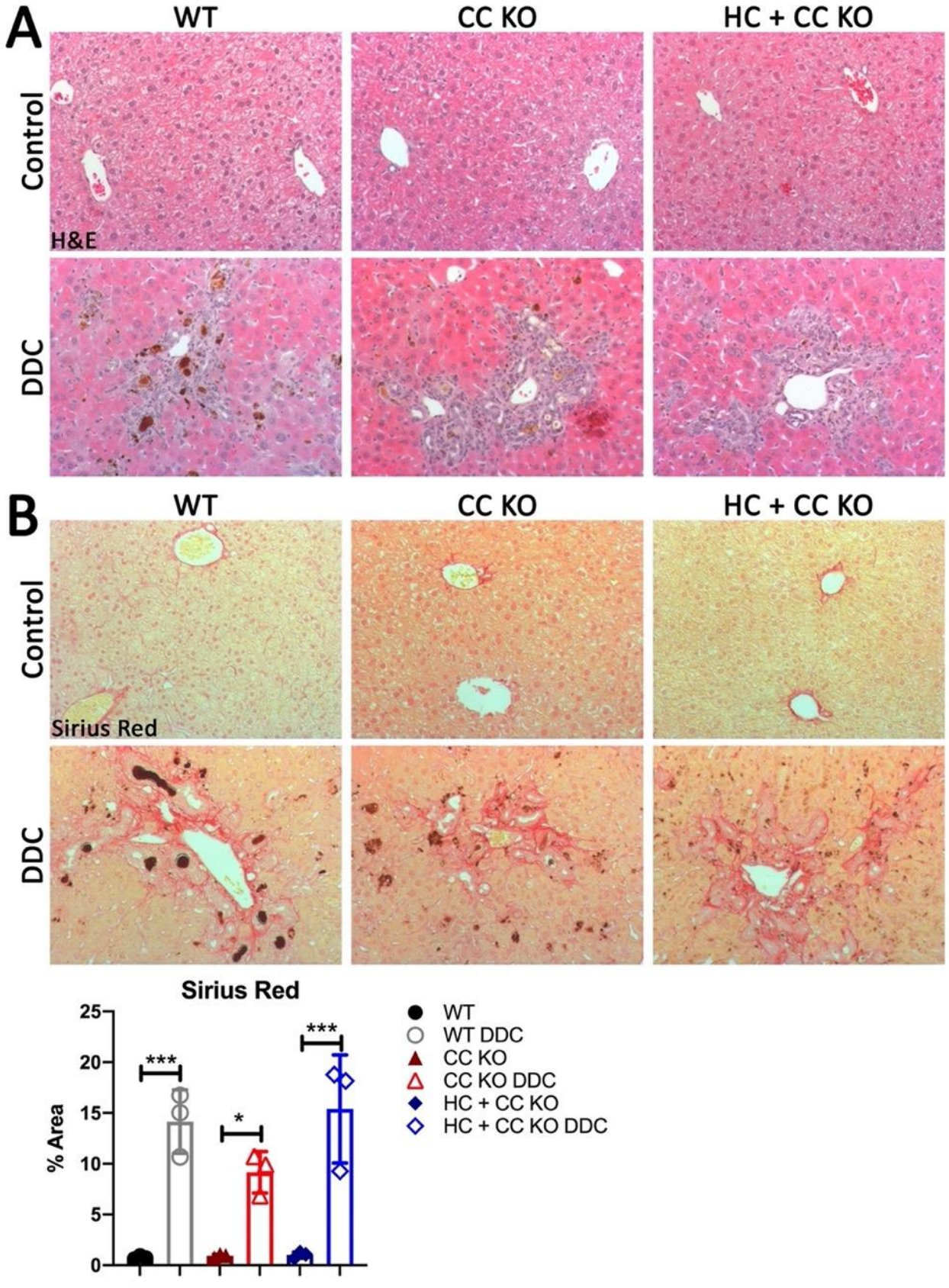
A
WT
CC KO
HC + CC KO
Control
DDC
H&E
B
WT
CC KO
HC + CC KO
Control
DDC
Sirius Red
Sirius Red
% Area
25
20
15
10
5
0
***
*
***
WT
WT DDC
CC KO
CC KO DDC
HC + CC KO
HC + CC KO DDC

Figure 33. Wnt7b KO has no effect on ductular response and fibrosis

(A) H&E stains of liver sections show no difference in parenchymal injury and ductular response between WT, CC KO, and HC + CC KO mice fed DDC diet. (B) Sirius red stains of liver sections and quantification of the images show no difference in fibrosis between the mice fed DDC diet; however the CC KO mice trend toward decreased fibrosis. $*P < 0.05$ and $***P < 0.001$. Original magnification, x200.

4.4.5 Wnt7b regulates cholangiocyte proliferation and ductular response *in vivo*

Since we have previously shown that loss of Wnt secretion from hepatocytes and cholangiocytes leads to fewer CK19+Ki67+ cells after DDC treatment, we next assessed the mitogenic role of Wnt7b *in vivo* by quantifying the number of proliferating cell nuclear antigen (PCNA)-positive cholangiocytes after DDC (69). As expected, both CC KO and HC + CC KO mice on DDC diet have significantly fewer PCNA-positive cholangiocytes compared to WT mice on DDC diet (Figure 34), indicating that loss of Wnt7b directly affects cholangiocyte proliferation. Quantitative RT-PCR analysis of cholangiocyte markers epithelial cell adhesion molecule (EpCAM), cytokeratin 19 (CK-19), and sex-determining region Y-box transcription factor 9 (Sox9) shows that CC KO mice on DDC diet have sustained expression of cholangiocyte markers compared to WT mice on DDC diet (Figure 35A). However, HC + CC KO mice on DDC diet trend toward decreased cholangiocyte marker expression compared to WT and CC KO on DDC diet (Figure 35A). These results are also mirrored in histological images of the early cholangiocyte marker A6. While CC KO mice have sustained ductular reaction compared to WT mice on DDC diet, HC + CC KO mice on DDC diet have significantly less ductular response compared to WT mice on DDC diet (Figure 35B-C). These results indicate that the suppressed ductular reaction seen in Wnt7b HC + CC KO is a result of decreased cholangiocyte proliferation.

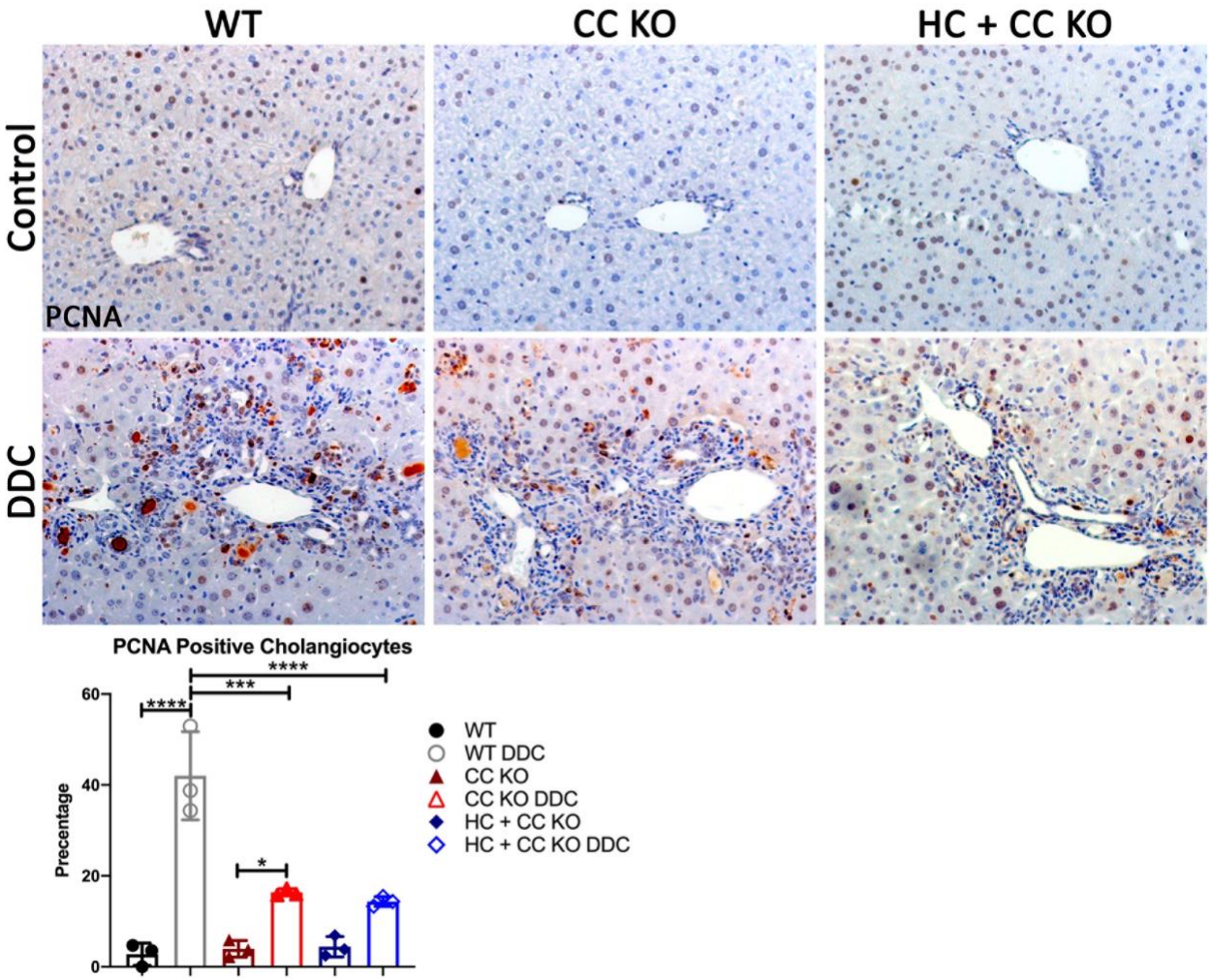

Figure 34. Wnt7b knockout inhibits cholangiocyte proliferation

Representative images and quantification of proliferation cell nuclear antigen (PCNA) show that Wnt7b knockout in both the cholangiocyte compartment and the cholangiocyte and hepatocyte compartment inhibits cholangiocyte proliferation in mice fed DDC diet. ∗P < 0.05, ∗∗∗P < 0.001, and ∗∗∗∗P < 0.0001. Original magnification, 200x.

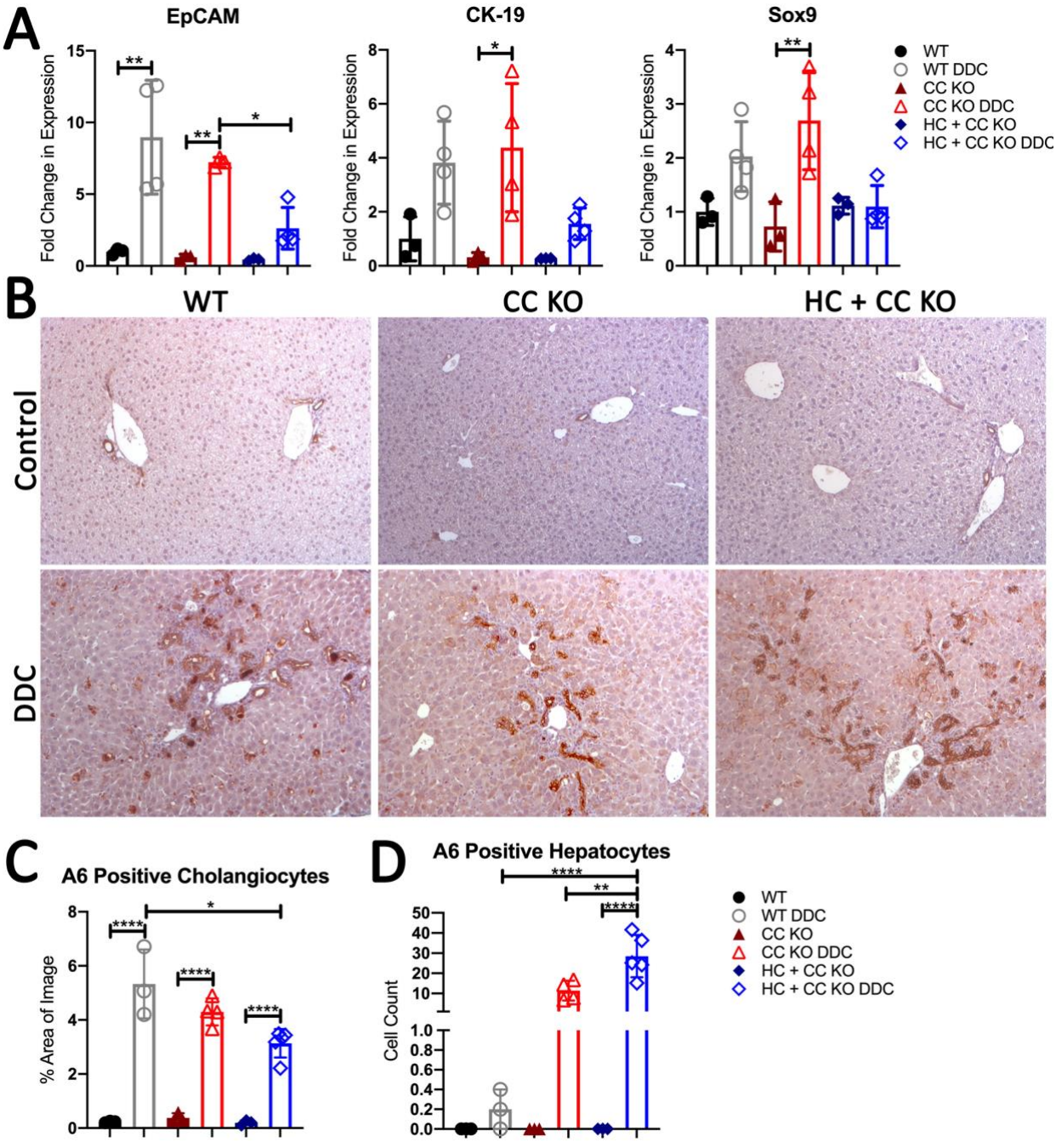

Figure 35. Wnt7b knockout suppresses ductular reaction and promotes hepatocyte expression of cholangiocyte markers

(A) Quantitative RT-PCR analysis of cholangiocyte markers EpCAM, CK-19, and Sox9 show a significant decrease in EpCAM and a trend toward lower CK-19 and Sox9 in HC + CC KO compared to WT after DDC. (B) su (C) Quantification of A6 positive cholangiocytes shows that HC + CC KO on DDC diet have significantly decreased ductular reaction compared to WT on DDC diet. D) Quantification of A6 positive hepatocytes shows that that HC + CC KO on DDC diet have significantly more A6 positive hepatocytes compared to WT and CC KO on DDC diet. ∗P < 0.05, ∗∗P < 0.01, ∗∗∗P < 0.001, and ∗∗∗∗P < 0.0001. Original magnification, 100x.

4.4.6 Wnt7b knockout promotes hepatocyte-to-cholangiocyte reprogramming

We also found A6 positive hepatocytes in our mice exposed to DDC diet. Interestingly CC KO mice on DDC have more A6 positive hepatocytes than WT mice on DDC diet, though the number is not significant (Figure 35D). However, HC + CC KO mice on DDC have a significant amount of A6 positive hepatocytes compared WT and CC KO mice on DDC diet (Figure 35D). These results indicate that loss of Wnt7b may promote hepatocyte expression of cholangiocyte markers, or hepatocyte-to-cholangiocyte reprogramming, when mice lacking Wnt7b in cholangiocyte and hepatocyte compartments are exposed to DDC diet.

4.4.7 β-catenin activation is increased in livers that lack Wnt7b in hepatocytes and cholangiocytes

Loss of Wnt7b may result in compensatory upregulation of other Wnts expressed during cholestasis. One of these is Wnt7a, which induces Sox9 expression in a β-catenin-dependent manner (69). To determine if upregulation of Wnt7a might be contributing to hepatocyte reprogramming, we examined its expression and found that DDC induced Wnt7a in all three mouse models; however, it was not significantly increased in either CC KO or HC + CC KO compared to WT (Figure 36A). Interestingly, however, non-phosphorylated β-catenin, which is an indicator of active canonical Wnt signaling, was higher in HC + CC KO on DDC compared to the same mice on normal diet, whereas phosphorylation of β-catenin at Serine 675, which occurs via the cAMP-dependent protein kinase A (PKA) pathway, was unchanged (Figure 36B) (30). Thus, the increased number of A6-expressing hepatocytes correlates with activation of

canonical β-catenin in HC + CC KO (and to a lesser extent in the CC KO), and this phenomenon is independent of Wnt7a.

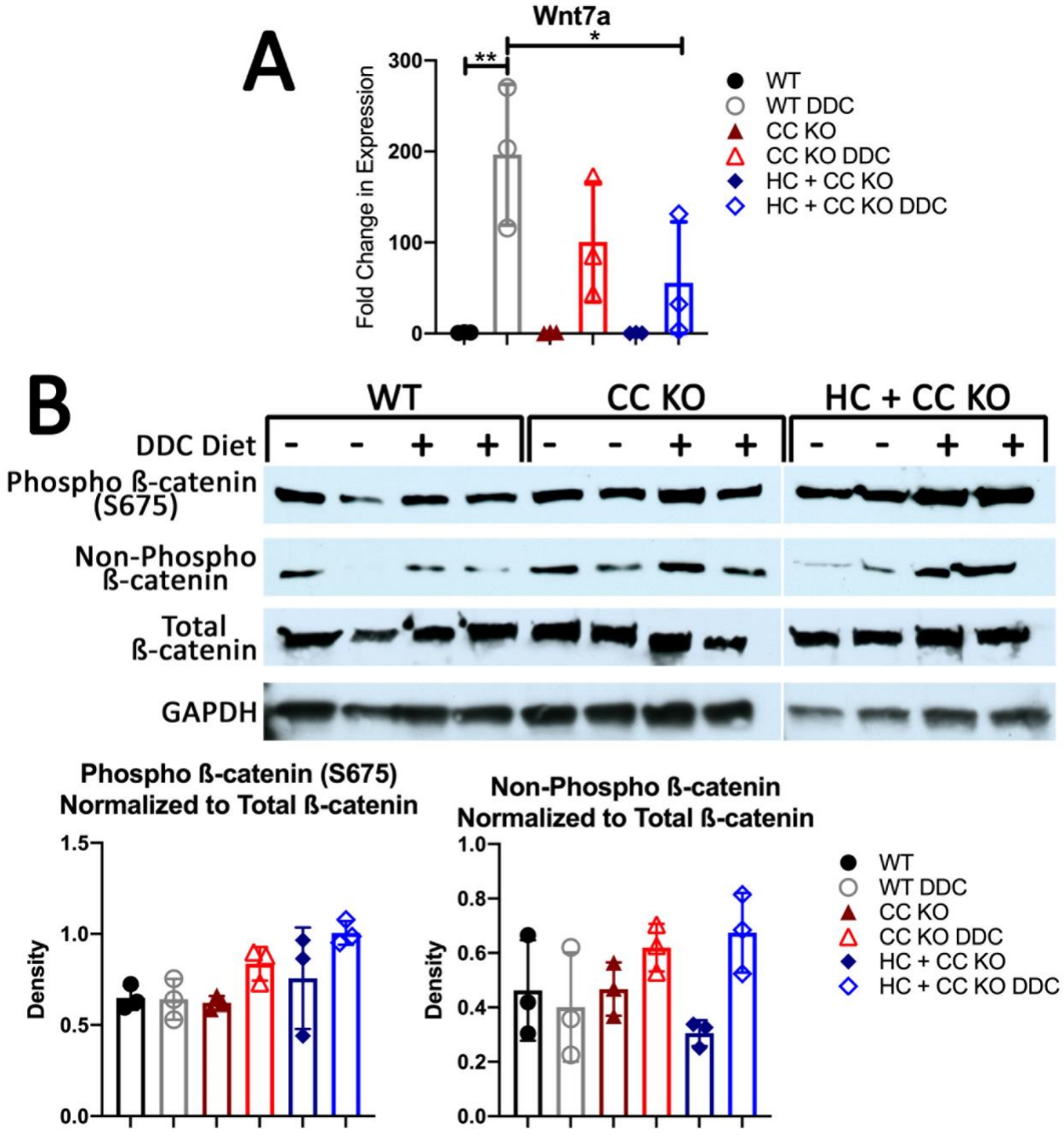

Figure 36. Wnt7a expression and β-catenin activity is upregulated in mice fed DDC diet
(A) Quantitative RT-PCR analysis of Wn7a shows that DDC diet induces expression of Wnt7a in all three genotypes. (B) Western blot and densitometry analyses for phosphorylated (S675), non-phosphorylated active, and total β-catenin shows that CC KO mice and HC + CC KO mice fed DDC diet trend toward an increase in Wnt-dependent active β-catenin. *P < 0.05, **P < 0.01.

4.5 Discussion

Previous studies have shown that in kidney cells macrophage-derived Wnt7b is critical for regeneration after injury by overcoming a G2 arrest in the cell cycle and preventing apoptosis (184). Additionally, Wnt7b is expressed in cholangiocarcinoma cells, and correlates with disease progression (269, 273). Though in vitro studies, we have also shown that Wnt7b plays a role in cholangiocyte proliferation during cholestatic liver injury (69). As expected, when Wnt7b was deleted from either cholangiocytes alone or hepatocytes and cholangiocytes *in vivo*, these KO mice had decreased numbers of proliferating cholangiocytes during cholestasis. Unexpectedly, despite our initial hypothesis that impaired ductular response would exacerbate cholestatic disease progression in response to DDC, Wnt7b KO mice are actually protected from biliary injury. There is almost a direct relationship between Wnt7b expression and ALP levels in serum; as Wnt7b is deleted from more cell types biliary injury improves. However, this decrease in injury is not due to the cholangiocytes' inability to proliferate, but instead related to hepatocytes' ability to transdifferentiate into a biliary-like phenotype.

It is well known that hepatocytes are remarkably plastic. When the biliary epithelium is critically injured, hepatocytes can function as "facultative stem cells," and undergo reprogramming from one epithelial cell type to the other to facilitate repair (216, 217). Typically, in rodent models, mature hepatocytes transdifferentiate into either fully-functional cholangiocytes or a cholangiocyte-like phenotype when there is extensive injury and resident cholangiocytes lose functionality and are incapable of adequately proliferating to compensate for the injury (218-221). Similar results have also been observed in humans. Hepatocytes from both pediatric and adult cholangiopathy patients have been reported to express the ductal marker OV-6 (227, 228), cholangiocyte-specific cytokeratins(229-231), and biliary transcription factors (222, 224). These

findings from both rodents and humans suggest that during biliary injury the number of hepatocytes expressing biliary markers increases over time. As cholestasis progresses, more and more hepatocytes compensate for the damage to and loss of the biliary epithelium.

In our models we found that as more cell types lost Wnt7b hepatocytes became more likely to express cholangiocyte markers. In WT mice on DDC diet biliary injury is repaired through Wnt7b driven cholangiocyte proliferation, and hepatocytes remain hepatocytes. CC KO mice have a few reprogrammed hepatocytes, which once converted to cholangiocytes will self-renew, since hepatocyte-derived cholangiocytes in the CC KO mice are able to express Wnt7b (Figure 37). In HC + CC KO mice even more hepatocytes are becoming biliary-like because the hepatocyte-derived cholangiocyte do not express Wnt7b; therefore, they cannot self-renew and more hepatocyte-derived cholangiocytes are needed to help repair the injured bile ducts (Figure 37). These findings are important because typically, hepatocytes do not undergo cellular reprogramming until biliary injury is so extensive that cholangiocytes are unable to compensate. Our study shows that by blocking cholangiocyte proliferation we can induce hepatocytes to begin reprogramming earlier to alleviate injury.

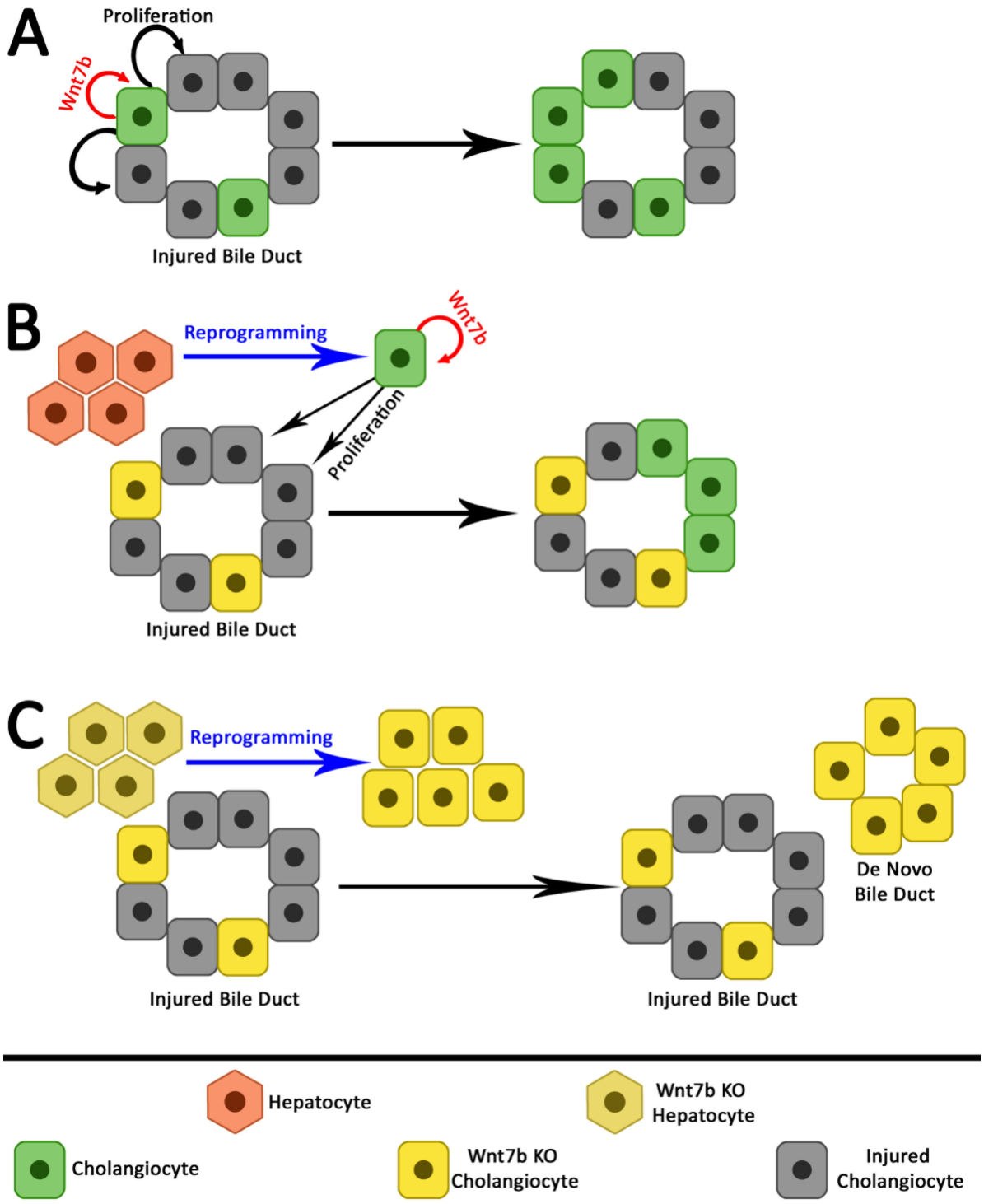

Figure 37. Schematic of how Wnt7b KO might promote hepatocyte-to-cholangiocyte reprogramming
(A) Cholangiocytes in WT mice exposed to biliary injury attempt to self-renew through Wnt7b expression to repair injured ducts. (B) In CC KO mice cholangiocytes lacking Wnt7b are unable to proliferate at an efficient rate, so a few hepatocytes begin expressing biliary markers; these cells then self-renew to repopulate the injured ducts. (C) In HC + CC KO mice cholangiocytes lacking Wnt7b are unable to proliferate, so hepatocytes become cholangiocyte-like. However, these hepatocyte-derived cholangiocytes are also unable to proliferate due to Wnt7b KO, so more hepatocytes must transdifferentiate to alleviate biliary injury.

Both Wnt7a and Wnt7b, along with Wnt10a, are highly expressed in models of cholestasis (69, 78). As Wnt7a induces cellular reprogramming in neighboring hepatocytes in a β-catenin-manner, we hypothesized a compensatory increase in Wnt7a in our Wnt7b KO models (CC or HC + CC) that might account for the increased number of reprogrammed hepatocytes. Interestingly, we do not see a further induction of Wnt7a in either KO. However, we did note an increase in non-phosphorylated, activated β-catenin, which has been shown previously to induce a biliary phenotype in hepatocytes (69, 180). Therefore, we believe that loss of Wnt7b activates β-catenin through some as-yet unknown mechanism to promote hepatocyte reprogramming. Indeed, TOPflash activity data suggests that overexpression of Wnt7b in cholangiocytes suppresses β-catenin activity, consistent with previous studies that demonstrated non-canonical Wnts can antagonize β-catenin activation (274-276). Further mechanistic studies will be needed to determine if the stoichiometry of Wnt7b/Frizzled receptor complex may out-compete binding of canonical Wnts in cholangiocytes during cholestasis.

Beyond its participation in cell cycle and repair processes, little else is known about the biological function of Wnt7b in the liver. We have shown that overexpression of Wnt7b in a cholangiocyte cell line stimulates secretion of certain cytokines associated with inflammation. During cholestasis cholangiocytes abandon a differentiated phenotype to repair the bile duct (181). Under normal conditions, cholangiocytes do not produce an abundance of growth factors and cytokines, but after exogenous or endogenous insult they acquire the ability to secrete factors that act in an autocrine and paracrine manner to promote remodeling (272). However, reactive cholangiocytes can also contribute to progression of liver injury by activating hepatic stellate cells and attracting immune cell populations that generate a persistent inflammatory response. Our data suggests that Wnt7b could be one of the switches driving this proliferative/inflammatory

phenotype during cholestasis, with unfavorable consequences for disease progression. Modulating this axis to block cholangiocyte proliferation and promote hepatocyte transdifferentiation could provide a novel treatment that would alleviate biliary injury in patients with PSC or other cholangiopathies.

5.0 Concluding Remarks and General Discussion

5.1 Significance

Though cholestatic liver diseases, such as primary sclerosing cholangitis (PSC), have a lower incidence than other causes of chronic liver diseases, such as viral hepatitis, alcoholic hepatitis, and non-alcoholic fatty liver disease, they still account for 8-11% of all liver transplants performed each year (277-279). The lack of donor organs and mortality of patients awaiting transplant, means alternative treatments for cholestatic liver disease patients is greatly needed (280). Therefore, the ability to promote healthy bile duct growth and regeneration in PSC patients could be the key in creating a new treatment, alleviating the needs for donor organs. In this dissertation, we determined that the Mdr2 KO mouse model has decreases levels of thyroid hormone receptor beta which causes hepatocytes to retain toxic bile injuring the liver. These findings could indicate that patients with PSC may also suffer similar side effects that cause exacerbated hepatic injury when treated with GC-1. This could be important knowledge to keep in mind when considering GC-1 as a treatment for PSC patients, as this treatment may put patients at higher risk of developing liver failure. Additionally, we have identified two potential methods to activate hepatocyte-to-cholangiocyte transdifferentiation and further elucidated the role that Wnt7b plays in cholangiocyte proliferation. These findings are both significant and exciting because they could help establish a foundation for new treatments for PSC.

Both hepatocytes and cholangiocytes are able to function as a type of “facultative stem cells,” and undergo reprogramming from one cell type to the other (216, 217). Specifically hepatocyte-to-cholangiocyte reprogramming has been well recorded *in vitro* in hepatic organoids

(222, 223), *in vivo* in both mice and rats (218-221, 223-226), and *in vivo* in human patients (222, 224, 227-231). However, despite this knowledge the mechanisms through which this reprogramming occurs are poorly understood. Excitingly, our findings indicate that β-catenin signaling is a driver of this reprogramming. We also found that whenWnt7b induced cholangiocyte proliferation is blocked during cholestatic injury, β-catenin activates and induces hepatocyte reprogramming as well. These findings together could help to develop a treatment for PSC patients that blocks injured cholangiocyte proliferation through inhibiting Wnt7b signaling and promoting hepatocytes to reprogram using β-catenin activation to create healthy bile ducts, alleviating cholestatic injury.

5.2 Future Directions: Wnt/β-catenin Driven Hepatocyte-to-Cholangiocyte Transdifferentiation

The current body of literature makes it well known that both hepatocyte and cholangiocytes exhibit remarkable plasticity, and under specific serious hepatic or biliary injury the two cell types can convert to one another in an attempt to alleviate said injury. However, the pathways involved in specifically hepatocyte-to-cholangiocyte transdifferentiation have not been fully studied. It has been found that these reprograming events involve a number of regenerative pathways including HGF signaling via MET, EGFR signaling, and potentially canonical Wnt/β-catenin signaling (69, 177, 180, 217, 281). Our findings that β-catenin signaling induces hepatocyte-to-cholangiocyte transdifferentiation in our mouse models further supports this knowledgebase. However, the Wnt ligand that induces this canonical signaling and hepatocyte reprogramming has not been fully determined. There is evidence that Wnt7a could be the ligand that induces this hepatocyte-to-

cholangiocyte transdifferentiation through canonical Wnt signaling, but further research is needed to confirm this hypothesis (69). Therefore, is it important in the future to determine whether Wnt7A, or another Wnt ligand, drives this canonical Wnt signaling induce hepatocyte-to-cholangiocyte conversion.

It also remains unknown whether hepatocyte-derived cholangiocytes fully commit to a cholangiocyte phenotype and remain cholangiocytes or revert back to hepatocytes after injury is reversed (225). Studies have shown that hepatocyte-derived cholangiocytes incorporate into biliary ductules, but no studies have compared their functionality to that native cholangiocytes (221, 224, 225, 232). Therefore, it would be necessary to test the incorporated hepatocyte-derived cells functionality compared to native cholangiocytes and determine if these cells remain cholangiocytes after cholestatic injury is alleviated. All of these questions will be undoubtedly answered in the future. Once we determine which Wnt ligand induces β-catenin driven hepatocyte reprogramming and how the newly derived cholangiocytes will act in the bile ducts, future patients with PSC will likely have a treatment option that does not rely on whole liver transplants.

5.3 Future Directions: Wnt7b Driven Cholangiocyte Proliferation

As we learn more information about the roles Wnt signaling plays in the liver, it is clear canonical Wnt signaling is involved in almost every aspect of liver function, from generation to metabolism to regeneration. Despite all that is known about Wnt/β-catenin signaling in the liver, there is still much to be learned about Wnt signaling, both canonical and non-canonical, in the liver, specifically in reference to the bile ducts. In our study we were able to further the knowledge of Wnt7b's role in cholangiocyte proliferation. However, very little is known about which Wnt

ligands interact with which Frizzled receptors in many cell types and if these interactions are altered in certain diseases. Elucidating this information becomes even more complex when faced with the knowledge that there are 19 Wnt ligands and 10 Frizzled receptors in the mammalian genome (57, 58). Therefore, determining which Frizzled receptor or receptors Wnt7b interacts with to induce cholangiocyte proliferation during cholestatic injury could be difficult to determine. Additionally, canonical Wnt signaling is well studied and understood in liver development, homeostasis, and regeneration; however, non-canonical Wnt signaling, which Wnt7b signals through to induce cholangiocyte proliferation, is not. This is further compounded with the fact that there are multiple non-canonical pathways through which Wnts can signal, making it trickier to study non-canonical Wnt signaling (46, 47, 51, 52). Finally, the role of non-canonical Wnt7b signaling in the pathobiology of cholestatic liver disease, such as PSC, in human patients will need to be investigated further as well. Undeniably, future research will fully identify the exciting role Wnt7b and non-canonical Wnt signaling play in in bile duct pathobiology and regeneration.

Bibliography

1.Barrott JJ, Cash GM, Smith AP, Barrow JR, Murtaugh LC. Deletion of mouse Porcn blocks Wnt ligand secretion and reveals an ectodermal etiology of human focal dermal hypoplasia/Goltz syndrome. Proc Natl Acad Sci U S A. 2011;108(31):12752-7.

2.Zhai L, Chaturvedi D, Cumberledge S. Drosophila Wnt-1 undergoes a hydrophobic modification and is targeted to lipid rafts, a process that requires porcupine. Journal of Biological Chemistry. 2004;279(32):33220-7.

3.Banziger C, Soldini D, Schutt C, Zipperlen P, Hausmann G, Basler K. Wntless, a conserved membrane protein dedicated to the secretion of Wnt proteins from signaling cells. Cell. 2006;125(3):509-22.

4.MacDonald BT, Tamai K, He X. Wnt/beta-catenin signaling: components, mechanisms, and diseases. Dev Cell. 2009;17(1):9-26.

5.Kimelman D, Xu W. beta-catenin destruction complex: insights and questions from a structural perspective. Oncogene. 2006;25(57):7482-91.

6.Rao TP, Kuhl M. An updated overview on Wnt signaling pathways: a prelude for more. Circ Res. 2010;106(12):1798-806.

7.Liu C, Li Y, Semenov M, Han C, Baeg GH, Tan Y, et al. Control of beta-catenin phosphorylation/degradation by a dual-kinase mechanism. Cell. 2002;108(6):837-47.

8.Hart M, Concordet JP, Lassot I, Albert I, del los Santos R, Durand H, et al. The F-box protein beta-TrCP associates with phosphorylated beta-catenin and regulates its activity in the cell. Curr Biol. 1999;9(4):207-10.

9.Aberle H, Bauer A, Stappert J, Kispert A, Kemler R. beta-catenin is a target for the ubiquitin-proteasome pathway. EMBO J. 1997;16(13):3797-804.

10.Bhanot P, Brink M, Samos CH, Hsieh JC, Wang Y, Macke JP, et al. A new member of the frizzled family from Drosophila functions as a Wingless receptor. Nature. 1996;382(6588):225-30.

11.Wehrli M, Dougan ST, Caldwell K, O'Keefe L, Schwartz S, Vaizel-Ohayon D, et al. arrow encodes an LDL-receptor-related protein essential for Wingless signalling. Nature. 2000;407(6803):527-30.

12.Tamai K, Semenov M, Kato Y, Spokony R, Liu C, Katsuyama Y, et al. LDL-receptor-related proteins in Wnt signal transduction. Nature. 2000;407(6803):530-5.

13.Tamai K, Zeng X, Liu C, Zhang X, Harada Y, Chang Z, et al. A mechanism for Wnt coreceptor activation. Mol Cell. 2004;13(1):149-56.

14.Clevers H. Wnt/beta-catenin signaling in development and disease. Cell. 2006;127(3):469-80.

15.Miller JR, Hocking AM, Brown JD, Moon RT. Mechanism and function of signal transduction by the Wnt/beta-catenin and Wnt/Ca2+ pathways. Oncogene. 1999;18(55):7860-72.

16.Knight C, James S, Kuntin D, Fox J, Newling K, Hollings S, et al. Epidermal growth factor can signal via beta-catenin to control proliferation of mesenchymal stem cells independently of canonical Wnt signalling. Cell Signal. 2019;53:256-68.

17.Krejci P, Aklian A, Kaucka M, Sevcikova E, Prochazkova J, Masek JK, et al. Receptor tyrosine kinases activate canonical WNT/beta-catenin signaling via MAP kinase/LRP6 pathway and direct beta-catenin phosphorylation. PLoS One. 2012;7(4):e35826.

18.Zhang X, Zhu J, Li Y, Lin T, Siclari VA, Chandra A, et al. Epidermal growth factor receptor (EGFR) signaling regulates epiphyseal cartilage development through beta-catenin-dependent and -independent pathways. J Biol Chem. 2013;288(45):32229-40.

19.Pascale RM, Feo F, Calvisi DF. An infernal cross-talk between oncogenic beta-catenin and c-Met in hepatocellular carcinoma: Evidence from mouse modeling. Hepatology. 2016;64(5):1421-3.

20.Purcell R, Childs M, Maibach R, Miles C, Turner C, Zimmermann A, et al. HGF/c-Met related activation of beta-catenin in hepatoblastoma. J Exp Clin Cancer Res. 2011;30:96.

21.Monga SP, Mars WM, Pediaditakis P, Bell A, Mule K, Bowen WC, et al. Hepatocyte growth factor induces Wnt-independent nuclear translocation of beta-catenin after Met-beta-catenin dissociation in hepatocytes. Cancer Res. 2002;62(7):2064-71.

22.Ranganathan S, Tan X, Monga SP. beta-Catenin and met deregulation in childhood Hepatoblastomas. Pediatr Dev Pathol. 2005;8(4):435-47.

23.Rubinfeld B, Albert I, Porfiri E, Fiol C, Munemitsu S, Polakis P. Binding of GSK3beta to the APC-beta-catenin complex and regulation of complex assembly. Science. 1996;272(5264):1023-6.

24.van Noort M, Meeldijk J, van der Zee R, Destree O, Clevers H. Wnt signaling controls the phosphorylation status of beta-catenin. J Biol Chem. 2002;277(20):17901-5.

25.Taurin S, Sandbo N, Qin Y, Browning D, Dulin NO. Phosphorylation of beta-catenin by cyclic AMP-dependent protein kinase. J Biol Chem. 2006;281(15):9971-6.

26.Hino S, Tanji C, Nakayama KI, Kikuchi A. Phosphorylation of beta-catenin by cyclic AMP-dependent protein kinase stabilizes beta-catenin through inhibition of its ubiquitination. Mol Cell Biol. 2005;25(20):9063-72.

27.Taurin S, Sandbo N, Yau DM, Sethakorn N, Dulin NO. Phosphorylation of beta-catenin by PKA promotes ATP-induced proliferation of vascular smooth muscle cells. Am J Physiol Cell Physiol. 2008;294(5):C1169-74.

28.Spirli C, Locatelli L, Morell CM, Fiorotto R, Morton SD, Cadamuro M, et al. Protein kinase A-dependent pSer(675) -beta-catenin, a novel signaling defect in a mouse model of congenital hepatic fibrosis. Hepatology. 2013;58(5):1713-23.

29.Alvarado TF, Puliga E, Preziosi M, Poddar M, Singh S, Columbano A, et al. Thyroid Hormone Receptor beta Agonist Induces beta-Catenin-Dependent Hepatocyte Proliferation in Mice: Implications in Hepatic Regeneration. Gene Expr. 2016;17(1):19-34.

30.Fanti M, Singh S, Ledda-Columbano GM, Columbano A, Monga SP. Tri-iodothyronine induces hepatocyte proliferation by protein kinase A-dependent beta-catenin activation in rodents. Hepatology. 2014;59(6):2309-20.

31.Wheelock MJ, Johnson KR. Cadherins as modulators of cellular phenotype. Annu Rev Cell Dev Biol. 2003;19:207-35.

32.Hartsock A, Nelson WJ. Adherens and tight junctions: Structure, function and connections to the actin cytoskeleton. Biochimica Et Biophysica Acta-Biomembranes. 2008;1778(3):660-9.

33.Brembeck FH, Rosario M, Birchmeier W. Balancing cell adhesion and Wnt signaling, the key role of beta-catenin. Curr Opin Genet Dev. 2006;16(1):51-9.

34.D'Souza-Schorey C. Disassembling adherens junctions: breaking up is hard to do. Trends in Cell Biology. 2005;15(1):19-26.

35.Chen YT, Stewart DB, Nelson WJ. Coupling assembly of the E-cadherin/beta-catenin complex to efficient endoplasmic reticulum exit and basal-lateral membrane targeting of E-cadherin in polarized MDCK cells. J Cell Biol. 1999;144(4):687-99.

36.Hinck L, Nathke IS, Papkoff J, Nelson WJ. Dynamics of cadherin/catenin complex formation: novel protein interactions and pathways of complex assembly. J Cell Biol. 1994;125(6):1327-40.

37.Miranda KC, Joseph SR, Yap AS, Teasdale RD, Stow JL. Contextual Binding of p120ctnto E-cadherin at the Basolateral Plasma Membrane in Polarized Epithelia. Journal of Biological Chemistry. 2003;278(44):43480-8.

38.Huber AH, Stewart DB, Laurents DV, Nelson WJ, Weis WI. The cadherin cytoplasmic domain is unstructured in the absence of beta-catenin - A possible-mechanism for regulating cadherin turnover. Journal of Biological Chemistry. 2001;276(15):12301-9.

39.Zeng G, Apte U, Micsenyi A, Bell A, Monga SP. Tyrosine residues 654 and 670 in beta-catenin are crucial in regulation of Met-beta-catenin interactions. Exp Cell Res. 2006;312(18):3620-30.

40.Lilien J, Balsamo J. The regulation of cadherin-mediated adhesion by tyrosine phosphorylation/dephosphorylation of beta-catenin. Current Opinion in Cell Biology. 2005;17(5):459-65.

41.Piedra J, Martinez D, Castano J, Miravet S, Dunach M, de Herreros AG. Regulation of beta-catenin structure and activity by tyrosine phosphorylation. J Biol Chem. 2001;276(23):20436-43.

42.Roura S, Miravet S, Piedra J, Garcia de Herreros A, Dunach M. Regulation of E-cadherin/Catenin association by tyrosine phosphorylation. J Biol Chem. 1999;274(51):36734-40.

43.Yeh TH, Krauland L, Singh V, Zou B, Devaraj P, Stolz DB, et al. Liver-specific beta-catenin knockout mice have bile canalicular abnormalities, bile secretory defect, and intrahepatic cholestasis. Hepatology. 2010;52(4):1410-9.

44.Pradhan-Sundd T, Kosar K, Saggi H, Zhang R, Vats R, Cornuet P, et al. Wnt/beta-Catenin Signaling Plays a Protective Role in the Mdr2 Knockout Murine Model of Cholestatic Liver Disease. Hepatology. 2020;71(5):1732-49.

45.Pradhan-Sundd T, Zhou L, Vats R, Jiang A, Molina L, Singh S, et al. Dual catenin loss in murine liver causes tight junctional deregulation and progressive intrahepatic cholestasis. Hepatology. 2018;67(6):2320-37.

46.Komiya Y, Habas R. Wnt signal transduction pathways. Organogenesis. 2008;4(2):68-75.

47.Nishita M, Yoo SK, Nomachi A, Kani S, Sougawa N, Ohta Y, et al. Filopodia formation mediated by receptor tyrosine kinase Ror2 is required for Wnt5a-induced cell migration. J Cell Biol. 2006;175(4):555-62.

48.Habas R, Dawid IB, He X. Coactivation of Rac and Rho by Wnt/Frizzled signaling is required for vertebrate gastrulation. Genes & Development. 2003;17(2):295-309.

49.Li L, Yuan H, Xie W, Mao J, Caruso AM, McMahon A, et al. Dishevelled proteins lead to two signaling pathways. Regulation of LEF-1 and c-Jun N-terminal kinase in mammalian cells. J Biol Chem. 1999;274(1):129-34.

50.Marlow F, Topczewski J, Sepich D, Solnica-Krezel L. Zebrafish Rho kinase 2 acts downstream of Wnt11 to mediate cell polarity and effective convergence and extension movements. Current Biology. 2002;12(11):876-84.

51.Li L, Hutchins BI, Kalil K. Wnt5a Induces Simultaneous Cortical Axon Outgrowth and Repulsive Axon Guidance through Distinct Signaling Mechanisms. Journal of Neuroscience. 2009;29(18):5873-83.

52.Nishita M, Enomoto M, Yamagata K, Minami Y. Cell/tissue-tropic functions of Wnt5a signaling in normal and cancer cells. Trends Cell Biol. 2010;20(6):346-54.

53.De A. Wnt/Ca2+ signaling pathway: a brief overview. Acta Biochim Biophys Sin (Shanghai). 2011;43(10):745-56.

54.Yamamoto H, Yoo SK, Nishita M, Kikuchi A, Minami Y. Wnt5a modulates glycogen synthase kinase 3 to induce phosphorylation of receptor tyrosine kinase Ror2. Genes Cells. 2007;12(11):1215-23.

55.Sheldahl LC, Park M, Malbon CC, Moon RT. Protein kinase C is differentially stimulated by Wnt and Frizzled homologs in a G-protein-dependent manner. Current Biology. 1999;9(13):695-8.

56.Kuhl M, Sheldahl LC, Malbon CC, Moon RT. Ca2+/calmodulin-dependent protein kinase II is stimulated by Wnt and frizzled homologs and promotes ventral cell fates in Xenopus. Journal of Biological Chemistry. 2000;275(17):12701-11.

57.Vincan E, Barker N. The upstream components of the Wnt signalling pathway in the dynamic EMT and MET associated with colorectal cancer progression. Clin Exp Metastasis. 2008;25(6):657-63.

58.Zeng G, Awan F, Otruba W, Muller P, Apte U, Tan X, et al. Wnt'er in liver: expression of Wnt and frizzled genes in mouse. Hepatology. 2007;45(1):195-204.

59.Bennett CN, Longo KA, Wright WS, Suva LJ, Lane TF, Hankenson KD, et al. Regulation of osteoblastogenesis and bone mass by Wnt10b. Proc Natl Acad Sci U S A. 2005;102(9):3324-9.

60.Lewis SL, Khoo PL, De Young RA, Steiner K, Wilcock C, Mukhopadhyay M, et al. Dkk1 and Wnt3 interact to control head morphogenesis in the mouse. Development. 2008;135(10):1791-801.

61.McMahon AP, Bradley A. The Wnt-1 (int-1) proto-oncogene is required for development of a large region of the mouse brain. Cell. 1990;62(6):1073-85.

62.Monkley SJ, Delaney SJ, Pennisi DJ, Christiansen JH, Wainwright BJ. Targeted disruption of the Wnt2 gene results in placentation defects. Development. 1996;122(11):3343-53.

63.Parr BA, Cornish VA, Cybulsky MI, McMahon AP. Wnt7b regulates placental development in mice. Dev Biol. 2001;237(2):324-32.

64.Teh C, Sun G, Shen H, Korzh V, Wohland T. Modulating the expression level of secreted Wnt3 influences cerebellum development in zebrafish transgenics. Development. 2015;142(21):3721-33.

65.Zheng HF, Tobias JH, Duncan E, Evans DM, Eriksson J, Paternoster L, et al. WNT16 influences bone mineral density, cortical bone thickness, bone strength, and osteoporotic fracture risk. PLoS Genet. 2012;8(7):e1002745.

66.Ding BS, Nolan DJ, Butler JM, James D, Babazadeh AO, Rosenwaks Z, et al. Inductive angiocrine signals from sinusoidal endothelium are required for liver regeneration. Nature. 2010;468(7321):310-5.

67.Yang J, Cusimano A, Monga JK, Preziosi ME, Pullara F, Calero G, et al. WNT5A inhibits hepatocyte proliferation and concludes beta-catenin signaling in liver regeneration. Am J Pathol. 2015;185(8):2194-205.

68.Wang B, Zhao L, Fish M, Logan CY, Nusse R. Self-renewing diploid Axin2(+) cells fuel homeostatic renewal of the liver. Nature. 2015;524(7564):180-5.

69.Okabe H, Yang J, Sylakowski K, Yovchev M, Miyagawa Y, Nagarajan S, et al. Wnt signaling regulates hepatobiliary repair following cholestatic liver injury in mice. Hepatology. 2016;64(5):1652-66.

70.Rodriguez-Seguel E, Mah N, Naumann H, Pongrac IM, Cerda-Esteban N, Fontaine JF, et al. Mutually exclusive signaling signatures define the hepatic and pancreatic progenitor cell lineage divergence. Genes Dev. 2013;27(17):1932-46.

71.Rosso SB, Sussman D, Wynshaw-Boris A, Salinas PC. Wnt signaling through Dishevelled, Rac and JNK regulates dendritic development. Nat Neurosci. 2005;8(1):34-42.

72.Tu X, Joeng KS, Nakayama KI, Nakayama K, Rajagopal J, Carroll TJ, et al. Noncanonical Wnt signaling through G protein-linked PKCdelta activation promotes bone formation. Dev Cell. 2007;12(1):113-27.

73.Zheng D, Decker KF, Zhou T, Chen J, Qi Z, Jacobs K, et al. Role of WNT7B-induced noncanonical pathway in advanced prostate cancer. Mol Cancer Res. 2013;11(5):482-93.

74.Arensman MD, Kovochich AN, Kulikauskas RM, Lay AR, Yang PT, Li X, et al. WNT7B mediates autocrine Wnt/beta-catenin signaling and anchorage-independent growth in pancreatic adenocarcinoma. Oncogene. 2014;33(7):899-908.

75.Davis EK, Zou YM, Ghosh A. Wnts acting through canonical and noncanonical signaling pathways exert opposite effects on hippocampal synapse formation. Neural Development. 2008;3.

76.Wang ZS, Shu WG, Lu MM, Morrisey EE. Wnt7b activates canonical signaling in epithelial and vascular smooth muscle cells through interactions with Fzd1, Fzd10, and LRP5. Molecular and Cellular Biology. 2005;25(12):5022-30.

77.Yu J, Carroll TJ, Rajagopal J, Kobayashi A, Ren Q, McMahon AP. A Wnt7b-dependent pathway regulates the orientation of epithelial cell division and establishes the cortico-medullary axis of the mammalian kidney. Development. 2009;136(1):161-71.

78.Itoh T, Kamiya Y, Okabe M, Tanaka M, Miyajima A. Inducible expression of Wnt genes during adult hepatic stem/progenitor cell response. FEBS Lett. 2009;583(4):777-81.

79.McLin VA, Rankin SA, Zorn AM. Repression of Wnt/beta-catenin signaling in the anterior endoderm is essential for liver and pancreas development. Development. 2007;134(12):2207-17.

80.Russell JO, Monga SP. Wnt/beta-Catenin Signaling in Liver Development, Homeostasis, and Pathobiology. Annu Rev Pathol. 2018;13:351-78.

81.Tan X, Yuan Y, Zeng G, Apte U, Thompson MD, Cieply B, et al. Beta-catenin deletion in hepatoblasts disrupts hepatic morphogenesis and survival during mouse development. Hepatology. 2008;47(5):1667-79.

82.Cadoret A, Ovejero C, Saadi-Kheddouci S, Souil E, Fabre M, Romagnolo B, et al. Hepatomegaly in transgenic mice expressing an oncogenic form of beta-catenin. Cancer Res. 2001;61(8):3245-9.

83.Tan X, Apte U, Micsenyi A, Kotsagrelos E, Luo JH, Ranganathan S, et al. Epidermal growth factor receptor: a novel target of the Wnt/beta-catenin pathway in liver. Gastroenterology. 2005;129(1):285-302.

84.Tan X, Behari J, Cieply B, Michalopoulos GK, Monga SP. Conditional deletion of beta-catenin reveals its role in liver growth and regeneration. Gastroenterology. 2006;131(5):1561-72.

85.Thorgeirsson SS. Hepatic stem cells in liver regeneration. FASEB J. 1996;10(11):1249-56.

86.Michalopoulos GK. Liver regeneration. J Cell Physiol. 2007;213(2):286-300.

87.Monga SP, Pediaditakis P, Mule K, Stolz DB, Michalopoulos GK. Changes in WNT/beta-catenin pathway during regulated growth in rat liver regeneration. Hepatology. 2001;33(5):1098-109.

88.Nelsen CJ, Rickheim DG, Timchenko NA, Stanley MW, Albrecht JH. Transient Expression of Cyclin D1 Is Sufficient to Promote Hepatocyte Replication and Liver Growth in Vivo. Cancer Research. 2001;61(23):8564-8.

89.Yang J, Mowry LE, Nejak-Bowen KN, Okabe H, Diegel CR, Lang RA, et al. beta-catenin signaling in murine liver zonation and regeneration: a Wnt-Wnt situation! Hepatology. 2014;60(3):964-76.

90.Apte U, Singh S, Zeng G, Cieply B, Virji MA, Wu T, et al. Beta-catenin activation promotes liver regeneration after acetaminophen-induced injury. Am J Pathol. 2009;175(3):1056-65.

91.Mossanen JC, Tacke F. Acetaminophen-induced acute liver injury in mice. Lab Anim. 2015;49(1 Suppl):30-6.

92.Zaher H, Buters JT, Ward JM, Bruno MK, Lucas AM, Stern ST, et al. Protection against acetaminophen toxicity in CYP1A2 and CYP2E1 double-null mice. Toxicol Appl Pharmacol. 1998;152(1):193-9.

93.Sekine S, Lan BY, Bedolli M, Feng S, Hebrok M. Liver-specific loss of beta-catenin blocks glutamine synthesis pathway activity and cytochrome p450 expression in mice. Hepatology. 2006;43(4):817-25.

94.Russell DW. The enzymes, regulation, and genetics of bile acid synthesis. Annu Rev Biochem. 2003;72:137-74.

95.Abou-Khalil JE, Bertens KA. Embryology, Anatomy, and Imaging of the Biliary Tree. Surg Clin North Am. 2019;99(2):163-74.

96.Sarnova L, Gregor M. Biliary System Architecture: Experimental Models and Visualization Techniques. Physiological Research. 2017:383-90.

97.Alpini G, Glaser S, Robertson W, Rodgers RE, Phinizy JL, Lasater J, et al. Large but not small intrahepatic bile ducts are involved in secretin-regulated ductal bile secretion. Am J Physiol. 1997;272(5 Pt 1):G1064-74.

98.Alpini G, Roberts S, Kuntz SM, Ueno Y, Gubba S, Podila PV, et al. Morphological, molecular, and functional heterogeneity of cholangiocytes from normal rat liver. Gastroenterology. 1996;110(5):1636-43.

99.Benedetti A, Bassotti C, Rapino K, Marucci L, Jezequel AM. A morphometric study of the epithelium lining the rat intrahepatic biliary tree. J Hepatol. 1996;24(3):335-42.

100.Ishii M, Vroman B, LaRusso NF. Isolation and morphologic characterization of bile duct epithelial cells from normal rat liver. Gastroenterology. 1989;97(5):1236-47.

101.Sasaki H, Schaffner F, Popper H. Bile ductules in cholestasis: morphologic evidence for secretion and absorption in man. Lab Invest. 1967;16(1):84-95.

102.Schaffner F, Popper H. Electron microscopic studies of normal and proliferated bile ductules. Am J Pathol. 1961;38:393-410.

103.Kanno N, LeSage G, Glaser S, Alvaro D, Alpini G. Functional heterogeneity of the intrahepatic biliary epithelium. Hepatology. 2000;31(3):555-61.

104.Marzioni M, Glaser SS, Francis H, Phinizy JL, LeSage G, Alpini G. Functional heterogeneity of cholangiocytes. Semin Liver Dis. 2002;22(3):227-40.

105.Tabibian JH, Masyuk AI, Masyuk TV, O'Hara SP, LaRusso NF. Physiology of cholangiocytes. Compr Physiol. 2013;3(1):541-65.

106.Theise ND, Saxena R, Portmann BC, Thung SN, Yee H, Chiriboga L, et al. The canals of Hering and hepatic stem cells in humans. Hepatology. 1999;30(6):1425-33.

107.Banales JM, Huebert RC, Karlsen T, Strazzabosco M, LaRusso NF, Gores GJ. Cholangiocyte pathobiology. Nat Rev Gastroenterol Hepatol. 2019;16(5):269-81.

108.Afroze S, Meng F, Jensen K, McDaniel K, Rahal K, Onori P, et al. The physiological roles of secretin and its receptor. Ann Transl Med. 2013;1(3):29.

109.Banales JM, Arenas F, Rodriguez-Ortigosa CM, Saez E, Uriarte I, Doctor RB, et al. Bicarbonate-rich choleresis induced by secretin in normal rat is taurocholate-dependent and involves AE2 anion exchanger. Hepatology. 2006;43(2):266-75.

110.Banales JM, Prieto J, Medina JF. Cholangiocyte anion exchange and biliary bicarbonate excretion. World J Gastroenterol. 2006;12(22):3496-511.

111.Lenzen R, Alpini G, Tavoloni N. Secretin stimulates bile ductular secretory activity through the cAMP system. Am J Physiol. 1992;263(4 Pt 1):G527-32.

112.Cohn JA, Strong TV, Picciotto MR, Nairn AC, Collins FS, Fitz JG. Localization of the cystic fibrosis transmembrane conductance regulator in human bile duct epithelial cells. Gastroenterology. 1993;105(6):1857-64.

113.Tietz PS, Marinelli RA, Chen XM, Huang B, Cohn J, Kole J, et al. Agonist-induced coordinated trafficking of functionally related transport proteins for water and ions in cholangiocytes. J Biol Chem. 2003;278(22):20413-9.

114.Dutta AK, Khimji AK, Kresge C, Bugde A, Dougherty M, Esser V, et al. Identification and functional characterization of TMEM16A, a Ca2+-activated Cl- channel activated by extracellular nucleotides, in biliary epithelium. J Biol Chem. 2011;286(1):766-76.

115.Dutta AK, Woo K, Khimji AK, Kresge C, Feranchak AP. Mechanosensitive Cl- secretion in biliary epithelium mediated through TMEM16A. Am J Physiol Gastrointest Liver Physiol. 2013;304(1):G87-98.

116.Feranchak AP, Fitz JG. Adenosine triphosphate release and purinergic regulation of cholangiocyte transport. Semin Liver Dis. 2002;22(3):251-62.

117.Woo K, Dutta AK, Patel V, Kresge C, Feranchak AP. Fluid flow induces mechanosensitive ATP release, calcium signalling and Cl- transport in biliary epithelial cells through a PKCzeta-dependent pathway. J Physiol. 2008;586(11):2779-98.

118.Marinelli RA, Tietz PS, Pham LD, Rueckert L, Agre P, LaRusso NF. Secretin induces the apical insertion of aquaporin-1 water channels in rat cholangiocytes. Am J Physiol. 1999;276(1):G280-6.

119.Masyuk AI, LaRusso NF. Aquaporins in the hepatobiliary system. Hepatology. 2006;43(2 Suppl 1):S75-81.

120.Beuers U, Hohenester S, de Buy Wenniger LJ, Kremer AE, Jansen PL, Elferink RP. The biliary HCO(3)(-) umbrella: a unifying hypothesis on pathogenetic and therapeutic aspects of fibrosing cholangiopathies. Hepatology. 2010;52(4):1489-96.

121.Chang JC, Go S, de Waart DR, Munoz-Garrido P, Beuers U, Paulusma CC, et al. Soluble Adenylyl Cyclase Regulates Bile Salt-Induced Apoptosis in Human Cholangiocytes. Hepatology. 2016;64(2):522-34.

122.Hohenester S, Wenniger LM, Paulusma CC, van Vliet SJ, Jefferson DM, Elferink RP, et al. A biliary HCO3- umbrella constitutes a protective mechanism against bile acid-induced injury in human cholangiocytes. Hepatology. 2012;55(1):173-83.

123.Hofmann AF. The enterohepatic circulation of bile acids in mammals: form and functions. Front Biosci (Landmark Ed). 2009;14:2584-98.

124.Lamri Y, Erlinger S, Dumont M, Roda A, Feldmann G. Immunoperoxidase localization of ursodeoxycholic acid in rat biliary epithelial cells. Evidence for a cholehepatic circulation. Liver. 1992;12(5):351-4.

125.Lazaridis KN, Pham L, Tietz P, Marinelli RA, deGroen PC, Levine S, et al. Rat cholangiocytes absorb bile acids at their apical domain via the ileal sodium-dependent bile acid transporter. J Clin Invest. 1997;100(11):2714-21.

126.Benedetti A, Di Sario A, Marucci L, Svegliati-Baroni G, Schteingart CD, Ton-Nu HT, et al. Carrier-mediated transport of conjugated bile acids across the basolateral membrane of biliary epithelial cells. Am J Physiol. 1997;272(6 Pt 1):G1416-24.

127.Kimura Y, Matsuo M, Takahashi K, Saeki T, Kioka N, Amachi T, et al. ATP hydrolysis-dependent multidrug efflux transporter: MDR1/P-glycoprotein. Curr Drug Metab. 2004;5(1):1-10.

128.Ober EA, Lemaigre FP. Development of the liver: Insights into organ and tissue morphogenesis. J Hepatol. 2018;68(5):1049-62.

129.Lemaigre FP. Molecular Mechanisms of Biliary Development. Development, Differentiation and Disease of the Para-Alimentary Tract. 2010;97:103-26.

130.Clotman F, Jacquemin P, Plumb-Rudewiez N, Pierreux CE, Van der Smissen P, Dietz HC, et al. Control of liver cell fate decision by a gradient of TGF beta signaling modulated by Onecut transcription factors. Genes Dev. 2005;19(16):1849-54.

131.Decaens T, Godard C, de Reynies A, Rickman DS, Tronche F, Couty JP, et al. Stabilization of beta-catenin affects mouse embryonic liver growth and hepatoblast fate. Hepatology. 2008;47(1):247-58.

132.So J, Khaliq M, Evason K, Ninov N, Martin BL, Stainier DYR, et al. Wnt/beta-catenin signaling controls intrahepatic biliary network formation in zebrafish by regulating notch activity. Hepatology. 2018;67(6):2352-66.

133.Tchorz JS, Kinter J, Muller M, Tornillo L, Heim MH, Bettler B. Notch2 signaling promotes biliary epithelial cell fate specification and tubulogenesis during bile duct development in mice. Hepatology. 2009;50(3):871-9.

134.Yanai M, Tatsumi N, Hasunuma N, Katsu K, Endo F, Yokouchi Y. FGF signaling segregates biliary cell-lineage from chick hepatoblasts cooperatively with BMP4 and ECM components in vitro. Dev Dyn. 2008;237(5):1268-83.

135.Hofmann JJ, Zovein AC, Koh H, Radtke F, Weinmaster G, Iruela-Arispe ML. Jagged1 in the portal vein mesenchyme regulates intrahepatic bile duct development: insights into Alagille syndrome. Development. 2010;137(23):4061-72.

136.Lemaigre FP. Notch signaling in bile duct development: new insights raise new questions. Hepatology. 2008;48(2):358-60.

137.Chiang JY. Regulation of bile acid synthesis: pathways, nuclear receptors, and mechanisms. J Hepatol. 2004;40(3):539-51.

138.Chiang JY. Regulation of bile acid synthesis. Front Biosci. 1998;3:d176-93.

139.Attili AF, Angelico M, Cantafora A, Alvaro D, Capocaccia L. Bile acid-induced liver toxicity: relation to the hydrophobic-hydrophilic balance of bile acids. Med Hypotheses. 1986;19(1):57-69.

140.Chiang JY. Bile acid metabolism and signaling. Compr Physiol. 2013;3(3):1191-212.

141.Falany CN, Johnson MR, Barnes S, Diasio RB. Glycine and taurine conjugation of bile acids by a single enzyme. Molecular cloning and expression of human liver bile acid CoA:amino acid N-acyltransferase. J Biol Chem. 1994;269(30):19375-9.

142.Kullak-Ublick GA, Stieger B, Meier PJ. Enterohepatic bile salt transporters in normal physiology and liver disease. Gastroenterology. 2004;126(1):322-42.

143.Hagenbuch B, Meier PJ. Sinusoidal (basolateral) bile salt uptake systems of hepatocytes. Semin Liver Dis. 1996;16(2):129-36.

144.Gartung C, Ananthanarayanan M, Rahman MA, Schuele S, Nundy S, Soroka CJ, et al. Down-regulation of expression and function of the rat liver Na+/bile acid cotransporter in extrahepatic cholestasis. Gastroenterology. 1996;110(1):199-209.

145.Lee JM, Trauner M, Soroka CJ, Stieger B, Meier PJ, Boyer JL. Expression of the bile salt export pump is maintained after chronic cholestasis in the rat. Gastroenterology. 2000;118(1):163-72.

146.Balistreri WF. Intrahepatic cholestasis. J Pediatr Gastroenterol Nutr. 2002;35 Suppl 1:S17-23.

147.Heathcote EJ. Diagnosis and management of cholestatic liver disease. Clin Gastroenterol Hepatol. 2007;5(7):776-82.

148.Lazaridis KN, LaRusso NF. The Cholangiopathies. Mayo Clin Proc. 2015;90(6):791-800.

149.Sclair SN, Little E, Levy C. Current Concepts in Primary Biliary Cirrhosis and Primary Sclerosing Cholangitis. Clin Transl Gastroenterol. 2015;6:e109.

150.LaRusso NF, Shneider BL, Black D, Gores GJ, James SP, Doo E, et al. Primary sclerosing cholangitis: summary of a workshop. Hepatology. 2006;44(3):746-64.

151.Lazaridis KN, LaRusso NF. Primary Sclerosing Cholangitis. N Engl J Med. 2016;375(12):1161-70.

152.Tabibian JH, Lindor KD. Primary sclerosing cholangitis: a review and update on therapeutic developments. Expert Rev Gastroenterol Hepatol. 2013;7(2):103-14.

153.Eaton JE, Talwalkar JA, Lazaridis KN, Gores GJ, Lindor KD. Pathogenesis of primary sclerosing cholangitis and advances in diagnosis and management. Gastroenterology. 2013;145(3):521-36.

154.Abdalian R, Heathcote EJ. Sclerosing cholangitis: a focus on secondary causes. Hepatology. 2006;44(5):1063-74.

155.Chapman R, Fevery J, Kalloo A, Nagorney DM, Boberg KM, Shneider B, et al. Diagnosis and management of primary sclerosing cholangitis. Hepatology. 2010;51(2):660-78.

156.Hirschfield GM, Karlsen TH, Lindor KD, Adams DH. Primary sclerosing cholangitis. The Lancet. 2013;382(9904):1587-99.

157.Alabraba E, Nightingale P, Gunson B, Hubscher S, Olliff S, Mirza D, et al. A re-evaluation of the risk factors for the recurrence of primary sclerosing cholangitis in liver allografts. Liver Transpl. 2009;15(3):330-40.

158.Campsen J, Zimmerman MA, Trotter JF, Wachs M, Bak T, Steinberg T, et al. Clinically recurrent primary sclerosing cholangitis following liver transplantation: a time course. Liver Transpl. 2008;14(2):181-5.

159.Graziadei IW. Recurrence of primary sclerosing cholangitis after liver transplantation. Liver Transpl. 2002;8(7):575-81.

160.Graziadei IW, Wiesner RH, Marotta PJ, Porayko MK, Hay JE, Charlton MR, et al. Long-term results of patients undergoing liver transplantation for primary sclerosing cholangitis. Hepatology. 1999;30(5):1121-7.

161.Alvaro D, Gigliozzi A, Attili AF. Regulation and deregulation of cholangiocyte proliferation. J Hepatol. 2000;33(2):333-40.

162.LeSage G, Glaser S, Alpini G. Regulation of cholangiocyte proliferation. Liver. 2001;21(2):73-80.

163.Desmet V, Roskams T, Van Eyken P. Ductular Reaction in the Livers. Pathology - Research and Practice. 1995;191(6):513-24.

164.Nakanuma Y, Ohta G. Immunohistochemical study on bile ductular proliferation in various hepatobiliary diseases. Liver. 1986;6(4):205-11.

165.Alpini G, Glaser SS, Ueno Y, Rodgers R, Phinizy JL, Francis H, et al. Bile acid feeding induces cholangiocyte proliferation and secretion: evidence for bile acid-regulated ductal secretion. Gastroenterology. 1999;116(1):179-86.

166.Alpini G, Lenzi R, Sarkozi L, Tavoloni N. Biliary physiology in rats with bile ductular cell hyperplasia. Evidence for a secretory function of proliferated bile ductules. J Clin Invest. 1988;81(2):569-78.

167.Goldfarb S, Singer EJ, Popper H. Experimental cholangitis due to alpha-naphthyl-isothiocyanate (ANIT). Am J Pathol. 1962;40(6):685-98.

168.James J, Lygidakis NJ, van Eyken P, Tanka AK, Bosch KS, Ramaekers FC, et al. Application of keratin immunocytochemistry and sirius red staining in evaluation of intrahepatic changes with acute extrahepatic cholestasis due to hepatic duct carcinoma. Hepatogastroenterology. 1989;36(3):151-5.

169.Palmer RH, Ruban Z. Production of bile duct hyperplasia and gallstones by lithocholic acid. J Clin Invest. 1966;45(8):1255-67.

170.LeSage GD, Benedetti A, Glaser S, Marucci L, Tretjak Z, Caligiuri A, et al. Acute carbon tetrachloride feeding selectively damages large, but not small, cholangiocytes from normal rat liver. Hepatology. 1999;29(2):307-19.

171.LeSage GD, Glaser SS, Marucci L, Benedetti A, Phinizy JL, Rodgers R, et al. Acute carbon tetrachloride feeding induces damage of large but not small cholangiocytes from BDL rat liver. Am J Physiol. 1999;276(5):G1289-301.

172.Desmet VJ, van Eyken P, Roskams T. Histopathology of vanishing bile duct diseases. Adv Clin Path. 1998;2(2):87-99.

173.Fickert P, Stoger U, Fuchsbichler A, Moustafa T, Marschall HU, Weiglein AH, et al. A new xenobiotic-induced mouse model of sclerosing cholangitis and biliary fibrosis. Am J Pathol. 2007;171(2):525-36.

174.LaRusso NF, Wiesner RH, Ludwig J, MacCarty RL. Current concepts. Primary sclerosing cholangitis. N Engl J Med. 1984;310(14):899-903.

175.Roskams TA, Theise ND, Balabaud C, Bhagat G, Bhathal PS, Bioulac-Sage P, et al. Nomenclature of the finer branches of the biliary tree: canals, ductules, and ductular reactions in human livers. Hepatology. 2004;39(6):1739-45.

176.Sell S. Comparison of liver progenitor cells in human atypical ductular reactions with those seen in experimental models of liver injury. Hepatology. 1998;27(2):317-31.

177.Thompson MD, Wickline ED, Bowen WB, Lu A, Singh S, Misse A, et al. Spontaneous repopulation of beta-catenin null livers with beta-catenin-positive hepatocytes after chronic murine liver injury. Hepatology. 2011;54(4):1333-43.

178.Kuhlmann WD, Wurster K. Correlation of histology and alpha 1-fetoprotein resurgence in rat liver regeneration after experimental injury by galactosamine. Virchows Arch A Pathol Anat Histol. 1980;387(1):47-57.

179.Nagore N, Howe S, Boxer L, Scheuer PJ. Liver cell rosettes: structural differences in cholestasis and hepatitis. Liver. 1989;9(1):43-51.

180.Thompson MD, Awuah P, Singh S, Monga SP. Disparate cellular basis of improved liver repair in beta-catenin-overexpressing mice after long-term exposure to 3,5-diethoxycarbonyl-1,4-dihydrocollidine. Am J Pathol. 2010;177(4):1812-22.

181.Lazaridis KN, Strazzabosco M, Larusso NF. The cholangiopathies: disorders of biliary epithelia. Gastroenterology. 2004;127(5):1565-77.

182.Strazzabosco M, Fiorotto R, Cadamuro M, Spirli C, Mariotti V, Kaffe E, et al. Pathophysiologic implications of innate immunity and autoinflammation in the biliary epithelium. Biochim Biophys Acta Mol Basis Dis. 2018;1864(4 Pt B):1374-9.

183.Xia X, Demorrow S, Francis H, Glaser S, Alpini G, Marzioni M, et al. Cholangiocyte injury and ductopenic syndromes. Semin Liver Dis. 2007;27(4):401-12.

184.Lin SL, Li B, Rao S, Yeo EJ, Hudson TE, Nowlin BT, et al. Macrophage Wnt7b is critical for kidney repair and regeneration. Proc Natl Acad Sci U S A. 2010;107(9):4194-9.

185.Liu Y, Han D, Wang L, Feng H. Down-regulation of Wnt10a affects odontogenesis and proliferation in mesenchymal cells. Biochem Biophys Res Commun. 2013;434(4):717-21.

186.Long A, Giroux V, Whelan KA, Hamilton KE, Tetreault MP, Tanaka K, et al. WNT10A promotes an invasive and self-renewing phenotype in esophageal squamous cell carcinoma. Carcinogenesis. 2015;36(5):598-606.

187.O'Hara SP, Karlsen TH, LaRusso NF. Cholangiocytes and the environment in primary sclerosing cholangitis: where is the link? Gut. 2017;66(11):1873-7.

188.O'Hara SP, Tabibian JH, Splinter PL, LaRusso NF. The dynamic biliary epithelia: molecules, pathways, and disease. J Hepatol. 2013;58(3):575-82.

189.Pinto C, Giordano DM, Maroni L, Marzioni M. Role of inflammation and proinflammatory cytokines in cholangiocyte pathophysiology. Biochim Biophys Acta Mol Basis Dis. 2018;1864(4 Pt B):1270-8.

190.Blechacz B, Gores GJ. Cholangiocarcinoma: advances in pathogenesis, diagnosis, and treatment. Hepatology. 2008;48(1):308-21.

191.Jensen K, Marzioni M, Munshi K, Afroze S, Alpini G, Glaser S. Autocrine regulation of biliary pathology by activated cholangiocytes. Am J Physiol Gastrointest Liver Physiol. 2012;302(5):G473-83.

192.Mederacke I, Hsu CC, Troeger JS, Huebener P, Mu X, Dapito DH, et al. Fate tracing reveals hepatic stellate cells as dominant contributors to liver fibrosis independent of its aetiology. Nat Commun. 2013;4:2823.

193.Campisi J, d'Adda di Fagagna F. Cellular senescence: when bad things happen to good cells. Nat Rev Mol Cell Biol. 2007;8(9):729-40.

194.Perez-Mancera PA, Young AR, Narita M. Inside and out: the activities of senescence in cancer. Nat Rev Cancer. 2014;14(8):547-58.

195.Meng L, Quezada M, Levine P, Han Y, McDaniel K, Zhou T, et al. Functional role of cellular senescence in biliary injury. Am J Pathol. 2015;185(3):602-9.

196.Coppe JP, Patil CK, Rodier F, Sun Y, Munoz DP, Goldstein J, et al. Senescence-associated secretory phenotypes reveal cell-nonautonomous functions of oncogenic RAS and the p53 tumor suppressor. PLoS Biol. 2008;6(12):2853-68.

197.Tchkonia T, Zhu Y, van Deursen J, Campisi J, Kirkland JL. Cellular senescence and the senescent secretory phenotype: therapeutic opportunities. J Clin Invest. 2013;123(3):966-72.

198.O'Hara SP, Splinter PL, Trussoni CE, Pisarello MJ, Loarca L, Splinter NS, et al. ETS Proto-oncogene 1 Transcriptionally Up-regulates the Cholangiocyte Senescence-associated Protein Cyclin-dependent Kinase Inhibitor 2A. J Biol Chem. 2017;292(12):4833-46.

199.Tabibian JH, O'Hara SP, Splinter PL, Trussoni CE, LaRusso NF. Cholangiocyte senescence by way of N-ras activation is a characteristic of primary sclerosing cholangitis. Hepatology. 2014;59(6):2263-75.

200.Desmet VJ. Ductal plates in hepatic ductular reactions. Hypothesis and implications. I. Types of ductular reaction reconsidered. Virchows Arch. 2011;458(3):251-9.

201.Sato K, Marzioni M, Meng F, Francis H, Glaser S, Alpini G. Ductular Reaction in Liver Diseases: Pathological Mechanisms and Translational Significances. Hepatology. 2019;69(1):420-30.

202.Carpino G, Cardinale V, Folseraas T, Overi D, Floreani A, Franchitto A, et al. Hepatic Stem/Progenitor Cell Activation Differs between Primary Sclerosing and Primary Biliary Cholangitis. American Journal of Pathology. 2018;188(3):627-39.

203.Govaere O, Cockell S, Van Haele M, Wouters J, Van Delm W, Van den Eynde K, et al. High-throughput sequencing identifies aetiology-dependent differences in ductular reaction in human chronic liver disease. J Pathol. 2019;248(1):66-76.

204.Fickert P, Pollheimer MJ, Beuers U, Lackner C, Hirschfield G, Housset C, et al. Characterization of animal models for primary sclerosing cholangitis (PSC). J Hepatol. 2014;60(6):1290-303.

205.Tephly TR, Gibbs AH, Ingall G, De Matteis F. Studies on the mechanism of experimental porphyria and ferrochelatase inhibition produced by 3,5-diethoxycarbonyl-1,4-dihydrocollidine. Int J Biochem. 1980;12(5-6):993-8.

206.Fickert P, Trauner M, Fuchsbichler A, Stumptner C, Zatloukal K, Denk H. Cytokeratins as targets for bile acid-induced toxicity. American Journal of Pathology. 2002;160(2):491-9.

207.Pose E, Sancho-Bru P, Coll M. 3,5-Diethoxycarbonyl-1,4-Dihydrocollidine Diet: A Rodent Model in Cholestasis Research. Methods Mol Biol. 2019;1981:249-57.

208.Smit JJ, Schinkel AH, Oude Elferink RP, Groen AK, Wagenaar E, van Deemter L, et al. Homozygous disruption of the murine mdr2 P-glycoprotein gene leads to a complete absence of phospholipid from bile and to liver disease. Cell. 1993;75(3):451-62.

209.Elferink RP, Tytgat GN, Groen AK. Hepatic canalicular membrane 1: The role of mdr2 P-glycoprotein in hepatobiliary lipid transport. FASEB J. 1997;11(1):19-28.

210.Ruetz S, Gros P. Phosphatidylcholine translocase: a physiological role for the mdr2 gene. Cell. 1994;77(7):1071-81.

211.Barrios JM, Lichtenberger LM. Role of biliary phosphatidylcholine in bile acid protection and NSAID injury of the ileal mucosa in rats. Gastroenterology. 2000;118(6):1179-86.

212.Fickert P, Zollner G, Fuchsbichler A, Stumptner C, Weiglein AH, Lammert F, et al. Ursodeoxycholic acid aggravates bile infarcts in bile duct-ligated and Mdr2 knockout mice via disruption of cholangioles. Gastroenterology. 2002;123(4):1238-51.

213.Van Nieuwkerk CM, Elferink RP, Groen AK, Ottenhoff R, Tytgat GN, Dingemans KP, et al. Effects of Ursodeoxycholate and cholate feeding on liver disease in FVB mice with a disrupted mdr2 P-glycoprotein gene. Gastroenterology. 1996;111(1):165-71.

214.Fickert P, Fuchsbichler A, Wagner M, Zollner G, Kaser A, Tilg H, et al. Regurgitation of bile acids from leaky bile ducts causes sclerosing cholangitis in Mdr2 (Abcb4) knockout mice. Gastroenterology. 2004;127(1):261-74.

215.Vierling JM. Animal models for primary sclerosing cholangitis. Best Pract Res Clin Gastroenterol. 2001;15(4):591-610.

216.Gracz AD, Fuller MK, Wang F, Li L, Stelzner M, Dunn JC, et al. Brief report: CD24 and CD44 mark human intestinal epithelial cell populations with characteristics of active and facultative stem cells. Stem Cells. 2013;31(9):2024-30.

217.Michalopoulos GK, Khan Z. Liver Stem Cells: Experimental Findings and Implications for Human Liver Disease. Gastroenterology. 2015;149(4):876-82.

218.Chen YH, Chen HL, Chien CS, Wu SH, Ho YT, Yu CH, et al. Contribution of Mature Hepatocytes to Biliary Regeneration in Rats with Acute and Chronic Biliary Injury. PLoS One. 2015;10(8):e0134327.

219.Kamath B, Mack C. From Hepatocyte to Cholangiocyte: The Remarkable Potential of Transdifferentiation to Treat Cholestatic Diseases. Hepatology. 2019;69(4):1828-30.

220.Michalopoulos GK, Barua L, Bowen WC. Transdifferentiation of rat hepatocytes into biliary cells after bile duct ligation and toxic biliary injury. Hepatology. 2005;41(3):535-44.

221.Sekiya S, Suzuki A. Hepatocytes, Rather than Cholangiocytes, Can Be the Major Source of Primitive Ductules in the Chronically Injured Mouse Liver. American Journal of Pathology. 2014;184(5):1468-78.

222.Limaye PB, Bowen WC, Orr AV, Luo J, Tseng GC, Michalopoulos GK. Mechanisms of hepatocyte growth factor-mediated and epidermal growth factor-mediated signaling in transdifferentiation of rat hepatocytes to biliary epithelium. Hepatology. 2008;47(5):1702-13.

223.Michalopoulos GK, Bowen WC, Mule K, Lopez-Talavera JC, Mars W. Hepatocytes undergo phenotypic transformation to biliary epithelium in organoid cultures. Hepatology. 2002;36(2):278-83.

224.Yanger K, Zong Y, Maggs LR, Shapira SN, Maddipati R, Aiello NM, et al. Robust cellular reprogramming occurs spontaneously during liver regeneration. Genes Dev. 2013;27(7):719-24.

225.Tarlow BD, Pelz C, Naugler WE, Wakefield L, Wilson EM, Finegold MJ, et al. Bipotential adult liver progenitors are derived from chronically injured mature hepatocytes. Cell Stem Cell. 2014;15(5):605-18.

226.Yanger K, Knigin D, Zong Y, Maggs L, Gu G, Akiyama H, et al. Adult hepatocytes are generated by self-duplication rather than stem cell differentiation. Cell Stem Cell. 2014;15(3):340-9.

227.Crosby HA, Hubscher S, Fabris L, Joplin R, Sell S, Kelly D, et al. Immunolocalization of putative human liver progenitor cells in livers from patients with end-stage primary biliary cirrhosis and sclerosing cholangitis using the monoclonal antibody OV-6. Am J Pathol. 1998;152(3):771-9.

228.Crosby HA, Hubscher SG, Joplin RE, Kelly DA, Strain AJ. Immunolocalization of OV-6, a putative progenitor cell marker in human fetal and diseased pediatric liver. Hepatology. 1998;28(4):980-5.

229.van Eyken P, Sciot R, Callea F, Desmet VJ. A cytokeratin-immunohistochemical study of focal nodular hyperplasia of the liver: further evidence that ductular metaplasia of hepatocytes contributes to ductular "proliferation". Liver. 1989;9(6):372-7.

230.Vandersteenhoven AM, Burchette J, Michalopoulos G. Characterization of ductular hepatocytes in end-stage cirrhosis. Arch Pathol Lab Med. 1990;114(4):403-6.

231.Butron Vila MM, Haot J, Desmet VJ. Cholestatic features in focal nodular hyperplasia of the liver. Liver. 1984;4(6):387-95.

232.Schaub JR, Huppert KA, Kurial SNT, Hsu BY, Cast AE, Donnelly B, et al. De novo formation of the biliary system by TGFbeta-mediated hepatocyte transdifferentiation. Nature. 2018;557(7704):247-51.

233.Tanimizu N, Mitaka T. Re-evaluation of liver stem/progenitor cells. Organogenesis. 2014;10(2):208-15.

234.Tanimizu N, Nishikawa Y, Ichinohe N, Akiyama H, Mitaka T. Sry HMG box protein 9-positive (Sox9+) epithelial cell adhesion molecule-negative (EpCAM-) biphenotypic cells derived from hepatocytes are involved in mouse liver regeneration. J Biol Chem. 2014;289(11):7589-98.

235.Brent GA. Mechanisms of thyroid hormone action. J Clin Invest. 2012;122(9):3035-43.

236.Gereben B, Zavacki AM, Ribich S, Kim BW, Huang SA, Simonides WS, et al. Cellular and molecular basis of deiodinase-regulated thyroid hormone signaling. Endocr Rev. 2008;29(7):898-938.

237.Hoffenberg R. Triiodothyronine. Clin Endocrinol (Oxf). 1973;2(1):75-87.

238.Gullberg H, Rudling M, Salto C, Forrest D, Angelin B, Vennstrom B. Requirement for thyroid hormone receptor beta in T3 regulation of cholesterol metabolism in mice. Mol Endocrinol. 2002;16(8):1767-77.

239.Kowalik MA, Perra A, Pibiri M, Cocco MT, Samarut J, Plateroti M, et al. TRbeta is the critical thyroid hormone receptor isoform in T3-induced proliferation of hepatocytes and pancreatic acinar cells. J Hepatol. 2010;53(4):686-92.

240.Ledda-Columbano GM, Molotzu F, Pibiri M, Cossu C, Perra A, Columbano A. Thyroid hormone induces cyclin D1 nuclear translocation and DNA synthesis in adult rat cardiomyocytes. FASEB J. 2006;20(1):87-94.

241.Chiellini G, Apriletti JW, Yoshihara HA, Baxter JD, Ribeiro RC, Scanlan TS. A high-affinity subtype-selective agonist ligand for the thyroid hormone receptor. Chem Biol. 1998;5(6):299-306.

242.Kosar K, Cornuet P, Singh S, Liu S, Nejak-Bowen K. The Thyromimetic Sobetirome (GC-1) Alters Bile Acid Metabolism in a Mouse Model of Hepatic Cholestasis. Am J Pathol. 2020;190(5):1006-17.

243.Dyson JK, Beuers U, Jones DEJ, Lohse AW, Hudson M. Primary sclerosing cholangitis. The Lancet. 2018;391(10139):2547-59.

244.Karlsen TH, Folseraas T, Thorburn D, Vesterhus M. Primary sclerosing cholangitis - a comprehensive review. J Hepatol. 2017;67(6):1298-323.

245.Monga SP. beta-Catenin Signaling and Roles in Liver Homeostasis, Injury, and Tumorigenesis. Gastroenterology. 2015;148(7):1294-310.

246.Saggi H, Maitra D, Jiang A, Zhang R, Wang P, Cornuet P, et al. Loss of hepatocyte beta-catenin protects mice from experimental porphyria-associated liver injury. J Hepatol. 2019;70(1):108-17.

247.Thompson MD, Moghe A, Cornuet P, Marino R, Tian J, Wang P, et al. beta-Catenin regulation of farnesoid X receptor signaling and bile acid metabolism during murine cholestasis. Hepatology. 2018;67(3):955-71.

248.Schindelin J, Arganda-Carreras I, Frise E, Kaynig V, Longair M, Pietzsch T, et al. Fiji: an open-source platform for biological-image analysis. Nat Methods. 2012;9(7):676-82.

249.Goodwin B, Jones SA, Price RR, Watson MA, McKee DD, Moore LB, et al. A regulatory cascade of the nuclear receptors FXR, SHP-1, and LRH-1 represses bile acid biosynthesis. Mol Cell. 2000;6(3):517-26.

250.Guo GL, Lambert G, Negishi M, Ward JM, Brewer HB, Jr., Kliewer SA, et al. Complementary roles of farnesoid X receptor, pregnane X receptor, and constitutive androstane receptor in protection against bile acid toxicity. J Biol Chem. 2003;278(46):45062-71.

251.Bai H, Zhang N, Xu Y, Chen Q, Khan M, Potter JJ, et al. Yes-associated protein regulates the hepatic response after bile duct ligation. Hepatology. 2012;56(3):1097-107.

252.Georgiev P, Jochum W, Heinrich S, Jang JH, Nocito A, Dahm F, et al. Characterization of time-related changes after experimental bile duct ligation. Br J Surg. 2008;95(5):646-56.

253.van Golen RF, Olthof PB, Lionarons DA, Reiniers MJ, Alles LK, Uz Z, et al. FXR agonist obeticholic acid induces liver growth but exacerbates biliary injury in rats with obstructive cholestasis. Sci Rep. 2018;8(1):16529.

254.Yokoyama Y, Nagino M, Nimura Y. Mechanism of impaired hepatic regeneration in cholestatic liver. J Hepatobiliary Pancreat Surg. 2007;14(2):159-66.

255.Fava G, Ueno Y, Glaser S, Francis H, DeMorrow S, Marucci L, et al. Thyroid hormone inhibits biliary growth in bile duct-ligated rats by PLC/IP3/Ca2+-dependent downregulation of SRC/ERK1/2. American Journal of Physiology-Cell Physiology. 2007;292(4):C1467-C75.

256.Sjouke B, Langslet G, Ceska R, Nicholls SJ, Nissen SE, Ohlander M, et al. Eprotirome in patients with familial hypercholesterolaemia (the AKKA trial): a randomised, double-blind, placebo-controlled phase 3 study. Lancet Diabetes Endocrinol. 2014;2(6):455-63.

257.Baghdasaryan A, Claudel T, Gumhold J, Silbert D, Adorini L, Roda A, et al. Dual farnesoid X receptor/TGR5 agonist INT-767 reduces liver injury in the Mdr2-/- (Abcb4-/-) mouse cholangiopathy model by promoting biliary HCO(-)(3) output. Hepatology. 2011;54(4):1303-12.

258.Bonde Y, Plosch T, Kuipers F, Angelin B, Rudling M. Stimulation of murine biliary cholesterol secretion by thyroid hormone is dependent on a functional ABCG5/G8 complex. Hepatology. 2012;56(5):1828-37.

259.Gullberg H, Rudling M, Forrest D, Angelin B, Vennstrom B. Thyroid hormone receptor beta-deficient mice show complete loss of the normal cholesterol 7alpha-hydroxylase (CYP7A) response to thyroid hormone but display enhanced resistance to dietary cholesterol. Mol Endocrinol. 2000;14(11):1739-49.

260.Angelin B, Rudling M. Lipid lowering with thyroid hormone and thyromimetics. Curr Opin Lipidol. 2010;21(6):499-506.

261.De Vree JM, Ottenhoff R, Bosma PJ, Smith AJ, Aten J, Oude Elferink RP. Correction of liver disease by hepatocyte transplantation in a mouse model of progressive familial intrahepatic cholestasis. Gastroenterology. 2000;119(6):1720-30.

262.Gautherot J, Claudel T, Cuperus F, Fuchs CD, Falguieres T, Trauner M. Thyroid hormone receptor beta1 stimulates ABCB4 to increase biliary phosphatidylcholine excretion in mice. J Lipid Res. 2018;59(9):1610-9.

263.Michalopoulos GK, Bowen WC, Mule K, Stolz DB. Histological organization in hepatocyte organoid cultures. Am J Pathol. 2001;159(5):1877-87.

264.Michalopoulos GK, Bowen WC, Zajac VF, Beer-Stolz D, Watkins S, Kostrubsky V, et al. Morphogenetic events in mixed cultures of rat hepatocytes and nonparenchymal cells maintained in biological matrices in the presence of hepatocyte growth factor and epidermal growth factor. Hepatology. 1999;29(1):90-100.

265.Gautam M, Cheruvattath R, Balan V. Recurrence of autoimmune liver disease after liver transplantation: a systematic review. Liver Transpl. 2006;12(12):1813-24.

266.Tamura S, Sugawara Y, Kaneko J, Togashi J, Matsui Y, Yamashiki N, et al. Recurrence of cholestatic liver disease after living donor liver transplantation. World J Gastroenterol. 2008;14(33):5105-9.

267.Limaye PB, Alarcon G, Walls AL, Nalesnik MA, Michalopoulos GK, Demetris AJ, et al. Expression of specific hepatocyte and cholangiocyte transcription factors in human liver disease and embryonic development. Lab Invest. 2008;88(8):865-72.

268.Carpino G, Nevi L, Overi D, Cardinale V, Lu WY, Di Matteo S, et al. Peribiliary Gland Niche Participates in Biliary Tree Regeneration in Mouse and in Human Primary Sclerosing Cholangitis. Hepatology. 2020;71(3):972-89.

269.Boulter L, Guest RV, Kendall TJ, Wilson DH, Wojtacha D, Robson AJ, et al. WNT signaling drives cholangiocarcinoma growth and can be pharmacologically inhibited. J Clin Invest. 2015;125(3):1269-85.

270.Wilson DH, Jarman EJ, Mellin RP, Wilson ML, Waddell SH, Tsokkou P, et al. Non-canonical Wnt signalling regulates scarring in biliary disease via the planar cell polarity receptors. Nat Commun. 2020;11(1):445.

271.Lindroos PM, Zarnegar R, Michalopoulos GK. Hepatocyte Growth-Factor (Hepatopoietin-a) Rapidly Increases in Plasma before DNA-Synthesis and Liver-Regeneration Stimulated by Partial-Hepatectomy and Carbon-Tetrachloride Administration. Hepatology. 1991;13(4):743-50.

272.Guicciardi ME, Trussoni CE, LaRusso NF, Gores GJ. The Spectrum of Reactive Cholangiocytes in Primary Sclerosing Cholangitis. Hepatology. 2020;71(2):741-8.

273.Loilome W, Bungkanjana P, Techasen A, Namwat N, Yongvanit P, Puapairoj A, et al. Activated macrophages promote Wnt/beta-catenin signaling in cholangiocarcinoma cells. Tumour Biol. 2014;35(6):5357-67.

274.MacLeod RJ, Hayes M, Pacheco I. Wnt5a secretion stimulated by the extracellular calcium-sensing receptor inhibits defective Wnt signaling in colon cancer cells. Am J Physiol Gastrointest Liver Physiol. 2007;293(1):G403-11.

275.Mikels AJ, Nusse R. Purified Wnt5a protein activates or inhibits beta-catenin-TCF signaling depending on receptor context. PLoS Biol. 2006;4(4):e115.

276.Topol L, Jiang X, Choi H, Garrett-Beal L, Carolan PJ, Yang Y. Wnt-5a inhibits the canonical Wnt pathway by promoting GSK-3-independent beta-catenin degradation. J Cell Biol. 2003;162(5):899-908.

277.Carbone M, Neuberger J. Liver transplantation in PBC and PSC: indications and disease recurrence. Clin Res Hepatol Gastroenterol. 2011;35(6-7):446-54.

278.Carrion AF, Bhamidimarri KR. Liver transplant for cholestatic liver diseases. Clin Liver Dis. 2013;17(2):345-59.

279.Schoning W, Schmeding M, Ulmer F, Andert A, Neumann U. Liver Transplantation for Patients with Cholestatic Liver Diseases. Viszeralmedizin. 2015;31(3):194-8.

280.Kwong A, Kim WR, Lake JR, Smith JM, Schladt DP, Skeans MA, et al. OPTN/SRTR 2018 Annual Data Report: Liver. Am J Transplant. 2020;20 Suppl s1:193-299.

281.Okabe M, Tsukahara Y, Tanaka M, Suzuki K, Saito S, Kamiya Y, et al. Potential hepatic stem cells reside in EpCAM+ cells of normal and injured mouse liver. Development. 2009;136(11):1951-60.